Effect of Pressure-Dependency of the Yield Criterion on the Strain Rate Intensity Factor

Sergei Alexandrov, Elena Lyamina and Yeau-Ren Jeng

Abstract In the case of several rigid plastic models, the equivalent strain rate (quadratic invariant of the strain rate tensor) approaches infinity in the vicinity of maximum friction surfaces. The strain rate intensity factor is the coefficient of the leading singular term in a series expansion of the equivalent strain rate in the vicinity of such surfaces. This coefficient controls the magnitude of the equivalent strain rate in a narrow material layer near maximum friction surfaces. On the other hand, the equivalent strain rate is involved in many conventional equations describing the evolution of parameters characterizing material properties. Experimental data show that a narrow layer in which material properties are quite different from those in the bulk often appears in the vicinity of surfaces with high friction in metal forming processes. This experimental fact is in qualitative agreement with the aforementioned evolution equations involving the equivalent strain rate. However, when the maximum friction law is adopted, direct use of such equations is impossible since the equivalent strain rate in singular. A possible way to overcome this difficulty is to develop a new type of evolution equations involving the strain rate intensity factor instead of the equivalent strain rate. This approach is somewhat similar to the conventional approach in the mechanics of cracks when fracture criteria from the strength of materials are replaced with criteria based on the stress intensity factor in the vicinity of crack tips. The development of the new approach requires a special experimental program to establish relations between the magnitude of the strain rate intensity factor and the

S. Alexandrov and E. Lyamina
A.Yu. Ishlinsky Institute for Problems in Mechanics, Russian Academy of Sciences, Moscow, Russia
e-mail: sergei_alexandrov@spartak.ru

E. Lyamina
e-mail: lyamina@inbox.ru

S. Alexandrov and Y.-R. Jeng
Department of Mechanical Engineering and Advanced Institute of Manufacturing with High-tech Innovations, National Chung Cheng University, Chia-Yi, Taiwan
e-mail: imeyrj@ccu.edu.tw

H. Altenbach and A. Öchsner (eds.), *Plasticity of Pressure-Sensitive Materials*, Engineering Materials, DOI: 10.1007/978-3-642-40945-5_5,

evolution of material properties in a narrow material layer near surfaces with high friction as well as a theoretical method to deal with singular solutions for rigid plastic solids. Since no numerical method has been yet developed to determine the strain rate intensity factor, the present chapter focuses on analytical and semi-analytical solutions from which the dependence of the strain rate intensity factor on process and material parameters are found. In particular, the effect of pressure-dependency of the yield criterion on the strain rate intensity factor is emphasized using the double shearing model.

1 Introduction

In the case of rigid perfectly plastic solids, the maximum friction surfaces are defined by the condition that the friction stress at sliding is equal to the shear yield stress of the material [1]. In the case of planar flow, this definition is equivalent to the statement that the maximum friction surface coincides with a characteristic or an envelope of characteristics. The latter definition is naturally generalized on the double shearing model [2]. A distinguished feature of maximum friction surfaces is that the second invariant of the strain rate tensor (this quantity is also called the equivalent strain rate) approaches infinity in the vicinity of such surfaces for several rigid plastic models [1–5]. This theoretical feature of the solutions can be related to the formation of a layer of intensive plastic deformation in the vicinity of frictional interfaces in real metal forming processes [6–8], though no specific theory is available. Therefore, it is of interest to understand the effect of material and process parameters on the magnitude of the strain rate intensity factor. The traditional finite element method cannot be used to find the strain rate intensity factor because it is the coefficient of a singular term. The extended finite element method [9] is in general applicable in this case but no specific code has been developed yet. Therefore, semi-analytical solutions available in the literature are used in the present chapter to reveal the effect of pressure-dependency of the yield criterion on the strain rate intensity factor. The solutions for pressure-independent material are based on Tresca's yield criterion and its associated flow rule. The solutions for pressure-dependent material are based on the double-shearing model [10].

2 Strain Rate Intensity Factor

The strain rate intensity factor has been previously introduced for several rigid plastic models. Most of solutions in which the strain rate intensity factor appears are available for the classical phenomenological theory of plasticity and the double shearing model. The former is a model of pressure-independent plasticity. A great account on this model is given in [11]. The double shearing model is a model of pressure-dependent plasticity based on the Mohr-Coulomb yield criterion. This model is described in detail in [10].

The constitutive equations of the rigid perfectly plastic pressure-independent model are a yield criterion and its associated flow rule. By assumption, the yield criterion is independent of the first invariant of the stress tensor (or the hydrostatic stress). Therefore, it can be represented by a locus in two-dimensional space, where the second and third invariants of the stress tensor are taken as Cartesian coordinates. The second invariant of the stress tensor is also called the equivalent stress, σ_{eq}. A number of yield criteria independent of the hydrostatic stress (pressure-independent yield criteria) have been proposed in the literature, though it is commonly accepted that the criteria due to von Mises and Tresca are most representative of initial yielding in isotropic, metallic materials [12]. The monograph [11] mainly deals with the von Mises criterion. It is worthy of note that the formulation of plane strain problems in dimensionless form is independent of the yield criterion chosen. In other words, any plane strain solution for the von Mises criterion is the solution for any other pressure-independent criterion. The model based on Tresca's yield criterion under conditions of axial symmetry is described in detail in [13, 14].

The constitutive equations of the double shearing model are the Mohr-Coulomb yield criterion, the equation of incompressibility and the equation that connects stresses and velocities. Extensions of this theory to include plastic volume change are also available in the literature (see, for example, [15]) but they are not considered in the present chapter. At a specific set of parameters, the double shearing model reduces to the model of classical pressure-independent plasticity based on Tresca's yield criterion. Since the objective of the present chapter is to demonstrate the effect of pressure-dependency of the yield criterion on the strain rate intensity factor, the Tresca's yield criterion will be used to determine the strain rate intensity factor in axisymmetric problems for pressure-independent materials.

The strain rate intensity factor has been defined in [1] as the coefficient of the leading singular term in a series expansion of the equivalent strain rate in the vicinity of maximum friction surfaces. This work has been restricted to the classical pressure-independent model. The term maximum friction surface is used to indicate that the maximum friction law is adopted on that surface. The original formulation of the maximum friction law for pressure-independent material is

$$\tau_f = \tau_s \tag{1}$$

at sliding. Here τ_f is the friction stress and τ_s is the shear yield stress. It is worthy to note that τ_s is constant for perfectly plastic materials. It is known from the general theory (see, for example, [14]) that the equations of plane strain and axisymmetric deformation are hyperbolic (in the latter case, Tresca's yield criterion should be adopted). Moreover, the characteristics for the stresses and the velocities coincide and, therefore, there are only two distinct characteristic directions at a point. The shear stress along the characteristic is equal to τ_s. Thus the boundary condition (1) is equivalent to the statement that the friction surface coincides with a characteristic or an envelope of characteristics. Let ϕ be the angle between the major principal stress σ_1 and the tangent to the friction surface, measured from the tangent anti-clockwise. In the case of the model of pressure-independent plasticity the characteristics are

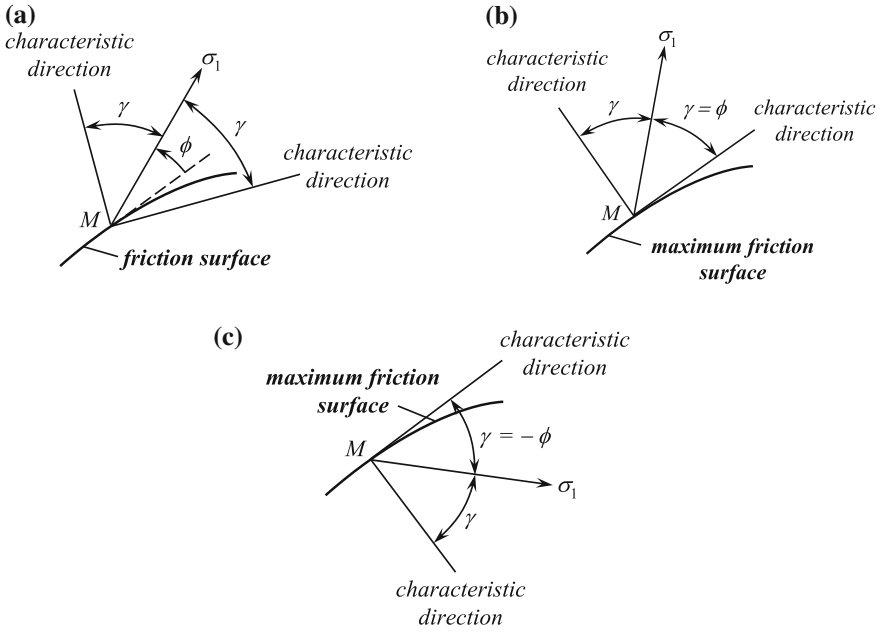

Fig. 1 Orientation of the characteristic directions relative to the tangent to friction surfaces. **a** arbitrary friction surface. **b** maximum friction surface with $\phi > 0$. **c** maximum friction surface with $\phi < 0$

inclined to the direction of σ_1 at $\pm\pi/4$. However, for later convenience it is assumed here that this angle is $\pm\gamma$. It is evident that the original case is obtained at $\gamma = \pi/4$. The characteristic directions at a generic point, M, on an arbitrary friction surface are illustrated in Fig. 1a. If the maximum friction law is valid on this surface then the orientation of the characteristics becomes such as shown in Fig. 1b, c. It is evident that $\phi = \gamma$ in Fig. 1b and $\phi = -\gamma$ in Fig. 1c. Therefore, since $\gamma = \pi/4$ in the case under consideration, the boundary condition (1) is equivalent to

$$\phi = \pm\frac{\pi}{4} \tag{2}$$

at sliding.

The equations of the double sharing model are also hyperbolic [10]. Therefore, the maximum friction law in the form of Eq. (2) can be extended to this model with no difficulty. In particular, it has been shown in [10] that in the case of plane strain and axisymmetric deformation $\gamma = \pi/4 + \varphi/2$ (Fig. 1). Here φ is the angle of internal friction, a material constant. Eq. (2) transforms to

$$\phi = \pm\left(\frac{\pi}{4} + \frac{\varphi}{2}\right) \tag{3}$$

at sliding. The strain rate intensity factor for this model has been introduced in [2].

When the maximum friction law is adopted, two qualitatively different options are possible. A natural way to distinguish these options is to use the maximum friction law in the form of Eqs. (2) and (3). Either of these equations is valid if the maximum friction surface coincides with (i) a characteristic or (ii) an envelope of characteristics. Option (i) imposes severe restrictions on the velocity field. In particular, the rate of extension along the friction surface is zero in the case of plane strain deformation of pressure-independent material. Therefore, in most cases Option (ii) occurs and it will be assumed throughout this chapter.

In order to precisely define the strain rate intensity factor, it is necessary to introduce the equivalent strain rate. The standard definition for this quantity involves the equivalent stress and the rate of plastic work [11]. In this chapter, however, the equivalent strain rate is understood as a pure kinematic quantity (the quadratic invariant of the strain rate tensor) defined by

$$\xi_{\mathrm{eq}} = \sqrt{\frac{2}{3}\xi_{ij}\xi_{ij}}, \tag{4}$$

where ξ_{ij} are the components of the strain rate tensor. This definition coincides with the standard definition for the von Mises yield criterion combined with its associated flow rule. The equivalent strain rate approaches infinity in the vicinity of maximum friction surfaces. In particular,

$$\xi_{\mathrm{eq}} = \frac{D}{\sqrt{s}} + o\left(\frac{1}{\sqrt{s}}\right) \quad \text{as} \quad s \to 0, \tag{5}$$

where s is the normal distance to the friction surface and D is the strain rate intensity factor. Under various assumptions concerning the pressure-independent yield criterion and modes of deformation, this result has been obtained in [1, 16–20]. For materials obeying the double shearing model the asymptotic expansion (5) for plane strain and axisymmetric flow has been found in [2, 21], respectively. Particular solutions show that (5) is also satisfied for other rigid plastic models [3–5, 22–25]. Reviews of solutions for the strain rate intensity factor are given in [26, 27].

It is always possible to choose such a coordinate system that the normal strain rates are bounded and one of the shear strain rates approaches infinity in the vicinity of maximum friction surfaces. Denote this shear strain rate by ξ_τ. Then, it follows from (4) and (5) that

$$|\xi_\tau| = \frac{\sqrt{3}}{2}\frac{D}{\sqrt{s}} + o\left(\frac{1}{\sqrt{s}}\right) \quad \text{as} \quad s \to 0. \tag{6}$$

In order to provide some insights into distinguished features of the maximum friction law and material models leading to (5), this asymptotic expansion is below derived for plane strain deformation of pressure-independent materials.

It is convenient to introduce a Cartesian coordinate system (x, y, z) whose z-axis is orthogonal to planes of flow. Let σ_{xx}, σ_{yy} and σ_{xy} be the components of the stress

tensor in this coordinate system. Then, any pressure-independent yield criterion can be written in the form

$$\left(\sigma_{xx}-\sigma_{yy}\right)^2+4\sigma_{xy}^2=4\tau_s^2. \tag{7}$$

The flow rule associated with this yield criterion is

$$\xi_{xx}=\lambda\left(\sigma_{xx}-\sigma_{yy}\right),\quad \xi_{yy}=\lambda\left(\sigma_{yy}-\sigma_{xx}\right),\quad \xi_{xy}=2\lambda\sigma_{xy} \tag{8}$$

where ξ_{xx}, ξ_{yy} and ξ_{xy} are the components of the strain rate tensor in the Cartesian coordinates and $\lambda\geq 0$. Eliminating λ in (8) gives

$$\xi_{xx}+\xi_{yy}=0,\quad \frac{\xi_{xy}}{\xi_{xx}-\xi_{yy}}=\frac{\sigma_{xy}}{\sigma_{xx}-\sigma_{yy}}. \tag{9}$$

The first equation of this system is the equation of incompressibility. The strain rate components are expressed through the velocity components, u_x and u_y, as

$$\xi_{xx}=\frac{\partial u_x}{\partial x},\quad \xi_{yy}=\frac{\partial u_y}{\partial y},\quad \xi_{xy}=\frac{1}{2}\left(\frac{\partial u_y}{\partial x}+\frac{\partial u_x}{\partial y}\right). \tag{10}$$

Substituting (10) into (9) yields

$$\frac{\partial u_x}{\partial x}+\frac{\partial u_y}{\partial y}=0,\quad \left(\frac{\partial u_x}{\partial y}+\frac{\partial u_y}{\partial x}\right)\left(\sigma_{xx}-\sigma_{yy}\right)=2\left(\frac{\partial u_x}{\partial x}-\frac{\partial u_y}{\partial y}\right)\sigma_{xy}. \tag{11}$$

The constitutive equations should be supplemented with the equilibrium equations

$$\frac{\partial \sigma_{xx}}{\partial x}+\frac{\partial \sigma_{xy}}{\partial y}=0,\quad \frac{\partial \sigma_{xy}}{\partial x}+\frac{\partial \sigma_{yy}}{\partial y}=0. \tag{12}$$

The system of five Eqs. (7), (11) and (12) in the five unknowns σ_{xx}, σ_{yy}, σ_{xy}, u_x, u_y, is the basis for the calculation of the distribution of stress and velocity in the plastic region. It is known that this system is hyperbolic [11]. The characteristic directions make an angle of $\pi/4$ with the major principal stress direction. Let ψ be the angle between the major principal stress σ_1 and the x-axis, measured from the axis anti-clockwise. Then, the orientation of the characteristic curves relative to the x-axis is (Fig. 2)

$$\phi_1=\psi-\frac{\pi}{4},\quad \phi_2=\psi+\frac{\pi}{4}. \tag{13}$$

Let ω be a tool surface (curve in planes of flow) where the condition (2) is satisfied, and consider Eqs. (7), (11) and (12) at an arbitrary point, M, on that surface. The tool is regarded as fixed. The Cartesian coordinate system is taken to be situated at M with the y-axis directed along the normal to ω, away from the rigid tool and

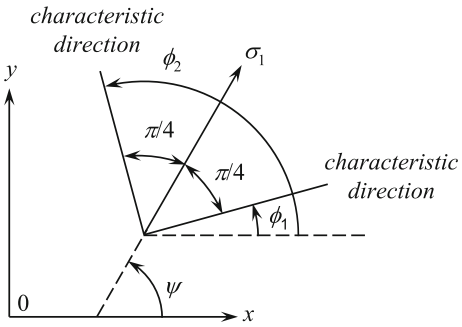

Fig. 2 Orientation of the major principal stress and characteristic directions relative to the x-axis

towards the plastic material (Fig. 3). Since the condition (2) is equivalent to (1), in this coordinate system

$$|\sigma_{xy}| = \tau_s \tag{14}$$

at M. Therefore, it follows from (7) that

$$\sigma_{xx} = \sigma_{yy} \tag{15}$$

at M. Using $(11)_1$ Eq. $(11)_2$ can be rewritten as

$$\left(\frac{\partial u_x}{\partial y} + \frac{\partial u_y}{\partial x}\right)(\sigma_{xx} - \sigma_{yy}) = 4\frac{\partial u_x}{\partial x}\sigma_{xy}. \tag{16}$$

Substituting (14) and (15) into (16) shows that it is necessary to examine the cases

$$\frac{\partial u_x}{\partial x} = 0 \quad \text{at} \quad y = 0 \tag{17}$$

and

$$\left|\frac{\partial u_x}{\partial y} + \frac{\partial u_y}{\partial x}\right| \to \infty \quad \text{as} \quad y \to 0. \tag{18}$$

It follows from (17) and the orientation of the x-axis (Fig. 3) that the rate of extension along the friction surface is zero. Since M is an arbitrary point on the friction surface, this means that a characteristic curve coincides with the friction surface. Such solutions have been excluded from consideration. Therefore, it is necessary to assume that Eq. (18) is valid. In order to determine the asymptotic behaviour of the velocity field in the vicinity of the friction surface, some additional assumptions are necessary. In particular,

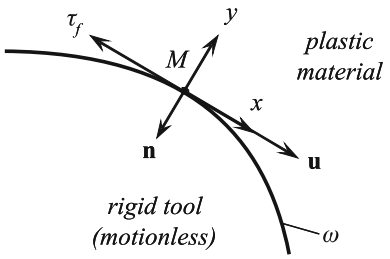

Fig. 3 Orientation of the local coordinate system at M

(i) Velocity components are bounded at M,
(ii) In-surface derivatives of the velocity components are bounded at M,
(iii) Solution can be represented by a power series in the vicinity of M.

With no loss of generality, it is possible to choose the direction of the x-axis such that $\xi_{xy} > 0$ at M. In particular, its direction should coincide with the direction of the velocity vector, $\mathbf{u}$, of a material particle located at M at a given instant (Fig. 3). In Fig. 3, $\mathbf{n}$ is the outer normal to the plastic material and τ_f is the friction stress applied to this material. Then, using assumptions (ii) and (iii) Eq. (18) transforms to

$$\frac{\partial u_x}{\partial y} = u_1 y^{-\alpha} + o\left(y^{-\alpha}\right) \quad \text{as} \quad y \to 0, \tag{19}$$

where u_1 may depend on x and $u_1 > 0$. Integrating (19) yields

$$u_x = u_0 + \frac{u_1}{(1-\alpha)} y^{1-\alpha} + o\left(y^{1-\alpha}\right) \quad \text{as} \quad y \to 0, \tag{20}$$

where u_0 may depend on x and $u_0 > 0$. It follows from assumption (i) and (20) that

$$\alpha < 1. \tag{21}$$

On the other hand, (18) is satisfied if and only if $\alpha > 0$ in (19). Combining this inequality and (21) leads to

$$0 < \alpha < 1. \tag{22}$$

Using (20) Eq. $(11)_1$ can be transformed to

$$\frac{du_0}{dx} + \frac{y^{1-\alpha}}{(1-\alpha)} \frac{du_1}{dx} + \frac{\partial u_y}{\partial y} + o\left(y^{1-\alpha}\right) = 0 \quad \text{as} \quad y \to 0. \tag{23}$$

Integrating with the boundary condition $u_y = 0$ for $y = 0$ (at point M) and taking into account (22) gives

$$u_y = -\frac{du_0}{dx} y + o(y) \quad \text{as} \quad y \to 0. \tag{24}$$

Using (10), (20) and (24) the non-zero strain rate components can be represented as

$$\xi_{xx} = -\xi_{yy} = \frac{du_0}{dx} + o(1), \quad \xi_{xy} = \frac{u_1}{2} y^{-\alpha} + o\left(y^{-\alpha}\right) \quad \text{as} \quad y \to 0. \tag{25}$$

It is worthy to note here that, by assumption, $\xi_{xx} \neq 0$ (or $du_0/dx \neq 0$) and $u_1 \neq 0$ at M. Since $\xi_{xy} > 0$ by the choice of the coordinate system, it follows from $(8)_3$ that $\sigma_{xy} > 0$ as well. Therefore, using assumption (iii) the distribution of stresses in the vicinity of the friction surface can be represented as

$$\begin{aligned} \sigma_{xx} &= \sigma_{xx}^{(0)} + \sigma_{xx}^{(1)} y^{\gamma_{11}} + o\left(y^{\gamma_{11}}\right), \\ \sigma_{yy} &= \sigma_{yy}^{(0)} + \sigma_{yy}^{(1)} y^{\gamma_{22}} + o\left(y^{\gamma_{22}}\right), \\ \sigma_{xy} &= \sigma_{xy}^{(0)} + \sigma_{xy}^{(1)} y^{\gamma_{12}} + o\left(y^{\gamma_{12}}\right) \end{aligned} \tag{26}$$

as $y \to 0$. Here $\sigma_{xx}^{(0)}$, $\sigma_{xx}^{(1)}$, $\sigma_{yy}^{(0)}$, $\sigma_{yy}^{(1)}$, $\sigma_{xy}^{(0)}$, and $\sigma_{xy}^{(1)}$ can depend on x. Equations (14) and (15) demand

$$\sigma_{xx}^{(0)} = \sigma_{yy}^{(0)} \quad \text{and} \quad \sigma_{xy}^{(0)} = \tau_s \tag{27}$$

at $x = 0$ (at point M). Substituting (19), (24) and (26) into (16) and using (27) yields

$$u_1 y^{-\alpha} \left(\sigma_{xx}^{(1)} y^{\gamma_{11}} - \sigma_{yy}^{(1)} y^{\gamma_{22}}\right) = 4 \frac{du_0}{dx} \tau_s \tag{28}$$

to leading order. Since the right hand side of this equation is $O(1)$ as $y \to 0$, it is necessary to examine the cases

$$\gamma_{11} - \alpha = 0 \tag{29}$$

and

$$\gamma_{22} - \alpha = 0. \tag{30}$$

Substituting (26) into (12) gives

$$\begin{aligned} \frac{d\sigma_{xx}^{(0)}}{dx} + \frac{d\sigma_{xx}^{(1)}}{dx} y^{\gamma_{11}} + \sigma_{xy}^{(1)} \gamma_{12} y^{\gamma_{12}-1} &= 0, \\ \frac{d\sigma_{xy}^{(0)}}{dx} + \frac{d\sigma_{xy}^{(1)}}{dx} y^{\gamma_{12}} + \sigma_{yy}^{(1)} \gamma_{22} y^{\gamma_{22}-1} &= 0 \end{aligned} \tag{31}$$

to leading order. Combining (30) and $(31)_2$ yields $\alpha = 1$ or $\gamma_{12} = \alpha - 1$. The former contradicts (22). The latter combined with (22) leads to $\gamma_{12} < 0$. According to (26) this inequality results in $|\sigma_{xy}| \to \infty$ as $y \to 0$. Therefore, it is necessary to assume that (29) is valid. Then, substituting (26) into (7) and using (27) yields

$$y^{2\alpha} \left[\sigma_{xx}^{(1)} - \sigma_{yy}^{(1)} y^{(\gamma_{22}-1)}\right]^2 + 4 \left[\tau_s + \sigma_{xy}^{(1)} y^{\gamma_{12}}\right]^2 = 4\tau_s^2 \tag{32}$$

as $y \to 0$. Using straight multiplication, Eq. (32) is simplified to

$$y^{2\alpha}\left[\sigma_{xx}^{(1)}\right]^2 + 8\tau_s\sigma_{xy}^{(1)}y^{\gamma_{12}} = 0 \quad \text{as} \quad y \to 0. \tag{33}$$

It follows from this equation that

$$2\alpha = \gamma_{12}. \tag{34}$$

Substituting (29) and (34) into $(31)_1$ shows that $2\alpha - 1 = \alpha$ or $2\alpha - 1 = 0$. The former gives $\alpha = 1$ and therefore contradicts (22). The latter results in

$$\alpha = \frac{1}{2}. \tag{35}$$

The asymptotic expansion (5) immediately follows from (4), (25) and (35).

3 Plane Strain Solutions for Pressure-Independent Material

3.1 Basic Equations

Section 3 is concerned with plane strain solutions for pressure-independent materials. In this section, two coordinate systems will be used, namely a Cartesian coordinate system $(x,\ y,\ z)$ and a cylindrical coordinate system $(r,\ \theta,\ z)$. All the solutions considered are independent of z. The constitutive equations in the Cartesian coordinate system are (7) and (9). The orientation of the characteristic curves relative to the x-axis is given by (13). The strain rate components ξ_{zz}, ξ_{xz} and ξ_{yz} as well as the stress components σ_{xz} and σ_{yz} vanish. The non-zero strain rate components are expressed through the velocity components according to (10). The equilibrium equations are given by (12). The transformation equations for stress components in xy-planes are (Fig. 2)

$$\sigma_{xx} = \frac{\sigma_1 + \sigma_2}{2} + \tau_s\cos 2\psi,\ \ \sigma_{yy} = \frac{\sigma_1 + \sigma_2}{2} - \tau_s\cos 2\psi,\ \ \sigma_{xy} = \tau_s\sin 2\psi. \tag{36}$$

It has been taken into account here that Eq. (7) in terms of the principal stresses σ_1 and σ_2 becomes

$$\sigma_1 - \sigma_2 = 2\tau_s. \tag{37}$$

Let σ_{rr}, $\sigma_{\theta\theta}$, σ_{zz}, σ_{rz}, $\sigma_{z\theta}$ and $\sigma_{r\theta}$ be the components of the stress tensor in the cylindrical coordinate system. The components σ_{rz} and $\sigma_{z\theta}$ vanish. The yield criterion (7) transforms to

$$(\sigma_{rr} - \sigma_{\theta\theta})^2 + 4\sigma_{r\theta}^2 = 4\tau_s^2. \tag{38}$$

Let ξ_{rr}, $\xi_{\theta\theta}$, ξ_{zz}, ξ_{rz}, $\xi_{z\theta}$ and $\xi_{r\theta}$ be the components of the strain rate tensor in the cylindrical coordinate system. The components ξ_{zz}, ξ_{rz} and $\xi_{z\theta}$ vanish. Equation (9) become

$$\xi_{rr} + \xi_{\theta\theta} = 0, \quad \frac{\xi_{r\theta}}{\xi_{rr} - \xi_{\theta\theta}} = \frac{\sigma_{r\theta}}{\sigma_{rr} - \sigma_{\theta\theta}}. \tag{39}$$

Equation (13) is valid but ψ is to be understood as the angle between the major principal stress σ_1 and the r-axis, measured from the axis anti-clockwise (Fig. 4). Thus the orientation of the characteristic directions relative to the r-axis is

$$\phi_1 = \psi - \frac{\pi}{4}, \quad \phi_2 = \psi + \frac{\pi}{4}. \tag{40}$$

The non-zero components of the strain rate tensor are

$$\xi_{rr} = \frac{\partial u_r}{\partial r}, \quad \xi_{\theta\theta} = \frac{1}{r}\left(\frac{\partial u_\theta}{\partial \theta} + u_r\right), \quad \xi_{r\theta} = \frac{1}{2}\left(\frac{\partial u_\theta}{\partial r} - \frac{u_\theta}{r} + \frac{1}{r}\frac{\partial u_r}{\partial \theta}\right), \tag{41}$$

where u_r and u_θ are the radial and circumferential velocities, respectively. The equilibrium equations are

$$\frac{\partial \sigma_{rr}}{\partial r} + \frac{1}{r}\frac{\partial \sigma_{r\theta}}{\partial r} + \frac{\sigma_{rr} - \sigma_{\theta\theta}}{r} = 0, \quad \frac{\partial \sigma_{r\theta}}{\partial r} + \frac{1}{r}\frac{\partial \sigma_{\theta\theta}}{\partial \theta} + \frac{2\sigma_{r\theta}}{r} = 0. \tag{42}$$

The transformation equations for stress components in $r\theta$-planes are (Fig. 4)

$$\sigma_{rr} = \frac{\sigma_1 + \sigma_2}{2} + \tau_s \cos 2\psi, \ \sigma_{\theta\theta} = \frac{\sigma_1 + \sigma_2}{2} - \tau_s \cos 2\psi, \ \sigma_{r\theta} = \tau_s \sin 2\psi. \tag{43}$$

Here Eq. (37) has been taken into account.

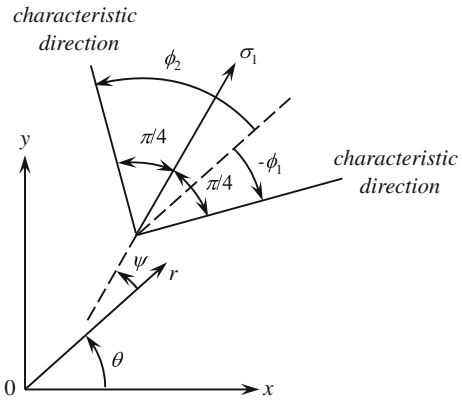

Fig. 4 Orientation of the major principal stress and characteristic directions relative to the r-axis

3.2 Compression of a Plastic Layer Between Parallel Plates

Consider compression of a wide plastic layer between two parallel plates. An approximate solution of this problem, known as Prandtl's problem, can be found in any monograph on plasticity theory (see, for example, [11]). The thickness of the layer is $2H$ and its width is $2L$. By assumption, $H/L \ll 1$. It is possible to choose the Cartesian coordinate system such that its axes x and y coincide with the axes of symmetry of the layer (Fig. 5). Therefore, it is sufficient to find the solution in the domain $0 \le x \le L$ and $0 \le y \le H$. The maximum friction law is valid at $y = H$. The velocity boundary conditions are

$$u_y = 0 \tag{44}$$

at $y = 0$,

$$u_y = -V \tag{45}$$

at $y = H$ and

$$u_x = 0 \tag{46}$$

at $x = 0$. Here V is the speed of the plate. The stress boundary conditions, in addition to the friction law, are

$$\sigma_{xy} = 0 \tag{47}$$

at $y = 0$, $x = 0$ and $x = L$ and

$$\sigma_{xx} = 0 \tag{48}$$

at $x = L$. The solution given in [11] ignores the boundary condition (47) at $x = 0$ and $x = L$. The boundary conditions (46) and (48) are replaced with the following integral conditions

$$\int_0^H u_x|_{x=0} dy = 0 \tag{49}$$

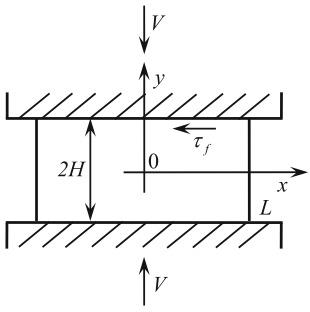

Fig. 5 Illustration of the boundary value problem

and

$$\int_0^H \sigma_{xx}|_{x=L} dy = 0, \tag{50}$$

respectively. Under the assumptions formulated, the velocity field satisfying Eq. (9) as well as the boundary conditions (44) and (45) is given by [11]

$$u_x = V\frac{x}{H} + 2V\left[1 - \left(\frac{y}{H}\right)^2\right]^{1/2} + U, \quad u_y = -V\frac{y}{H}, \tag{51}$$

where U is a constant of integration. Its value can be determined from the boundary condition (49). However, it has no effect on the strain rate intensity factor and, therefore, is not found here. It has been shown in [11] that the stress field used to determine the value of the right hand side of $(9)_2$ satisfies Eqs. (7) and (12) as well as the boundary conditions (1) at $y = H$, (47) at $y = 0$ and (50). Using (10) the components of the strain rate tensor are determined from (51). Then, the equivalent strain rate is found from (4) as

$$\xi_{\text{eq}} = \frac{2}{\sqrt{3}}\frac{V}{\sqrt{H^2 - y^2}}. \tag{52}$$

In the case under consideration $s = H - y$. Therefore, Eq. (52) can be represented in the form

$$\xi_{\text{eq}} = \sqrt{\frac{2}{3}}\frac{V}{\sqrt{s}\sqrt{H}} + o\left(\frac{1}{\sqrt{s}}\right) \quad \text{as} \quad s \to 0. \tag{53}$$

Comparing (5) and (53) gives

$$D = \sqrt{\frac{2}{3}}\frac{V}{\sqrt{H}}. \tag{54}$$

3.3 *Flow of Plastic Material Through an Infinite Wedge-Shaped Channel*

This is also one of the classical problems of plasticity. Its solution used in this section has been given in [11]. The process is illustrated in Fig. 6. Material flows to the line of intersection of two plates. The plates are inclined to each other at an angle 2α. The axis $\theta = 0$ of the cylindrical coordinate system coincides with the axis of symmetry of the flow. Therefore, it is sufficient to find the solution in the domain $0 \le \theta \le \alpha$. The maximum friction law is supposed at $\theta = \alpha$. The velocity boundary conditions are

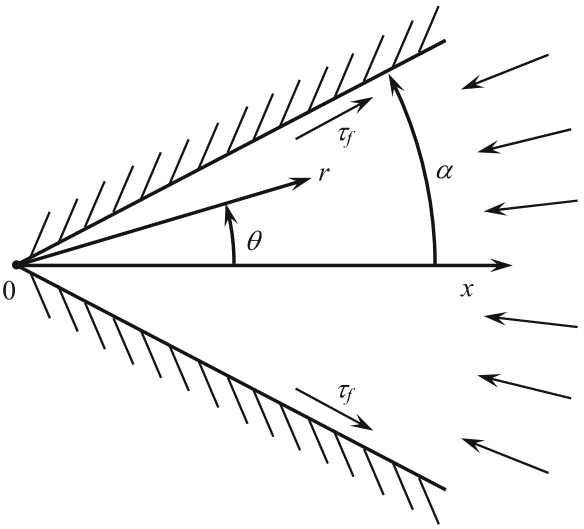

Fig. 6 Illustration of the boundary value problem

$$u_\theta = 0 \tag{55}$$

at $\theta = 0$ and $\theta = \alpha$. The stress boundary condition, in addition to the friction law, is

$$\sigma_{r\theta} = 0 \tag{56}$$

at $\theta = 0$. The velocity field satisfying Eq. (39) as well as the boundary conditions (55) are

$$u_r = -\frac{B}{r\,(c - 2\cos 2\psi)}, \quad u_\theta = 0, \tag{57}$$

where B is proportional to the material flux, c can be determined numerically using the maximum friction law and the boundary condition (56), and ψ is related to θ by the following equation

$$\cos 2\psi \left(\frac{d\psi}{d\theta} + 1\right) = \frac{c}{2} \tag{58}$$

whose solution is

$$\theta = -\psi + c \arctan\left[\left(\frac{c+2}{c-2}\right)^{1/2} \tan\psi\right]\left(c^2 - 4\right)^{-1/2}. \tag{59}$$

It has been shown in [11] that the stress field used to determine the value of the right hand side of $(39)_2$ satisfies Eqs. (38) and (42).

The maximum friction surface is determined by the equation $\theta = \alpha$. Therefore, $\phi_1 = 0$ or $\phi_2 = 0$ in (40). In order to choose between these two options, it is necessary to take into account that $\sigma_{r\theta} > 0$ at $\theta = \alpha$ (Fig. 6). Then, it is evident from (43) that $0 < \psi < \pi/2$ at $\theta = \alpha$. The equation $\phi_2 = 0$ contradicts this inequality. Therefore, $\phi_1 = 0$ and $\psi = \pi/4$ at $\theta = \alpha$. The equation for c is obtained from (59) at $\theta = \alpha$ and $\psi = \pi/4$. The resulting equation has been solved numerically and its solution is illustrated in Fig. 7. Using (41) the components of the strain rate tensor are determined from (57). Then, the equivalent strain rate is found from (4) as

$$\xi_{\text{eq}} = \frac{2}{\sqrt{3}} \frac{B}{r^2 (c - 2\cos 2\psi) \cos 2\psi}. \tag{60}$$

Expanding the right hand side of this expression in a series near $\psi = \pi/4$ and using (59) give

$$\xi_{\text{eq}} = \frac{\sqrt{2}B}{\sqrt{3} r^2 c \sqrt{c}\, (\alpha - \theta)^{1/2}} + o\left[(\alpha - \theta)^{-1/2}\right] \quad \text{as} \quad \theta \to \alpha. \tag{61}$$

Comparing (5) and (61) it is possible to conclude that the strain rate intensity factor is

$$D = \sqrt{\frac{2}{3}} \frac{B}{(rc)^{3/2}}. \tag{62}$$

Let Q be the material flux per unit length. Then,

$$Q = -2 \int_0^{\alpha} u_r r d\theta. \tag{63}$$

Substituting (57) into (63) and replacing integration with respect to θ with integration with respect to ψ by means of (58) result in

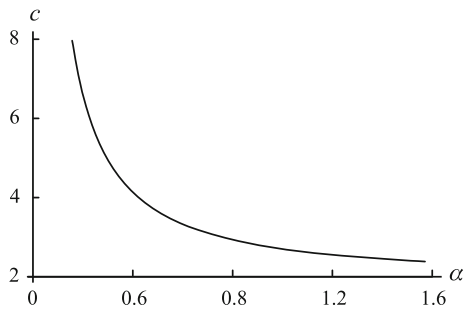

Fig. 7 Variation of c with α

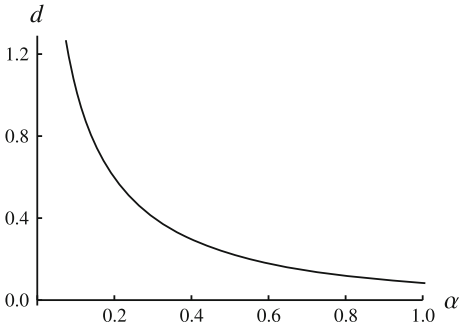

Fig. 8 Variation of the dimensionless strain rate intensity factor with α

$$B = \frac{Q}{4}\left[\int_0^{\pi/4} \frac{\cos 2\psi}{(c - 2\cos 2\psi)^2} d\psi\right]^{-1}. \tag{64}$$

Eliminating B in (62) by means of (64) shows that the strain rate intensity factor is a linear function of Q. In order to reveal the effect of α on the strain rate intensity factor, it is convenient to introduce its dimensionless representation by

$$d = \frac{Dr^{3/2}}{Q}. \tag{65}$$

It follows from (62), (64) and (65) that

$$d = \frac{1}{2\sqrt{6}c^{3/2}}\left[\int_0^{\pi/4} \frac{\cos 2\psi}{(c - 2\cos 2\psi)^2} d\psi\right]^{-1}. \tag{66}$$

Since the dependence of c on α has been found (Fig. 7), the variation of d with α is immediately determined from (66). This dependence is illustrated in Fig. 8.

3.4 Compression of a Plastic Layer Between Cylindrical Surfaces

The boundary value problem is illustrated in Fig. 9. Its solution has been given in [28]. The outer surface of radius R_2 is rigid and motionless whereas the inner surface of current radius R_1 expands. The rate of this expansion is $\dot{R}_1$. The solution is restricted to instantaneous flow. It is natural to use the cylindrical coordinate system shown in Fig. 9. The flow is symmetric with respect to the axis $\theta = 0$. It is therefore sufficient to obtain the solution in the region $0 \le \theta \le \theta_0$ where θ_0 is the orientation of the edge of the layer. The velocity boundary conditions are

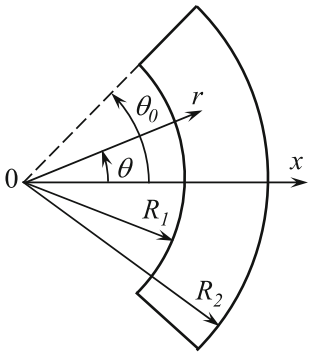

Fig. 9 Illustration of the boundary value problem

$$u_r = 0 \quad \text{at} \quad r = R_2, \tag{67}$$

$$u_r = \dot{R}_1 \quad \text{at} \quad r = R_1 \tag{68}$$

and

$$u_\theta = 0 \quad \text{at} \quad \theta = 0. \tag{69}$$

The stress boundary conditions, in addition to the maximum friction law, are

$$\sigma_{r\theta} = 0 \quad \text{at} \quad \theta = 0 \quad \text{and} \quad \theta = \theta_0, \tag{70}$$

and

$$\sigma_{\theta\theta} = 0 \quad \text{at} \quad \theta = \theta_0. \tag{71}$$

It is evident that the problem under consideration can be viewed as a generalization of the Prandtl's problem (Sect. 3.2). Therefore, the same assumptions are made. In particular, end effects are neglected such that the solution is not valid in the vicinity of $\theta = 0$ and $\theta = \theta_0$. Accordingly, the boundary conditions (70) are ignored, and the boundary conditions (69) and (71) should be replaced with integral conditions. On the other hand, the boundary conditions at $r = R_1$ and $r = R_2$ are exactly satisfied. These boundary conditions include (67), (68) and the maximum friction law at $r = R_1$ and $r = R_2$. Since the maximum friction law acts on both contact surfaces, two strain rate intensity factors are obtained. The velocity field satisfying Eqs. (39) as well as the boundary conditions (67) and (68) are [28]

$$\frac{u_r}{\dot{R}_1} = U_r(r), \quad \frac{u_\theta}{\dot{R}_1} = -\left(r\frac{dU_r}{dr} + U_r\right)\theta + U_\theta(r), \tag{72}$$

where $U_r(r)$ and $U_\theta(r)$ are functions of r given by

$$U_r = \frac{R_1\left(r^2 - R_2^2\right)}{r\left(R_1^2 - R_2^2\right)},$$

$$U_\theta = \frac{\sqrt{2}R_2}{\left[R_2^2 + R_1^2 + \left(R_2^2 - R_1^2\right)\sin 2\psi\right]^{1/2}} \times \\ \times \left\{ u_0 + \int_{\pi/4}^{\psi} \frac{\left[R_2^2 + 3R_1^2 + \left(R_2^2 - R_1^2\right)\sin 2\gamma\right]\sin 2\gamma}{\left[R_2^2 + R_1^2 + \left(R_2^2 - R_1^2\right)\sin 2\gamma\right]} d\gamma \right\},$$

where γ is a dummy variable of integration and ψ is related to r by the following equation

$$\sin 2\psi = \frac{2R_1^2 R_2^2}{\left(R_2^2 - R_1^2\right)r^2} - \frac{\left(R_2^2 + R_1^2\right)}{\left(R_2^2 - R_1^2\right)}. \tag{73}$$

It has been shown in [28] that the stress field used to determine the value of the right hand side of $(39)_2$ satisfies Eqs. (38) and (42) as well as the boundary condition (1) at $r = R_1$ and $r = R_2$. Using (41) the components of the strain rate tensor are determined from (72) and (73) as

$$\xi_{rr} = -\xi_{\theta\theta} = \frac{\dot{R}_1 R_1\left(r^2 + R_2^2\right)}{\left(R_1^2 - R_2^2\right)r^2}, \quad \xi_{r\theta} = \frac{\dot{R}_1 R_1\left(R_2^2 + r^2\right)}{\left(R_1^2 - R_2^2\right)r^2}\tan 2\psi.$$

Then, the equivalent strain rate is found from (4) as

$$\xi_{\text{eq}} = \frac{2\dot{R}_1 R_1\left(R_2^2 + r^2\right)}{\sqrt{3}\left(R_2^2 - R_1^2\right)r^2\cos 2\psi}. \tag{74}$$

It has been assumed here that $-\pi/4 \le \psi \le \pi/4$. It follows from (73) that $\psi = \pi/4$ at $r = R_1$ and $\psi = -\pi/4$ at $r = R_2$. Eliminating in (74) the value of r by means of (73) and expanding the right hand side of (74) in a series in the vicinity of $\psi = \pi/4$ (or $r = R_1$) and $\psi = -\pi/4$ (or $r = R_2$) gives

$$\begin{aligned} \xi_{\text{eq}} &= \frac{\dot{R}_1\left(R_2^2 + R_1^2\right)}{\sqrt{3}R_1\left(R_2^2 - R_1^2\right)(\pi/4 - \psi)} + o\left[\left(\frac{\pi}{4} - \psi\right)^{-1}\right] \quad \text{as} \quad \psi \to \frac{\pi}{4} \\ \xi_{\text{eq}} &= \frac{2\dot{R}_1 R_1}{\sqrt{3}\left(R_2^2 - R_1^2\right)(\psi + \pi/4)} + o\left[\left(\psi + \frac{\pi}{4}\right)^{-1}\right] \quad \text{as} \quad \psi \to -\frac{\pi}{4}. \end{aligned} \tag{75}$$

On the other hand, Eq. (73) in the vicinity of the maximum friction surfaces is represented in the form

$$\begin{aligned}\frac{\pi}{4}-\psi &= \frac{\sqrt{2}R_2\sqrt{r-R_1}}{\sqrt{R_1\left(R_2^2-R_1^2\right)}}+o\left(\sqrt{r-R_1}\right) \quad \text{as} \quad r\to R_1,\\ \frac{\pi}{4}+\psi &= \frac{\sqrt{2}R_1\sqrt{R_2-r}}{\sqrt{R_2\left(R_2^2-R_1^2\right)}}+o\left(\sqrt{R_2-r}\right) \quad \text{as} \quad r\to R_2.\end{aligned} \tag{76}$$

Substituting (76) into (75) leads to

$$\begin{aligned}\xi_{\text{eq}} &= \frac{\dot{R}_1\left(R_2^2+R_1^2\right)}{\sqrt{6}R_2\sqrt{R_1\left(R_2^2-R_1^2\right)}\sqrt{r-R_1}}+o\left(\frac{1}{\sqrt{r-R_1}}\right), \quad \text{as} \quad r\to R_1\\ \xi_{\text{eq}} &= \sqrt{\frac{2}{3}}\frac{\dot{R}_1\sqrt{R_2}}{\sqrt{R_2^2-R_1^2}\sqrt{R_2-r}}+o\left[\frac{1}{\sqrt{R_2-r}}\right] \quad \text{as} \quad r\to R_2.\end{aligned} \tag{77}$$

Comparing (5) and (77) it is possible to find that the strain rate intensity factors are

$$D_1=\frac{\dot{R}_1\left(1+R_1^2/R_2^2\right)}{\sqrt{6}\sqrt{R_1}\sqrt{1-R_1^2/R_2^2}}, \qquad D_2=\frac{2\dot{R}_1}{\sqrt{6}\sqrt{R_2}\sqrt{1-R_1^2/R_2^2}}. \tag{78}$$

Here D_1 corresponds to the maximum friction surface $r=R_1$ and D_2 to the maximum friction surface $r=R_2$. It is convenient to represent the final result in the form of the ratio D_1/D_2 because it is non-dimensional. It follows from (78) that

$$\Delta=\frac{D_1}{D_2}=\frac{1+R_1^2/R_2^2}{2\left(R_1/R_2\right)^{1/2}}.$$

The variation of Δ with R_1/R_2 is depicted in Fig. 10. It is seen from this figure that $\Delta>1$ in the region $R_1/R_2<r_{\text{cr}}$ and $\Delta<1$ in the region $R_1/R_2>r_{\text{cr}}$ where $r_{\text{cr}}\approx 0.3$. Using the hypothesis that the strain rate intensity factor controls the formation of the layer of intensive plastic deformation in the vicinity of friction

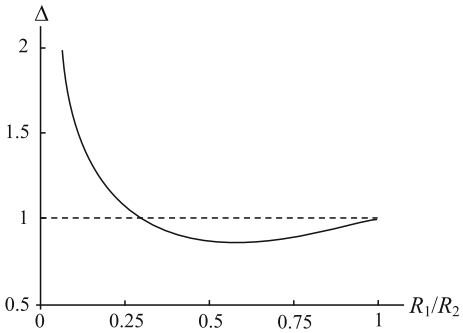

Fig. 10 Variation of Δ with the ratio of the radii

surfaces [8], it is possible to conclude from these inequalities that the thickness of this layer is larger near the friction surface $r = R_1$ if $R_1/R_2 < r_{\rm cr}$, and it is larger near the friction surface $r = R_2$ if $R_1/R_2 > r_{\rm cr}$.

3.5 Compression of a Plastic Layer Between Rotating Plates I

The boundary value problem is illustrated in Fig. 11. Two semi-infinite rough plates hinged together at their ends and inclined to each other at an angle 2α rotate towards each other with angular velocity of magnitude ω about an axis O through the hinge. The cylindrical coordinate system is taken with $\theta = 0$ taken as the perpendicular bisector of the angle 2α. Since $\theta = 0$ is an axis of symmetry for the flow, it is sufficient to find the solution in the region $\theta \geq 0$. By definition, ω is taken to be positive for the clockwise rotation of the upper plate. The maximum friction law is assumed at $\theta = \alpha$. The solution of this problem has been proposed in [29]. In fact, that solution was given for tension of the layer and, moreover, a velocity discontinuity surface appeared instead of the maximum friction surface in the problem under consideration. However, since the model is pressure-independent, these distinctions have no effect on the velocity field other than the sense of the velocity components. Qualitative behavior of the solution depends on the value of α. In particular, the solution exhibits sticking at the plates together with a rigid zone in the region adjacent to the plates for $\alpha > \pi/4$. In this case the velocity field is not singular and, therefore, the solution is not of interest for the purpose of the present chapter. The sliding regime of friction accompanied by a singular velocity field occurs for $\alpha < \pi/4$. The special case $\alpha = \pi/4$ will be treated separately.

The velocity boundary conditions are

$$u_\theta = 0 \quad \text{at} \quad \theta = 0 \tag{79}$$

and

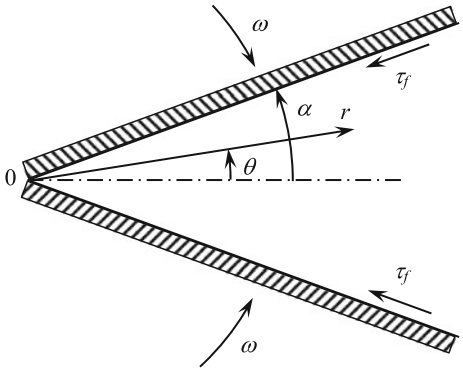

Fig. 11 Illustration of the boundary value problem

$$u_\theta = -\omega r \quad \text{at} \quad \theta = \alpha. \tag{80}$$

It is also assumed that there is no material flux through O. The stress boundary condition, in addition to the maximum friction law, is

$$\sigma_{r\theta} = 0 \quad \text{at} \quad \theta = 0. \tag{81}$$

The velocity field found in [29] is

$$u_r = -\frac{\omega r}{2}\left(c - 2\cos 2\psi\right), \quad u_\theta = \omega r \sin 2\psi, \tag{82}$$

where c is constant and ψ is related to θ by the following equation

$$\frac{d\psi}{d\theta} = \frac{(c - 2\cos 2\psi)}{2\cos 2\psi}. \tag{83}$$

The constraints imposed on the flow demand $u_r > 0$ and $\sigma_{rr} \geq \sigma_{\theta\theta}$. A consequence of the former inequality is $\sigma_{r\theta} < 0$ at $\theta = \alpha$. It follows from this inequality, the inequality $\sigma_{rr} \geq \sigma_{\theta\theta}$ and Eq. (43) that

$$-\frac{\pi}{4} \leq \psi \leq 0. \tag{84}$$

Since the friction surface is determined by the equation $\theta = \alpha$, the maximum friction law demands $\phi_1 = 0$ or $\phi_2 = 0$ in (40). Using (84) it is possible to conclude that $\phi_2 = 0$ and, therefore, $\psi = -\pi/4$ for $\theta = \alpha$. The solution of Eq. (83) satisfying this condition is

$$\theta = \alpha + 2\int_{-\pi/4}^{\psi} \frac{\cos 2\gamma d\gamma}{(c - 2\cos 2\gamma)}, \tag{85}$$

where γ is a dummy variable of integration. Substituting the condition $\psi = -\pi/4$ at $\theta = \alpha$ into (82) also shows that the boundary condition (80) is satisfied. It follows from (43), (81) and (84) that $\psi = 0$ at $\theta = 0$. Therefore, the equation for c is obtained from (85) in the form

$$\alpha = -2\int_{-\pi/4}^{0} \frac{\cos 2\gamma d\gamma}{(c - 2\cos 2\gamma)}. \tag{86}$$

Substituting the condition $\psi = 0$ at $\theta = 0$ into (82) also shows that the boundary condition (79) is satisfied. The variation of c with α found from (86) is depicted in Fig. 12. Expanding the right hand site of (83) in a series in the vicinity of $\psi = -\pi/4$ gives

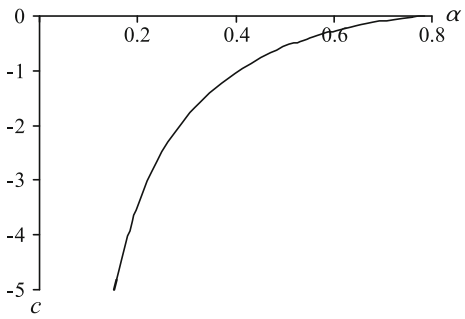

Fig. 12 Variation of c with α

$$\left[\frac{4}{c}\left(\psi+\frac{\pi}{4}\right)+o\left(\psi+\frac{\pi}{4}\right)\right]d\psi=d\theta \quad \text{as} \quad \psi\to-\frac{\pi}{4}.$$

Integrating with the use of the boundary condition $\psi=-\pi/4$ for $\theta=\alpha$ results in

$$\psi+\frac{\pi}{4}=\frac{\sqrt{-c\,(\alpha-\theta)}}{\sqrt{2}}+o\left(\sqrt{\alpha-\theta}\right) \quad \text{as} \quad \theta\to\alpha. \tag{87}$$

It is worthy to note here that $c\le 0$ (Fig. 12). The strain rate components are found from (41), (82) and (83) as

$$\xi_{rr}=-\xi_{\theta\theta}=-\frac{\omega}{2}\left(c-2\cos 2\psi\right), \quad \xi_{r\theta}=\frac{\omega}{2}\tan 2\psi\left(c-2\cos 2\psi\right).$$

Then, it follows from (4) that

$$\xi_{\text{eq}}=\frac{\omega}{\sqrt{3}}\frac{(2\cos 2\psi-c)}{\cos 2\psi}. \tag{88}$$

It has been taken into account there that $c\le 0$ (Fig. 12) and $\cos 2\psi\ge 0$ according to (84). Using (87), Eq. (88) in the vicinity of the maximum friction surface is represented as

$$\xi_{\text{eq}}=\frac{\omega\sqrt{-c}}{\sqrt{6}\sqrt{\alpha-\theta}}+o\left[\frac{1}{\sqrt{\alpha-\theta}}\right] \quad \text{as} \quad \theta\to\alpha. \tag{89}$$

Comparing (5) and (89) leads to the strain rate intensity factor in the form

$$D=\omega\sqrt{\frac{-cr}{6}}. \tag{90}$$

It follows from the solution that c vanishes at $\alpha=\pi/4$. Then, it is evident from (90) that the strain rate intensity factor vanishes at $\alpha=\pi/4$. Therefore, the solution

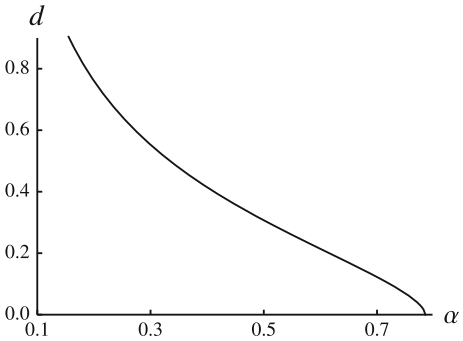

Fig. 13 Variation of the dimensionless strain rate intensity factor with α

is singular for $0 < \alpha < \pi/4$ and is not singular at $\alpha = \pi/4$. The variation of the dimensionless strain rate intensity factor defined by $d = D/\left(\omega\sqrt{r}\right)$ with α is illustrated in Fig. 13.

3.6 Compression of a Plastic Layer Between Rotating Plates II

The statement of the boundary value problem solved in the previous section is now slightly modified assuming that $u_r < 0$. This change in the direction of the radial velocity leads to the corresponding change in the direction of the friction stress (Fig. 14). The boundary conditions (79), (80) and (81) are valid. The maximum friction law is supposed at $\theta = \alpha$. As before, it is sufficient to find the solution in the region $\theta \geq 0$. The stress boundary conditions coincide with those in Sect. 3.3. Since ψ is solely determined from the stress equations, Eq. (58) is valid in the case under consideration. The velocity field is sought in the form

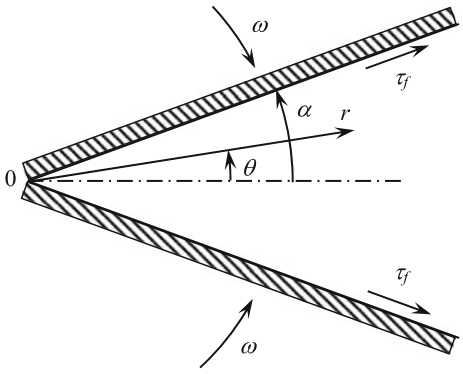

Fig. 14 Illustration of the boundary value problem

$$u_r = \frac{\omega r}{2}\frac{dg\,(\psi)}{d\theta} + \omega\frac{G\,(\psi)}{r}, \quad u_\theta = -\omega r g\,(\psi)\,, \tag{91}$$

where $g\,(\psi)$ and $G\,(\psi)$ are arbitrary functions of ψ. It is possible to verify by inspection that the velocity field (91) automatically satisfies the incompressibility Eq. $(39)_1$. The inequality $u_r < 0$ demands $\sigma_{r\theta} > 0$ at $\theta = \alpha$. Therefore, it follows from (43) that $\pi/2 \geq \psi \geq 0$. The constraints imposed on the flow demand $\sigma_{rr} > \sigma_{\theta\theta}$. A consequence of this inequality and (43) is $\pi/4 \geq \psi \geq -\pi/4$. Finally,

$$\frac{\pi}{4} \geq \psi \geq 0. \tag{92}$$

Since the friction surface is determined by the equation $\theta = \alpha$, the maximum friction law demands $\phi_1 = 0$ or $\phi_2 = 0$ in (40). Using (92) it is possible to conclude that $\phi_1 = 0$ and, therefore, $\psi = \pi/4$ for $\theta = \alpha$. The same boundary condition was used in Sect. 3.3. Therefore, the solution (59) of Eq. (58) is valid in the case under consideration. The variation of c with α is depicted in Fig. 7.

Substituting (91) into (41) yields

$$\xi_{rr} = -\xi_{\theta\theta} = \frac{\omega}{2}\frac{dg}{d\psi}\frac{d\psi}{d\theta} - \frac{\omega G}{r^2},$$
$$\xi_{r\theta} = \frac{\omega}{4}\frac{d^2g}{d\theta^2} + \frac{\omega}{2r^2}\frac{dG}{d\psi}\frac{d\psi}{d\theta} = \frac{\omega}{4}\left[\frac{d^2g}{d\psi^2}\left(\frac{d\psi}{d\theta}\right)^2 + \frac{dg}{d\psi}\frac{d^2\psi}{d\theta^2}\right] + \frac{\omega}{2r^2}\frac{dG}{d\psi}\frac{d\psi}{d\theta}.$$

Eliminating here $d\psi/d\theta$ and $d^2\psi/d\theta^2$ by means of (58) gives

$$\begin{aligned}
\xi_{rr} &= -\xi_{\theta\theta} = \frac{\omega}{4}\frac{(c - 2\cos 2\psi)}{\cos 2\psi}\frac{dg}{d\psi} - \frac{\omega G}{r^2},\\
\xi_{r\theta} &= \frac{\omega\,(c - 2\cos 2\psi)}{16\cos^2 2\psi}\left[(c - 2\cos 2\psi)\,\frac{d^2g}{d\psi^2} + 2c\tan 2\psi\frac{dg}{d\psi}\right]\\
&\quad + \frac{\omega}{4r^2}\frac{(c - 2\cos 2\psi)}{\cos 2\psi}\frac{dG}{d\psi}.
\end{aligned} \tag{93}$$

Substituting (93) into $(39)_2$ and eliminating stress components by means of (43) result in

$$\frac{(c - 2\cos 2\psi)^2}{16\cos^2 2\psi}\left(\frac{d^2g}{d\psi^2} + 2\tan 2\psi\frac{dg}{d\psi}\right) + \left[\frac{(c - 2\cos 2\psi)}{4\cos 2\psi}\frac{dG}{d\psi} + G\tan 2\psi\right]\frac{1}{r^2} = 0.$$

This equation may have a solution if and only if

$$\cos 2\psi\frac{d^2g}{d\psi^2} + 2\sin 2\psi\frac{dg}{d\psi} = 0, \quad (c - 2\cos 2\psi)\,\frac{dG}{d\psi} + 4G\sin 2\psi = 0. \tag{94}$$

Using (91) and taking into account that $\psi = 0$ at $\theta = 0$ and $\psi = \pi/4$ at $\theta = \alpha$ the boundary conditions (79) and (80) are transformed to

$$g = 0 \tag{95}$$

at $\psi = 0$ and

$$g = 1 \tag{96}$$

at $\psi = \pi/4$, respectively. The solution to $(94)_1$ satisfying these boundary conditions is

$$g = \sin 2\psi. \tag{97}$$

The general solution to $(94)_2$ is

$$G = \frac{G_0}{c - 2\cos 2\psi}, \tag{98}$$

where G_0 is a constant of integration. In order to find its value, a boundary condition in integral form similar to (49) should be prescribed. For example,

$$\int_0^\alpha u_r|_{r=R}\, d\theta = 0, \tag{99}$$

where the value of R should be prescribed. Using (91) and taking into account (95) and (96) the condition (99) is written in the form

$$1 + \frac{2}{R^2}\int_0^\alpha G d\theta = 0.$$

Replacing here integration with respect to θ with integration with respect to ψ by means of (58) and using (98) yields

$$G_0 = -\frac{R^2}{4}\left[\int_0^{\pi/4} \frac{\cos 2\psi}{(c - 2\cos 2\psi)^2} d\psi\right]^{-1}. \tag{100}$$

It follows from (93), (97) and (98) that

$$\begin{aligned} \xi_{rr} = -\xi_{\theta\theta} &= \frac{\omega}{2}(c - 2\cos 2\psi) - \frac{\omega G_0}{r^2 (c - 2\cos 2\psi)}, \\ \xi_{r\theta} &= \frac{\omega}{2\cos 2\psi}\left[(c - 2\cos 2\psi)\sin 2\psi - \frac{2G_0}{r^2}\frac{\sin 2\psi}{(c - 2\cos 2\psi)}\right]. \end{aligned} \tag{101}$$

It is evident that the normal strain rates are bounded and $|\xi_{r\theta}| \to \infty$ as $\psi \to \pi/4$. Therefore, Eq. (6) in which ξ_τ is replaced with $\xi_{r\theta}$ is valid. Using (101) the shear strain rate in the vicinity of the friction surface is represented as

$$\xi_{r\theta} = \frac{\omega c}{4\,(\pi/4 - \psi)} \left[1 - \frac{2G_0}{r^2 c^2}\right] + o\left(\frac{1}{\pi/4 - \psi}\right) \quad \text{as} \quad \psi \to \frac{\pi}{4}. \tag{102}$$

Equation (58) transforms to

$$\frac{d\theta}{d\psi} = \frac{4}{c}\left(\frac{\pi}{4} - \psi\right) + o\left(\frac{\pi}{4} - \psi\right) \quad \text{as} \quad \psi \to \frac{\pi}{4}.$$

Integrating with the boundary condition $\theta = \alpha$ at $\psi = \pi/4$ gives

$$\alpha - \theta = \frac{2}{c}\left(\frac{\pi}{4} - \psi\right)^2 + o\left[\left(\frac{\pi}{4} - \psi\right)^2\right] \quad \text{as} \quad \psi \to \frac{\pi}{4}. \tag{103}$$

Replacing $\pi/4 - \psi$ in (102) with $\alpha - \theta$ by means of (103) results in

$$\xi_{r\theta} = \frac{\omega\sqrt{2c}}{4\sqrt{\alpha - \theta}}\left(1 - \frac{2G_0}{r^2 c^2}\right) + o\left(\frac{1}{\sqrt{\alpha - \theta}}\right) \quad \text{as} \quad \theta \to \alpha. \tag{104}$$

It is seen from Fig. 7 that $c > 2$ and from Eq. (100) that $G_0 < 0$. Therefore, $\xi_{r\theta} > 0$. Then, combining (6) and (104) gives

$$D = \frac{\omega\sqrt{c}\sqrt{r}}{\sqrt{6}}\left(1 - \frac{2G_0}{r^2 c^2}\right). \tag{105}$$

Since the dependence of c on α is known (Fig. 7), it follows from (100) that the dimensionless strain rate intensity factor defined by $d = D/\left(\omega\sqrt{r}\right)$ depends on α and the ratio r/R. Its variation with r/R at several values of α is depicted in Fig. 15 (curve 1 corresponds to $\alpha = \pi/36$, curve 2 to $\alpha = \pi/18$, curve 3 to $\alpha = \pi/12$, curve 4 to $\alpha = \pi/9$, and curve 5 to $\alpha = \pi/6$). In the solution for compression of a plastic layer between parallel plates (see Sect. 3.2) a rigid zone appears at the center of the layer [11]. The length of this zone at the friction surface is of order of the thickness of the layer. By analogy to this solution it is reasonable to assume that there is a rigid zone near the cross-section $r = R$ and that its length at the friction surface is equal to $R\alpha$. The solution found is not valid in the rigid zone. Therefore, the right ends of the curves in Fig. 15 are determined by the equation $r/R = 1 - \alpha$. The dependence of d on α at several values of r/R is illustrated in Fig. 16 (curve 1 corresponds to $r/R = 0.4$, curve 2 to $r/R = 0.3$, curve 3 to $r/R = 0.25$, and curve 4 to $r/R = 0.2$).

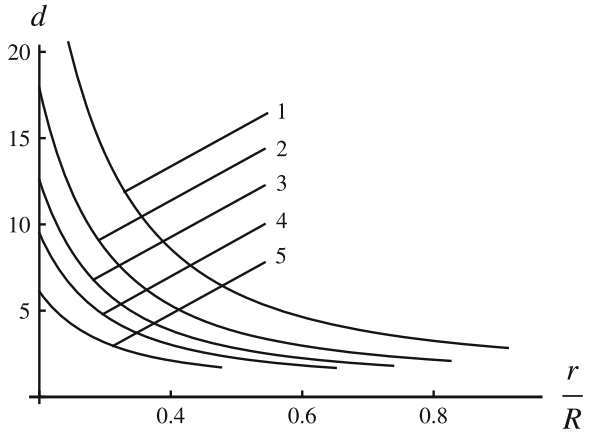

Fig. 15 Variation of the dimensionless strain rate intensity factor with r/R at several α- values

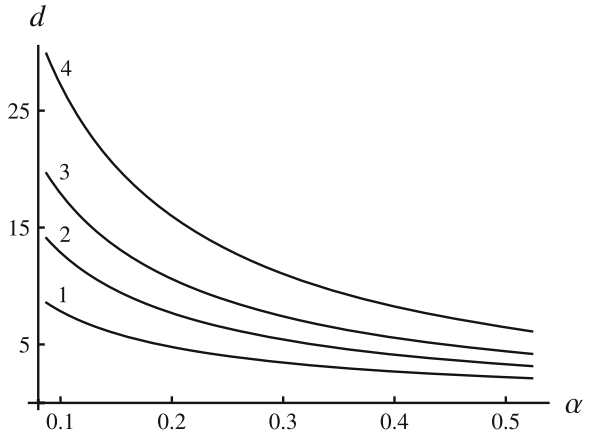

Fig. 16 Variation of the dimensionless strain rate intensity factor with α at several r/R- values

3.7 Simultaneous Shearing and Expansion of a Hollow Cylinder

The boundary value problem considered in this section consists of a planar deformation comprising the simultaneous shearing and expansion of a hollow cylinder (Fig. 17). The internal and external radii of the cylinder are denoted by a and b, respectively. It is convenient to use the cylindrical coordinates whose z-axis coincides the axis of the cylinder. In this coordinate system, the internal surface of the cylinder is determined by the equation $r = a$ and the external surface by the equation $r = b$. The deformation of the cylinder is caused by an expanding and rotating rod inserted into its hole. The radius of the rod is a and the rate of its expansion is $\dot{a}$. The angular velocity of the rod is ω and its direction is shown in Fig. 17. The external

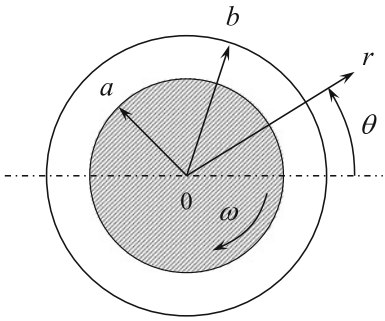

Fig. 17 Illustration of the boundary value problem

radius of the cylinder is fixed against rotation. Therefore, the velocity boundary conditions are

$$u_r = \dot{a} \tag{106}$$

for $r = a$ and

$$u_\theta = 0 \tag{107}$$

for $r = b$. One of the stress boundary conditions is $\sigma_{rr} = -p_a < 0$ for $r = a$. p_a is given, but its value has no effect of the strain rate intensity factor. The final boundary condition is the maximum friction law at $r = a$. In general, two different regimes may be identified at this boundary, sticking and sliding. However, the velocity field is singular if and only if the regime of sliding occurs. Therefore, the solution considered in this section is restricted to this regime. The general solution is provided in [30]. The direction of ω requires $\sigma_{r\theta} > 0$. On the other hand, it is evident that $\sigma_{rr} < \sigma_{\theta\theta}$. Therefore, it follows from (43) that

$$\frac{\pi}{4} \le \psi < \frac{\pi}{2}. \tag{108}$$

The maximum friction surface is orthogonal to the r-axis. Therefore, the maximum friction law demands $\phi_1 = \pi/2$ or $\phi_2 = \pi/2$ at $r = a$. Comparing (40) and (108) gives

$$\psi = \frac{\pi}{4} \tag{109}$$

for $r = a$.

The solution satisfying Eqs. (38), (39) and (42) as well as the boundary conditions formulated has been given in [30]. The regime of sliding when (109) is valid requires

$$\omega a > \dot{a}\sqrt{1 - \frac{a^4}{b^4}}.$$

The velocity field in the case of sliding is

$$u_r = \frac{\dot{a}a}{r}, \quad u_\theta = -\frac{\dot{a}r}{a}\left(\sqrt{1-\frac{a^4}{b^4}} - \sqrt{1-\frac{a^4}{r^4}}\right). \tag{110}$$

Substituting (110) into (41) leads to

$$\xi_{rr} = -\xi_{\theta\theta} = -\frac{\dot{a}a}{r^2}, \quad \xi_{r\theta} = \frac{\dot{a}a^3}{r^4}\left(1-\frac{a^4}{r^4}\right)^{-1/2}.$$

Then, the equivalent strain rate follows from (4) as

$$\xi_{\text{eq}} = \frac{2}{\sqrt{3}}\frac{\dot{a}a}{\sqrt{r^4-a^4}}.$$

Expanding the right hand side of this equation is a series in the vicinity of the surface $r = a$ gives

$$\xi_{\text{eq}} = \frac{\dot{a}}{\sqrt{3}\sqrt{a}\sqrt{r-a}} + o\left(\frac{1}{\sqrt{r-a}}\right) \quad \text{as} \quad r \to a. \tag{111}$$

It follows from (5) and (111) that the strain rate intensity factor is

$$D = \frac{\dot{a}}{\sqrt{3}\sqrt{a}}. \tag{112}$$

4 Axisymmetric Solutions for Pressure-Independent Material

4.1 Basic Equations

Section 4 is concerned with axisymmetric solutions for pressure-independent material. In this section, two coordinate systems will be used, namely a cylindrical coordinate system (r, θ, z) and a spherical coordinate system (r, θ, ϑ). The solutions in the cylindrical coordinate system are independent of θ and the solutions in the spherical coordinate system are independent of ϑ. Let σ_1, σ_2 and σ_3 be the principal stresses. Then, Tresca's yield criterion adopted in this section can be written in the form

$$|\sigma_1 - \sigma_2| \le 2\tau_s, \quad |\sigma_2 - \sigma_3| \le 2\tau_s, \quad |\sigma_3 - \sigma_1| \le 2\tau_s. \tag{113}$$

This yield criterion is represented by a regular hexagonal prism in a three-dimensional space where the principal stresses are taken as Cartesian coordinates. The cross-section of this prism by the plane $\sigma_1 + \sigma_2 + \sigma_3 = 0$ is shown in Fig. 18. It is seen

Fig. 18 Tresca's yield locus

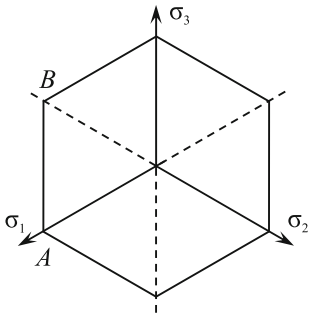

from this figure that the yield surface is singular. Therefore, various plastic regimes can in general arise. However, of particular interest are those corresponding to edges of the yield surface (corners in Fig. 18). The circumferential stress is one of the principal stresses. It is possible to assume that σ_3 is the circumferential stress. It is also possible to assume, with no loss of generality, that $\sigma_1 \geq \sigma_2$. The case $\sigma_1 = \sigma_2$ is not considered here. Therefore, $\sigma_1 > \sigma_2$ and Eqs. (113) reduce to

$$\sigma_1 - \sigma_2 = 2\tau_s, \quad \sigma_1 - \sigma_3 = 2\tau_s \tag{114}$$

or

$$\sigma_1 - \sigma_2 = 2\tau_s, \quad \sigma_3 - \sigma_2 = 2\tau_s. \tag{115}$$

Equations (114) correspond to point A and Eq. (115) to point B (Fig. 18).

Let $\sigma_{rr}, \sigma_{\theta\theta}, \sigma_{zz}, \sigma_{rz}, \sigma_{z\theta}$ and $\sigma_{r\theta}$ be the components of the stress tensor, and ξ_{rr}, $\xi_{\theta\theta}$, $\xi_{zz}, \xi_{rz}, \xi_{z\theta}$ and $\xi_{r\theta}$ be the components of the strain rate tensor in the cylindrical coordinate system. In the case under consideration, $\xi_{r\theta} = \xi_{z\theta} = 0$, $\sigma_{r\theta} = \sigma_{z\theta} = 0$ and the circumferential velocity $u_\theta = 0$. The non-zero strain rate components are expressed through the velocity components, u_r and u_z, as

$$\xi_{rr} = \frac{\partial u_r}{\partial r}, \quad \xi_{\theta\theta} = \frac{u_r}{r}, \quad \xi_{zz} = \frac{\partial u_z}{\partial z}, \quad \xi_{rz} = \frac{1}{2}\left(\frac{\partial u_r}{\partial z} + \frac{\partial u_z}{\partial r}\right). \tag{116}$$

The equilibrium equations are

$$\frac{\partial \sigma_{rr}}{\partial r} + \frac{\partial \sigma_{rz}}{\partial z} + \frac{\sigma_{rr} - \sigma_{\theta\theta}}{r} = 0, \quad \frac{\partial \sigma_{rz}}{\partial r} + \frac{\partial \sigma_{zz}}{\partial z} + \frac{\sigma_{rz}}{r} = 0. \tag{117}$$

Taking into account (114) or (115) the transformation equations for stress components in rz-planes are represented as

$$\sigma_{rr} = \frac{1}{2}(\sigma_1 + \sigma_2) + \tau_s \cos 2\psi, \quad \sigma_{zz} = \frac{1}{2}(\sigma_1 + \sigma_2) - \tau_s \cos 2\psi, \tag{118}$$
$$\sigma_{rz} = \tau_s \sin 2\psi,$$

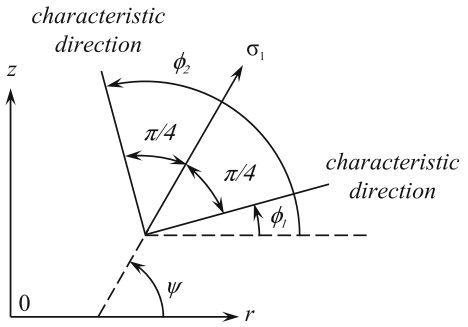

Fig. 19 Orientation of the major principal stress and characteristic directions relative to the r-axis of cylindrical coordinates

where ψ is the orientation of the principal stress σ_1 relative to the r-axis (Fig. 19). These equations show that $\sigma_{rr} + \sigma_{zz} = \sigma_1 + \sigma_2$. Then, it follows from Eqs. (114) and (115) that

$$\sigma_3 = \sigma_{\theta\theta} = \frac{1}{2}(\sigma_{rr} + \sigma_{zz}) + \varepsilon\tau_s, \tag{119}$$

where ε can take the values ± 1. It is evident that $\varepsilon = -1$ corresponds to point A and $\varepsilon = +1$ to point B (Fig. 18).

The flow rule associated with the yield criterion (114) or (115) leads to the equation of incompressibility and the isotropy condition. Using (116) the equation of incompressibility $\xi_{rr} + \xi_{\theta\theta} + \xi_{zz} = 0$ is transformed to

$$\frac{\partial u_r}{\partial r} + \frac{u_r}{r} + \frac{\partial u_z}{\partial z} = 0. \tag{120}$$

The isotropy condition is

$$\frac{\sigma_{rz}}{(\sigma_{rr} - \sigma_{zz})} = \frac{\xi_{rz}}{(\xi_{rr} - \xi_{zz})}.$$

Substituting (118) into this equation gives

$$\frac{2\xi_{rz}}{(\xi_{rr} - \xi_{zz})} = \tan 2\psi. \tag{121}$$

The conditions that an element of the material shall be in a state of stress corresponding to points A and B (Fig. 18) are that the associated velocity field satisfies the inequalities

$$\varepsilon u_r \geq 0, \quad (\xi_{rr} - \xi_{zz})^2 + 4\xi_{rz}^2 \geq \frac{u_r^2}{r^2}. \tag{122}$$

It is known (see, for example, [14]) that the characteristic directions make angles $\pm\pi/4$ with the direction of the principal stress σ_1. Therefore (Fig. 19),

$$\phi_1 = \psi - \frac{\pi}{4}, \quad \phi_2 = \psi + \frac{\pi}{4} \tag{123}$$

where ϕ_1 and ϕ_2 are the angles between the characteristic directions and the r-axis.

Let $\sigma_{rr}, \sigma_{\theta\theta}, \sigma_{\vartheta\vartheta}, \sigma_{r\vartheta}, \sigma_{\vartheta\theta}$ and $\sigma_{r\theta}$ be the components of the stress tensor, and ξ_{rr}, $\xi_{\theta\theta}, \xi_{\vartheta\vartheta}, \xi_{r\vartheta}, \xi_{\vartheta\theta}$ and $\xi_{r\theta}$ be the components of the strain rate tensor in the spherical coordinate system. In the case under consideration, $\xi_{r\vartheta} = \xi_{\vartheta\theta} = 0$, $\sigma_{r\vartheta} = \sigma_{\vartheta\theta} = 0$ and the circumferential velocity $u_\vartheta = 0$. The non-zero strain rate components are expressed through the velocity components, u_r and u_θ, as

$$\xi_{rr} = \frac{\partial u_r}{\partial r}, \ \xi_{\theta\theta} = \frac{1}{r}\left(\frac{\partial u_\theta}{\partial \theta} + u_r\right),$$
$$\xi_{\vartheta\vartheta} = \frac{1}{r\sin\theta}\left(u_r \sin\theta + u_\theta \cos\theta\right), \ \xi_{r\theta} = \frac{1}{2}\left(\frac{\partial u_\theta}{\partial r} - \frac{u_\theta}{r} + \frac{1}{r}\frac{\partial u_r}{\partial \theta}\right). \tag{124}$$

The equilibrium equations are

$$\frac{\partial \sigma_{rr}}{\partial r} + \frac{1}{r}\frac{\partial \sigma_{r\theta}}{\partial \theta} + \frac{(2\sigma_{rr} - \sigma_{\theta\theta} - \sigma_{\vartheta\vartheta} + \sigma_{r\theta}\cot\theta)}{r} = 0, \tag{125}$$
$$\frac{\partial \sigma_{r\theta}}{\partial r} + \frac{1}{r}\frac{\partial \sigma_{\theta\theta}}{\partial \theta} + \frac{(\sigma_{\theta\theta} - \sigma_{\vartheta\vartheta})\cot\theta + 3\sigma_{r\theta}}{r} = 0.$$

Taking into account (114) or (115) the transformation equations for stress components in $r\theta$-planes are represented as

$$\sigma_{rr} = \frac{1}{2}(\sigma_1 + \sigma_2) + \tau_s \cos 2\psi, \quad \sigma_{\theta\theta} = \frac{1}{2}(\sigma_1 + \sigma_2) - \tau_s \cos 2\psi, \tag{126}$$
$$\sigma_{r\theta} = \tau_s \sin 2\psi,$$

where ψ is the orientation of the principal stress σ_1 relative to the r-axis (Fig. 20). These equations show that $\sigma_{rr} + \sigma_{\theta\theta} = \sigma_1 + \sigma_2$. Then, it follows from Eqs. (114) and (115) that

$$\sigma_3 = \sigma_{\vartheta\vartheta} = \frac{1}{2}(\sigma_{rr} + \sigma_{\theta\theta}) + \varepsilon\tau_s. \tag{127}$$

As before, $\varepsilon = -1$ corresponds to point A and $\varepsilon = +1$ to point B (Fig. 18).

Using (124) the equation of incompressibility, $\xi_{rr} + \xi_{\theta\theta} + \xi_{\vartheta\vartheta} = 0$, is transformed to

$$\frac{\partial u_r}{\partial r} + \frac{1}{r}\left(\frac{\partial u_\theta}{\partial \theta} + u_r\right) + \frac{1}{r\sin\theta}\left(u_r \sin\theta + u_\theta \cos\theta\right) = 0. \tag{128}$$

Using (126) the isotropy condition, $\sigma_{r\theta}(\xi_{rr} - \xi_{\theta\theta}) = (\sigma_{rr} - \sigma_{\theta\theta})\xi_{r\theta}$, is written as

$$\frac{2\xi_{r\theta}}{(\xi_{rr} - \xi_{\theta\theta})} = \tan 2\psi. \tag{129}$$

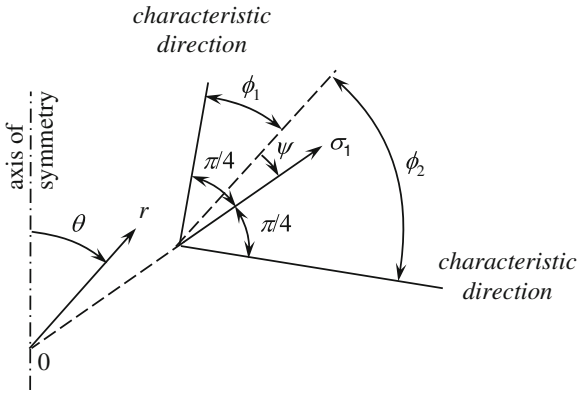

Fig. 20 Orientation of the major stress and characteristic directions relative to the r-axis of spherical coordinates

The inequalities (122) in the spherical coordinate system become

$$\varepsilon\,(u_r \sin\theta + u_\theta \cos\theta) \geq 0,\ \ (\xi_{rr} - \xi_{\theta\theta})^2 + 4\xi_{r\theta}^2 \geq \frac{(u_r \sin\theta + u_\theta \cos\theta)^2}{r^2 \sin^2\theta}. \quad (130)$$

Since the characteristic directions make angles $\pm\pi/4$ with the direction of the principal stress σ_1, it is seen from Fig. 20 that

$$\phi_1 = \psi - \frac{\pi}{4}, \quad \phi_2 = \psi + \frac{\pi}{4}, \quad (131)$$

where ϕ_1 and ϕ_2 are the angles between the characteristic directions and the r-axis.

4.2 Compression of a Hollow Cylinder on a Rigid Fibre

The boundary value problem is illustrated in Fig. 21. An axisymmetric hollow cylinder of internal radius a and external radius b is subject to compression by pressure p uniformly distributed over its outer surface. The length of the cylinder is $2L$. A rigid fibre of radius a is inserted into the hole of the cylinder. The cylindrical coordinate system is chosen such that the plane $z = 0$ coincides with the plane of symmetry of the cylinder. Then, it is sufficient to find the solution in the domain $0 \leq z \leq L$. Symmetry demands

$$u_z = 0 \quad (132)$$

and

$$\sigma_{rz} = 0 \quad (133)$$

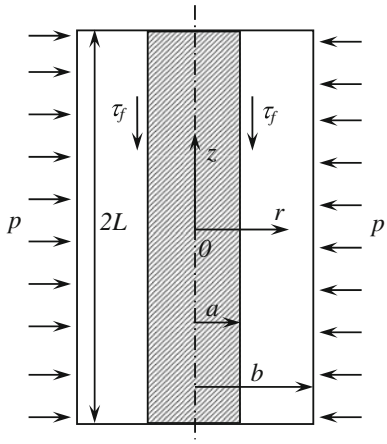

Fig. 21 Illustration of the boundary value problem

for $z = 0$. Since the fibre is rigid,

$$u_r = 0 \tag{134}$$

for $r = a$. The rate of contraction of the external radius of the cylinder is denoted by U. Then,

$$u_r = -U \tag{135}$$

for $r = b$. The surface $z = L$ is traction free. Therefore,

$$\sigma_{rz} = 0 \tag{136}$$

and

$$\sigma_{zz} = 0 \tag{137}$$

for $z = L$. By assumption, the surface $r = b$ is free of shear stress. Then,

$$\sigma_{rz} = 0 \tag{138}$$

for $r = b$. The final boundary condition is the maximum friction law at $r = a$. The direction of the friction stress is shown in Fig. 21. Therefore, the maximum friction law becomes

$$\sigma_{rz} = \tau_s \tag{139}$$

for $r = a$. The boundary value problem defined is an axisymmetric analogue to the problem considered in Sect. 3.2. Its approximate solution proposed in [31] ignores the boundary conditions (133) and (136). The boundary conditions (132) and (137) are replaced with the following integral conditions

$$\int_a^b u_z|_{z=0}\, r dr = 0 \tag{140}$$

and

$$\int_a^b \sigma_{zz}|_{z=L}\, r dr = 0, \tag{141}$$

respectively. Thus the solution is not valid in the vicinity of $z = 0$ and $z = L$.

The velocity field proposed in [31] is

$$\frac{u_r}{U} = -\frac{b\left(r^2 - a^2\right)}{r\left(b^2 - a^2\right)}, \tag{142}$$

$$\frac{u_z}{U} = \frac{b}{\left(b^2 - a^2\right)}\left[2z + \int \frac{\left(3r^2 + a^2\right) f\,(r)}{r^2\sqrt{1 - f\,(r)^2}} dr\right] + K, \quad f\,(r) = \frac{a\left(b^2 - r^2\right)}{r\left(b^2 - a^2\right)}.$$

Here K is the constant of integration. Its value can be found by means of the boundary condition (140). However, it is not necessary for determining the strain rate intensity factor. It is possible to verify by inspection that the velocity field (142) satisfies the equation of incompressibility (120). It has been shown in [31] that the velocity field also satisfies the inequalities (122) if $\varepsilon = -1$. Then, the associated state of stress must correspond to point A (Fig. 18). Such a stress field satisfying Eqs. (114), (117), (119) and (121) as well as the boundary conditions (138), (139) and (141) has been found in [31]. Substituting (142) into (116) yields

$$\xi_{rr} = -\frac{Ub\left(r^2 + a^2\right)}{r^2\left(b^2 - a^2\right)}, \quad \xi_{\theta\theta} = -\frac{Ub\left(r^2 - a^2\right)}{r^2\left(b^2 - a^2\right)}, \quad \xi_{zz} = \frac{2Ub}{\left(b^2 - a^2\right)}, \tag{143}$$

$$\xi_{rz} = \frac{Ub\left(3r^2 + a^2\right) f\,(r)}{2\left(b^2 - a^2\right) r^2\sqrt{1 - f\,(r)^2}}.$$

Since $f\,(a) = 1$, it is evident that the normal strain rates are bounded and $\xi_{rz} \to \infty$ as $r \to a$. Therefore, Eq. (6) in which ξ_τ is replaced with ξ_{rz} is valid. Eliminating the function $f(r)$ in (143) by means of (142) the shear strain rate in the vicinity of the maximum friction surface $r = a$ is represented as

$$\xi_{rz} = \frac{\sqrt{2}Ub\sqrt{a}}{\sqrt{b^4 - a^4}\sqrt{r - a}} + o\left(\frac{1}{\sqrt{r - a}}\right) \quad \text{as} \quad r \to a. \tag{144}$$

Combining (6) and (144) gives

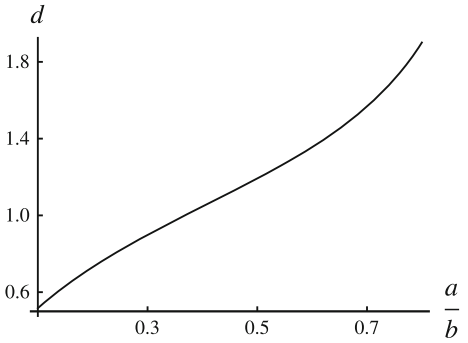

Fig. 22 Variation of the dimensionless strain rate intensity factor with the ratio a/b

$$D = \frac{2\sqrt{2}Ub\sqrt{a}}{\sqrt{3}\sqrt{b^4 - a^4}}. \tag{145}$$

It is convenient to introduce the dimensionless strain rate intensity factor by

$$d = D\sqrt{b}/U.$$

Then, it follows from (145) that

$$d = \frac{2\sqrt{2a}}{\sqrt{3b}}\left(1 - \frac{b^4}{a^4}\right)^{-1/2}. \tag{146}$$

The variation of d with a/b is shown in Fig. 22.

4.3 *Flow of Plastic Material Through an Converging Conical Channel*

Consider a converging conical channel (total angle 2α) through which plastic material is being forced (Fig. 23). The material flows to the virtual apex O. The origin of the spherical coordinate system is taken at O and the surface of the channel is determined by the equation $\theta = \alpha$. The maximum friction law is supposed at $\theta = \alpha$. The direction of friction stresses τ_f is dictated by the direction of flow (Fig. 23). The solution used in this section has been proposed in [32]. The velocity boundary conditions are

$$u_\theta = 0 \tag{147}$$

at $\theta = 0$ and $\theta = \alpha$. The stress boundary condition, in addition to the maximum friction law, is

$$\sigma_{r\theta} = 0 \tag{148}$$

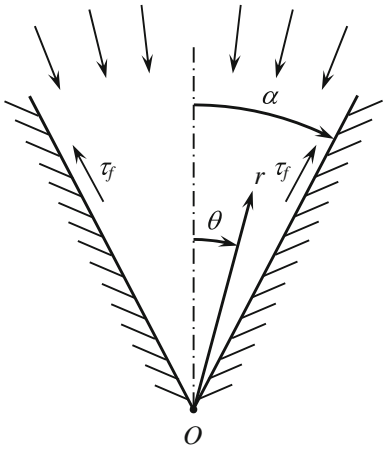

Fig. 23 Illustration of the boundary value problem

at $\theta = 0$. It is assumed in [32] that $u_\theta = 0$ everywhere. Then, the boundary conditions (147) are automatically satisfied. In the case of Tresca's yield criterion the radial velocity is given by [32]

$$u_r = -\frac{B}{r^2} \exp\left[-3 \int_\alpha^\theta \frac{t}{\sqrt{1-t^2}} d\gamma\right], \tag{149}$$

where B is proportional to the material flux, t is a function of θ and γ is a dummy variable of integration. The function $t\,(\theta)$ is determined by the following equation

$$\frac{dt}{d\theta} + t \cot\theta + 3\sqrt{1-t^2} = c, \tag{150}$$

where c is a constant of integration. The physical meaning of the function $t\,(\theta)$ is that $\sigma_{r\theta} = \tau_s t\,(\theta)$. Therefore, it follows from (148) and the maximum friction law (1) that

$$t = 0 \tag{151}$$

at $\theta = 0$ and

$$t = 1 \tag{152}$$

at $\theta = \alpha$. It is convenient to introduce the following substitution

$$t = \cos\mu. \tag{153}$$

Then, Eq. (150) transforms to

$$-\sin\mu\frac{d\mu}{d\theta}+\cos\mu\cot\theta+3\sin\mu=c \tag{154}$$

and the boundary conditions (151) and (152) to

$$\mu=\frac{\pi}{2} \quad \text{at} \quad \theta=0 \tag{155}$$

and

$$\mu=0 \quad \text{at} \quad \theta=\alpha, \tag{156}$$

respectively. It is seen from (155) that the second term in (154) reduces to the expression $0\cdot\infty$ at $\theta=0$. Assume that

$$\mu=\frac{\pi}{2}+a_1\theta+o(\theta) \quad \text{as} \quad \theta\to 0. \tag{157}$$

Substituting (157) into (154) it is possible to express a_1 in terms of c. Then, (157) becomes

$$\mu=\frac{\pi}{2}+\frac{(3-c)}{2}\theta+o(\theta) \quad \text{as} \quad \theta\to 0. \tag{158}$$

Since the coefficient of the derivative in (154) vanishes at $\theta=\alpha$, it is convenient to rewrite this equation as

$$\frac{d\theta}{d\mu}=\frac{\sin\mu}{3\sin\mu+\cos\mu\cot\theta-c}. \tag{159}$$

Using (158) the function $\theta(\mu)$ is represented as

$$\theta=\frac{2}{(c-3)}\left(\frac{\pi}{2}-\mu\right)+o\left(\frac{\pi}{2}-\mu\right) \quad \text{as} \quad \mu\to\frac{\pi}{2}. \tag{160}$$

It follows from this equation that

$$\theta_a=\frac{2\delta_a}{(c-3)} \tag{161}$$

to leading order. Here $\delta_a=\pi/2-\mu_a<<1$. Using the boundary condition $\theta=\theta_a$ for $\mu=\mu_a$ at some value of c Eq. (159) can be solved numerically in the range $0\le\mu\le\mu_a$. Then, an iterative procedure should be adopted to find the value of c satisfying the boundary condition (156). The variation of c with α is depicted in Fig. 24. It has been shown in [32] that there exists a distribution of the normal stresses associated with the velocity field considered and the solution of Eq. (159) found. The state of stresses corresponds to point A of the yield surface (Fig. 18) and satisfies the equilibrium Eq. (125).

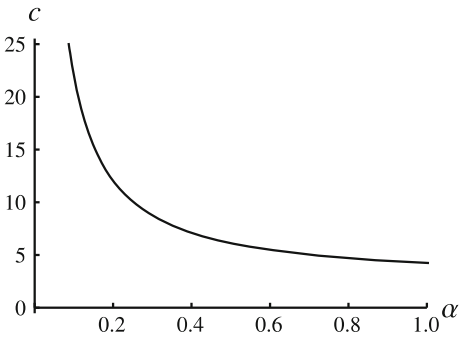

Fig. 24 Variation of c with α

Using (153) Eq. (149) transforms to

$$u_r = -\frac{B}{r^2}\exp\left[-3\int_{\alpha}^{\theta}\cot\mu d\gamma\right]. \tag{162}$$

The components of the strain rate tensor are determined from (124). It is evident that the normal strain rates are bounded and $\xi_{r\theta} \to \infty$ as $\theta \to \alpha$. Therefore, Eq. (6) in which ξ_τ is replaced with $\xi_{r\theta}$ is valid. Using (124) and (162) the shear strain rate in the vicinity of the maximum friction surface $\theta = \alpha$ is represented as

$$\xi_{r\theta} = \frac{U}{r^3}\mu^{-1} + o\left(\mu^{-1}\right) \quad \text{as} \quad \mu \to 0, \tag{163}$$

where

$$U = \frac{3B}{2}\exp\left(3\int_{0}^{\alpha}\cot\mu d\theta\right). \tag{164}$$

Equation (159) in the vicinity of the friction surface $\theta = \alpha$ can be written as

$$\frac{d\theta}{d\mu} = \frac{\mu}{\cot\alpha - c} \quad \text{as} \quad \theta \to \alpha.$$

Integrating with the boundary condition (156) yields

$$\mu = \sqrt{c - \cot\alpha}\sqrt{\alpha - \theta} + o\left(\sqrt{\alpha - \theta}\right) \quad \text{as} \quad \theta \to \alpha. \tag{165}$$

Substituting (165) into (163) gives

$$\xi_{r\theta} = \frac{U}{r^3\sqrt{c - \cot\alpha}\sqrt{\alpha - \theta}} + o\left(\frac{1}{\sqrt{\alpha - \theta}}\right) \quad \text{as} \quad \theta \to \alpha. \tag{166}$$

Comparing (6) and (166) shows that

$$D = \frac{2}{\sqrt{3}} \frac{U}{\sqrt{c - \cot \alpha}} r^{-5/2}. \tag{167}$$

The material flux is defined by

$$Q = -2\pi \int_0^{\alpha} u_r r^2 \sin \theta d\theta. \tag{168}$$

Substituting (162) into (168) gives

$$Q = 2\pi B \int_0^{\alpha} \exp \left[-3 \int_{\alpha}^{\theta} \cot \mu d\gamma \right] \sin \theta d\theta. \tag{169}$$

It is convenient to introduce the dimensionless strain rate intensity factor as

$$d = \frac{Dr^{5/2}}{Q}. \tag{170}$$

Then, it follows from (164), (167), (169), and (170) that

$$d = \frac{\sqrt{3}}{2\pi \sqrt{c - \cot \alpha}} \exp \left(3 \int_0^{\alpha} \cot \mu d\theta \right) \left\{ \int_0^{\alpha} \exp \left[3 \int_{\theta}^{\alpha} \cot \mu d\gamma \right] \sin \theta d\theta \right\}^{-1}. \tag{171}$$

Using the solution of Eq. (159) along with the value of c found (Fig. 24) the integrals involved in this equation can be evaluated. As a result, the variation of d with α is obtained. This variation is illustrated in Fig. 25.

4.4 Radial Flow Between Two Conical Surfaces

Consider radial flow between two conical surfaces shown in Fig. 26. The material flows to the virtual apex O. The origin of the spherical coordinate system is taken at O and the surfaces of the channel are determined by the equations $\theta = \theta_0$ and $\theta = \theta_1$. The maximum friction law is supposed at both $\theta = \theta_0$ and $\theta = \theta_1$. The direction of friction stresses τ_f is dictated by the direction of flow (Fig. 26). A solution to this problem for the von Mises yield criterion has been proposed in [33]. It was based on the general solution given in [32] where the solution for the Tresca yield criterion considered in the previous section was also proposed. The latter will be adopted in the present section to describe radial flow between two conical surfaces.

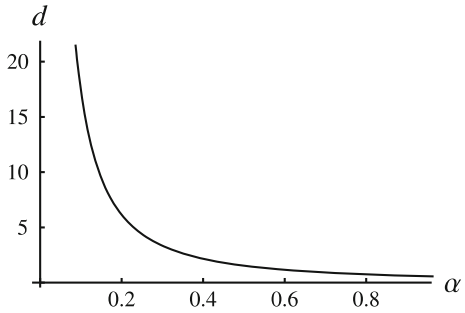

Fig. 25 Variation of the dimensionless strain rate intensity factor with α

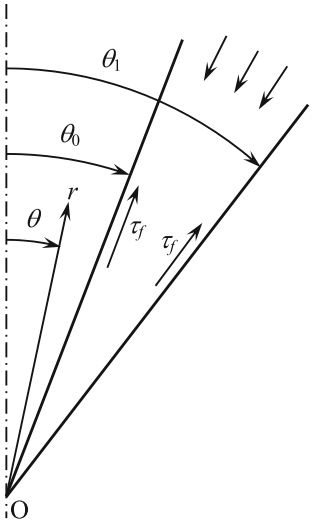

Fig. 26 Illustration of the boundary value problem

The velocity boundary conditions are

$$u_\theta = 0 \quad \text{at} \quad \theta = \theta_0 \quad \text{and} \quad \theta = \theta_1. \tag{172}$$

Therefore, the assumption that $u_\theta = 0$ everywhere adopted in the previous section is applicable in the case under consideration. Then, the radial velocity is given by (149). Using (153) this equation is transformed to (162). Equations (154) and (159) are valid. However, the boundary conditions (155) and (156) are replaced with

$$\mu = \pi \quad \text{at} \quad \theta = \theta_0 \tag{173}$$

and

$$\mu = 0 \quad \text{at} \quad \theta = \theta_1. \tag{174}$$

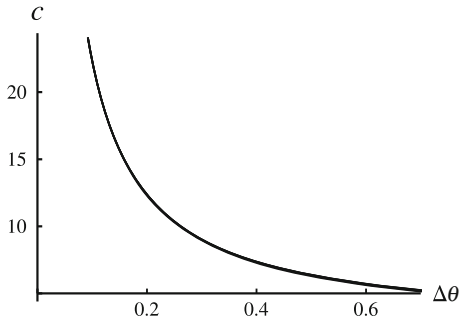

Fig. 27 Variation of c with $\Delta\theta$

Solving Eq. (159) along with the boundary conditions (173) and (174) numerically gives the dependence of c on θ_0 and θ_1. The variation of c with $\Delta\theta = \theta_1 - \theta_0$ at several values of θ_0 in the range $\pi/36 \le \theta_0 \le \pi/4$ is depicted in Fig. 27. It is seen from this figure that the value of c is practically independent of θ_0 and θ_1 separately (no difference between the curves is visible in the figure). Equation (162) is replaced with

$$u_r = -\frac{B}{r^2} \exp\left[-3 \int_{\theta_0}^{\theta} \cot \mu d\gamma\right]. \tag{175}$$

The components of the strain rate tensor are determined from (124). It is evident that the normal strain rates are bounded and $|\xi_{r\theta}| \to \infty$ as $\theta \to \theta_0$ and $\theta \to \theta_1$. Therefore, Eq. (6) in which ξ_τ is replaced with $\xi_{r\theta}$ is valid. Using (124) and (175) the shear strain rate in the vicinity of the maximum friction surfaces $\theta = \theta_1$ and $\theta = \theta_0$ is represented as

$$\xi_{r\theta} = \frac{U}{r^3}\mu^{-1} + o\left(\mu^{-1}\right) \quad \text{as} \quad \mu \to 0 \tag{176}$$

and

$$\xi_{r\theta} = -\frac{3B}{2r^3}(\pi - \mu)^{-1} + o\left[(\pi - \mu)^{-1}\right] \quad \text{as} \quad \mu \to \pi, \tag{177}$$

respectively. Here

$$U = \frac{3B}{2} \exp\left(-3 \int_{\theta_0}^{\theta_1} \cot \mu d\theta\right). \tag{178}$$

Using (173) and (174) Eq. (154) in the vicinity of points $\mu = 0$ and $\mu = \pi$ can be represented as

$$\frac{d\mu}{d\theta} = \frac{\cot\theta_0 + c}{\mu - \pi} + o\left[(\mu - \pi)^{-1}\right] \quad \text{as} \quad \mu \to \pi \tag{179}$$

and

$$\frac{d\mu}{d\theta} = \frac{\cot\theta_1 - c}{\mu} + o\left(\frac{1}{\mu}\right) \quad \text{as} \quad \mu \to 0. \tag{180}$$

Integrating (179) and (180) with the use of the boundary conditions (173) and (174) yields

$$\pi - \mu = \sqrt{2\,(\cot\theta_0 + c)}\sqrt{\theta - \theta_0} + o\left(\sqrt{\theta - \theta_0}\right) \quad \text{as} \quad \theta \to \theta_0 \tag{181}$$

and

$$\mu = \sqrt{2\,(c - \cot\theta_1)}\sqrt{\theta_1 - \theta} + o\left(\sqrt{\theta_1 - \theta}\right) \quad \text{as} \quad \theta \to \theta_1. \tag{182}$$

Substituting (181) into (177) and (182) into (176) gives

$$\xi_{r\theta} = -\frac{3B}{2r^3\sqrt{2\,(\cot\theta_0 + c)}\sqrt{\theta - \theta_0}} + o\left(\frac{1}{\sqrt{\theta - \theta_0}}\right) \quad \text{as} \quad \theta \to \theta_0 \tag{183}$$

and

$$\xi_{r\theta} = \frac{U}{r^3\sqrt{2\,(c - \cot\theta_1)}\sqrt{\theta_1 - \theta}} + o\left(\frac{1}{\sqrt{\theta_1 - \theta}}\right) \quad \text{as} \quad \theta \to \theta_1, \tag{184}$$

respectively. Comparing (6) with (183) and (184) gives

$$D_{in} = \frac{\sqrt{3}}{\sqrt{2}}\frac{B}{\sqrt{\cot\theta_0 + c}}r^{-5/2} \tag{185}$$

and

$$D_{\text{ex}} = \frac{\sqrt{2}}{\sqrt{3}}\frac{U}{\sqrt{c - \cot\theta_1}}r^{-5/2}. \tag{186}$$

Here D_{in} is the strain rate intensity factor related to the inner friction surface $\theta = \theta_0$ and D_{ex} is the strain rate intensity factor related to the outer friction surface $\theta = \theta_1$.

The material flux is defined by

$$Q = -2\pi\int_{\theta_0}^{\theta_1} u_r r^2 \sin\theta d\theta. \tag{187}$$

Substituting (175) into (187) gives

$$Q = 2\pi B \int_{\theta_0}^{\theta_1} \exp\left[-3\int_{\theta_0}^{\theta} \cot\mu d\gamma\right] \sin\theta d\theta. \tag{188}$$

As before, it is convenient to introduce the dimensionless strain rate intensity factor by Eq. (170). Then, it follows from (170), (178), (185), (186), and (188) that

$$d_{in} = \frac{\sqrt{6}}{4\pi\sqrt{\cot\theta_0 + c}} \left\{\int_{\theta_0}^{\theta_1} \exp\left[-3\int_{\theta_0}^{\theta} \cot\mu d\gamma\right] \sin\theta d\theta\right\}^{-1} \tag{189}$$

and

$$d_{\text{ex}} = \frac{\sqrt{6}}{4\pi\sqrt{c - \cot\theta_1}} \exp\left(-3\int_{\theta_0}^{\theta_1} \cot\mu d\theta\right) \left\{\int_{\theta_0}^{\theta_1} \exp\left[-3\int_{\theta_0}^{\theta} \cot\mu d\gamma\right] \sin\theta d\theta\right\}^{-1}. \tag{190}$$

Using (159) the integrals involved in these equations are represented as

$$\int_{\theta_0}^{\theta_1} \cot\mu d\theta = -\int_0^{\pi} \frac{\cos\mu}{(3\sin\mu + \cos\mu\cot\theta - c)} d\mu,$$

$$\int_{\theta_0}^{\theta_1} \exp\left[-3\int_{\theta_0}^{\theta} \cot\mu d\gamma\right] \sin\theta d\theta$$

$$= -\int_0^{\pi} \exp\left[3\int_{\mu}^{\pi} \frac{\cos\gamma}{(3\sin\gamma + \cos\gamma\cot\theta - c)} d\gamma\right] \frac{\sin\theta\sin\mu}{(3\sin\mu + \cos\mu\cot\theta - c)} d\mu.$$

Using the solution of Eq. (159) along with the value of c found (Fig. 27) these integrals can be evaluated. As a result, the variation of d_{in} and d_{ex} with θ_0 and θ_1 is obtained. As before, it is convenient to use the parameters θ_0 and $\Delta\theta$ instead of θ_0 and θ_1. Figures 28 and 29 illustrate the dependence of d_{in} and d_{ex} on $\Delta\theta$ at several values of θ_0. It is also of great interest to understand the variation of the ratio $d_r = d_{\text{ex}}/d_{in} = D_{\text{ex}}/D_{in}$ with process parameters. Its dependence on $\Delta\theta$ at several values of θ_0 is illustrated in Fig. 30. In Figs. 28, 29 and 30, curve 1 corresponds to $\theta_0 = \pi/36$, curve 2 to $\theta_0 = \pi/18$, curve 3 to $\theta_0 = \pi/9$, curve 4 to $\theta_0 = \pi/6$, and curve 5 to $\theta_0 = \pi/4$.

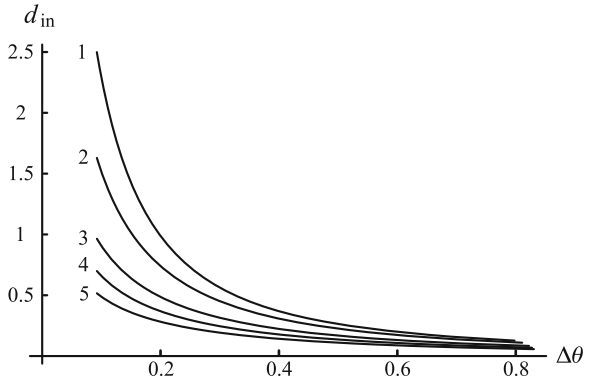

Fig. 28 Variation of the dimensionless strain rate intensity factor d_{in} with $\Delta\theta$ at several θ_0-values

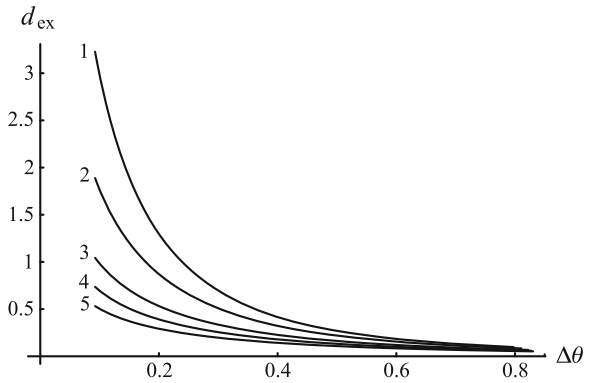

Fig. 29 Variation of the dimensionless strain rate intensity factor d_{ex} with $\Delta\theta$ at several θ_0-values

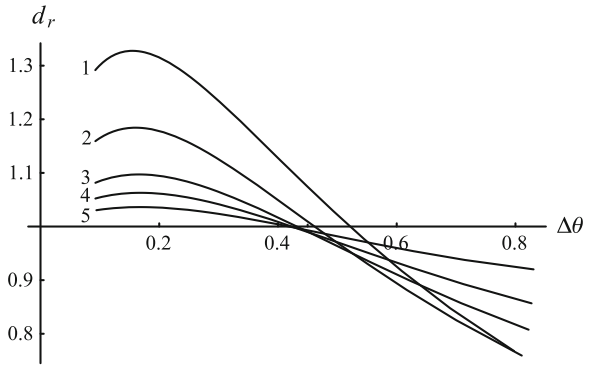

Fig. 30 Variation of the ratio of the strain rate intensity factors with $\Delta\theta$ at several θ_0-values

5 Plane Strain Solutions for the Double-Shearing Model

5.1 Basic Equations

Section 5 is concerned with plane strain solutions for the double-shearing model. In this section, two coordinate systems will be used, namely a Cartesian coordinate system (x, y, z) and a cylindrical coordinate system (r, θ, z). All the solutions considered are independent of z. The principal stress coinciding with the stress σ_{zz} is denoted by σ_3. The constitutive equations in terms of stress and strain rate have been given in [10, 34]. In particular, the Coulomb-Mohr yield criterion is

$$q - p \sin \varphi = k \cos \varphi \tag{191}$$

where k is the cohesion and

$$p = -\frac{\sigma_1 + \sigma_2}{2}, \quad q = \frac{\sigma_1 - \sigma_2}{2} > 0. \tag{192}$$

Using the transformation equations for stress components in xy-planes and (192) the stress components in the Cartesian coordinates are expressed as (Fig. 2)

$$\sigma_{xx} = -p + q \cos 2\psi, \quad \sigma_{yy} = -p - q \cos 2\psi, \quad \sigma_{xy} = q \sin 2\psi. \tag{193}$$

It follows from these equations that

$$p = -\frac{\sigma_{xx} + \sigma_{yy}}{2}, \quad q = \frac{1}{2}\sqrt{\left(\sigma_{xx} - \sigma_{yy}\right)^2 + 4\sigma_{xy}^2}. \tag{194}$$

It is seen from this equation that the yield criterion (191) reduces to the pressure-independent yield criterion (7) at $\varphi = 0$ assuming that $\tau_s = k$. The velocity equations are

$$\xi_{xx} + \xi_{yy} = 0, \quad 2\xi_{xy} \cos 2\psi - \left(\xi_{xx} - \xi_{yy}\right) \sin 2\psi + 2 \sin \varphi \left(\omega_{xy} + \dot{\psi}\right) = 0, \tag{195}$$

where ω_{xy} is the component of spin relative to the Cartesian coordinates. By definition,

$$\omega_{xy} = \frac{1}{2}\left(\frac{\partial u_x}{\partial y} - \frac{\partial u_y}{\partial x}\right), \quad \dot{\psi} = \frac{\partial \psi}{\partial t} + u_x \frac{\partial \psi}{\partial x} + u_y \frac{\partial \psi}{\partial y}, \tag{196}$$

where $\partial\psi/\partial t$ is the derivative of ψ at a point which is fixed relative to the Cartesian coordinates. Equation $(195)_1$ coincides with $(9)_1$. Using (193) to eliminate ψ Eq. $(195)_2$ is reduced to $(9)_2$ at $\varphi = 0$. Substituting (10) and $(196)_1$ into (195) yields

$$\frac{\partial u_x}{\partial x} + \frac{\partial u_y}{\partial y} = 0,$$
$$(\cos 2\psi + \sin\varphi)\frac{\partial u_x}{\partial y} + (\cos 2\psi - \sin\varphi)\frac{\partial u_y}{\partial x} \tag{197}$$
$$-\left(\frac{\partial u_x}{\partial x} - \frac{\partial u_y}{\partial y}\right)\sin 2\psi + 2\sin\varphi\dot{\psi} = 0.$$

The constitutive equations should be supplemented with the equilibrium Eq. (12). It is known that the resulting system is hyperbolic [34]. The stress and velocity characteristics coincide. The orientation of the characteristic curves relative to the x-axis is

$$\phi_1 = \psi - \frac{\pi}{4} - \frac{\varphi}{2}, \quad \phi_2 = \psi + \frac{\pi}{4} + \frac{\varphi}{2}. \tag{198}$$

Figure 2 can serve as a geometric interpretation of these relations if $\pi/4$ is replaced with $\pi/4 + \varphi/2$.

Similar equations are valid in the cylindrical coordinates. In particular,

$$\sigma_{rr} = -p + q\cos 2\psi, \quad \sigma_{\theta\theta} = -p - q\cos 2\psi, \quad \sigma_{r\theta} = q\sin 2\psi, \tag{199}$$

where

$$p = -\frac{\sigma_{rr} + \sigma_{\theta\theta}}{2}, \quad q = \frac{1}{2}\sqrt{(\sigma_{rr} - \sigma_{\theta\theta})^2 + 4\sigma_{r\theta}^2}. \tag{200}$$

As before, ψ is now understood as the orientation of the stress σ_1 relative to the r-axis (Fig. 4). The velocity equations are

$$\xi_{rr} + \xi_{\theta\theta} = 0, \quad 2\xi_{r\theta}\cos 2\psi - (\xi_{rr} - \xi_{\theta\theta})\sin 2\psi + 2\sin\varphi\left(\omega_{r\theta} + \dot{\psi}\right) = 0, \tag{201}$$

where

$$\omega_{r\theta} = \frac{1}{2}\left(\frac{\partial u_r}{r\partial\theta} - \frac{\partial u_\theta}{\partial r} - \frac{u_\theta}{r}\right), \quad \dot{\psi} = \frac{\partial\psi}{\partial t} + u_r\frac{\partial\psi}{\partial r} + \frac{u_\theta}{r}\frac{\partial\psi}{\partial\theta}. \tag{202}$$

Substituting (41) and $(202)_1$ into (201) yields

$$r\frac{\partial u_r}{\partial r} + \frac{\partial u_\theta}{\partial\theta} + u_r = 0,$$
$$(\cos 2\psi - \sin\varphi)\frac{\partial u_\theta}{\partial r} + \left(\frac{\partial u_r}{r\partial\theta} - \frac{u_\theta}{r}\right)(\cos 2\psi + \sin\varphi) \tag{203}$$
$$-\left(\frac{\partial u_r}{\partial r} - \frac{\partial u_\theta}{r\partial\theta} - \frac{u_r}{r}\right)\sin 2\psi + 2\sin\varphi\dot{\psi} = 0.$$

The constitutive equations should be supplemented with the equilibrium Eq. (42). The orientation of the characteristic curves relative to the r-axis is given by the following equations similar to (198)

$$\phi_1 = \psi - \frac{\pi}{4} - \frac{\varphi}{2}, \quad \phi_2 = \psi + \frac{\pi}{4} + \frac{\varphi}{2}. \tag{204}$$

Figure 4 can serve as a geometric interpretation of these relations if $\pi/4$ is replaced with $\pi/4 + \varphi/2$.

5.2 Compression of a Plastic Layer Between Parallel Plates

This boundary value problem has been formulated and solved for pressure-independent material in Sect. 3.2 (see Fig. 5). An extension of this solution to the double shearing model has been proposed in [35]. In particular, the velocity field is given by

$$\frac{u_x}{V} = \frac{x}{H} - \frac{\cos 2\psi}{A} + U, \quad \frac{u_y}{V} = -\frac{y}{H}, \tag{205}$$

where U and A are constants of integration and ψ is related to y by the following equation

$$(\sin\phi + \cos 2\psi)\,\frac{d\psi}{dy} = \frac{A}{H}. \tag{206}$$

The value of U is not essential for determining the strain rate intensity factor. It is evident that the distribution of u_y in (205) satisfies the boundary conditions (44) and (45). The maximum friction surface is determined by the equation $y = H$. Therefore, $\phi_1 = 0$ or $\phi_2 = 0$ at $y = H$ in (198). The direction of the friction stress (Fig. 5) dictates that $\sigma_{xy} < 0$ at $y = H$. Therefore, it follows from (193) that $-\pi/2 < \psi < 0$ at $y = H$. Equation $\phi_1 = 0$ contradicts this inequality. Therefore, $\phi_2 = 0$ and

$$\psi = \psi_w = -\frac{\pi}{4} - \frac{\varphi}{2} \tag{207}$$

at $y = H$. On the other hand, it is reasonable to assume that $\sigma_{xx} > \sigma_{yy}$ at $y = 0$. Then, taking into account the boundary condition (47) at $y = 0$ and (193) it is possible to conclude that

$$\psi = 0 \tag{208}$$

at $y = 0$. Integrating (206) with the use of the boundary condition (207) results in

$$2A\left(\frac{y}{H} - 1\right) = 2\sin\varphi\left(\psi + \frac{\pi}{4} + \frac{\varphi}{2}\right) + \sin 2\psi + \cos\varphi. \tag{209}$$

Substituting the boundary condition (208) into this solution determines A as

$$A = -\sin\varphi\left(\frac{\pi}{4} + \frac{\varphi}{2}\right) - \frac{\cos\varphi}{2}. \tag{210}$$

Eliminating A in (206) by means of (210) it is possible to represent the resulting equation in the vicinity of the friction surface as

$$\frac{d\psi}{dy} = -\frac{\tan\varphi\,(\pi + 2\varphi) + 2}{8H\,(\psi - \psi_w)} + o\left[(\psi - \psi_w)^{-1}\right] \quad \text{as} \quad \psi \to \psi_w. \tag{211}$$

Integrating with the use of the boundary condition $\psi = \psi_w$ at $y = H$ yields

$$(\psi - \psi_w)^2 = \frac{[\tan\varphi\,(\pi + 2\varphi) + 2]}{4H}\,(H - y) + o\,(H - y) \quad \text{as} \quad y \to H. \tag{212}$$

Substituting (205) into (10) and using (206) give

$$\xi_{xx} = \frac{V}{H}, \quad \xi_{yy} = -\frac{V}{H}, \quad \xi_{xy} = \frac{V}{H}\frac{\sin 2\psi}{(\sin\varphi + \cos 2\psi)}. \tag{213}$$

Substituting (213) into (4) and expanding in a series in the vicinity of $\psi = \psi_w$ yield

$$\begin{aligned} \xi_{\text{eq}} &= \frac{2}{\sqrt{3}}\frac{V}{H}\sqrt{1 + \frac{\sin^2 2\psi}{(\sin\varphi + \cos 2\psi)^2}} \\ &= \frac{V}{\sqrt{3}H\,(\psi - \psi_w)} + o\left[(\psi - \psi_w)^{-1}\right] \quad \text{as} \quad \psi \to \psi_w. \end{aligned} \tag{214}$$

Combining (212) and (214) gives

$$\xi_{\text{eq}} = \frac{2V}{\sqrt{3H\,[\tan\varphi\,(\pi + 2\varphi) + 2]}\sqrt{H - y}} + o\left(\frac{1}{\sqrt{H - y}}\right) \text{ as } y \to H. \tag{215}$$

It follows from (5) and (215) that

$$D = \frac{2V}{\sqrt{3H\,[\tan\varphi\,(\pi + 2\varphi) + 2]}}. \tag{216}$$

The strain rate intensity factor given by (54) is recovered from (216) at $\varphi = 0$. In order to demonstrate the effect of pressure-dependency of the yield criterion on the strain rate intensity factor, it is convenient to introduce the dimensionless strain rate intensity factor, d, as the ratio of the strain rate intensity factor given by (216) to the strain rate intensity factor given by (54). As a result,

$$d = \frac{\sqrt{2}}{\sqrt{\tan\varphi\,(\pi + 2\varphi) + 2}}. \tag{217}$$

The variation of d with φ is depicted in Fig. 31. It is seen from this figure that the strain rate intensity factor decreases as the value of φ increases.

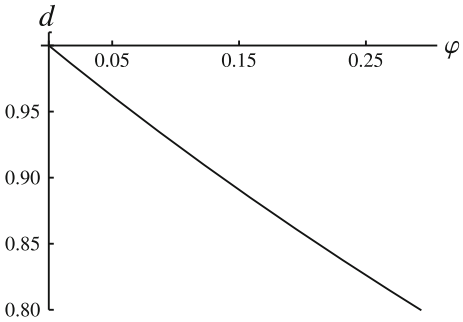

Fig. 31 Variation of the dimensionless strain rate intensity factor with φ

5.3 Flow of Plastic Material Through an Infinite Wedge-Shaped Channel

This boundary value problem has been formulated and solved for pressure-independent material in Sect. 3.3 (see Fig. 6). An extension of this solution to the double shearing model has been proposed in [36]. In particular, the velocity field is given by

$$u_r = -\frac{B}{r\,(\cos 2\psi + \sin\varphi - c)}, \quad u_\theta = 0, \tag{218}$$

where B and c are constants of integration and ψ is related to θ by the following equation

$$(\sin\varphi + \cos 2\psi)\left(\frac{d\psi}{d\theta} + 1\right) = c. \tag{219}$$

It is evident that the distribution of u_θ in (218) satisfies the boundary condition (55) at $\theta = 0$ and $\theta = \alpha$. The maximum friction surface is determined by the equation $\theta = \alpha$. Therefore, $\phi_1 = 0$ or $\phi_2 = 0$ in (204). The direction of the friction stress (Fig. 6) dictates that $\sigma_{r\theta} > 0$ at $\theta = \alpha$. The equation $\phi_2 = 0$ contradicts this inequality. Therefore, $\phi_1 = 0$ and

$$\psi = \psi_w = \frac{\pi}{4} + \frac{\varphi}{2} \tag{220}$$

at $\theta = \alpha$. On the other hand, it is reasonable to assume that $\sigma_{rr} > \sigma_{\theta\theta}$ at $\theta = 0$. Then, taking into account the boundary condition (56) and (199) it is possible to conclude that

$$\psi = 0 \tag{221}$$

at $\theta = 0$. The solution to Eq. (219) satisfying the boundary condition (220) is

$$\theta = \alpha - \int_{\psi}^{\psi_w} \frac{(\sin\varphi + \cos 2\gamma)}{(c - \sin\varphi - \cos 2\gamma)} d\gamma. \tag{222}$$

Here γ is a dummy variable of integration. Substituting the boundary condition (221) into the solution (222) gives the following equation for c

$$\alpha = \int_{0}^{\psi_w} \frac{(\sin\varphi + \cos 2\gamma)}{(c - \sin\varphi - \cos 2\gamma)} d\gamma. \tag{223}$$

This equation has been solved numerically. The variation of c with α for several φ-values is shown in Fig. 32. The broken line corresponds to $\varphi = 0$ (pressure-independent material), curve 1 to $\varphi = 0.1$, curve 2 to $\varphi = 0.2$, and curve 3 to $\varphi = 0.3$. Equation (219) in the vicinity of the maximum friction surface is represented as

$$\frac{d\psi}{d\theta} = \frac{c}{2\cos\varphi\,(\psi_w - \psi)} + o\left[(\psi_w - \psi)^{-1}\right] \quad \text{as} \quad \psi \to \psi_w. \tag{224}$$

Integrating with the use of the boundary condition (220) yields

$$\psi_w - \psi = \left(\frac{c}{\cos\varphi}\right)^{1/2} (\alpha - \theta)^{1/2} + o\left[(\alpha - \theta)^{1/2}\right] \quad \text{as} \quad \theta \to \alpha. \tag{225}$$

It has been taken into account here that $c > 0$ (Fig. 32). The shear strain rate is determined from (41), (218) and (219) as

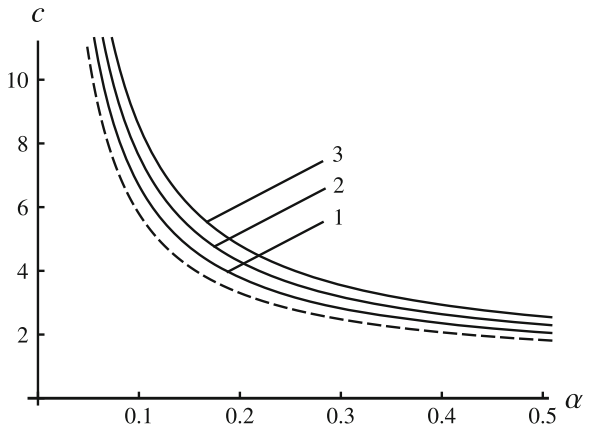

Fig. 32 Variation of c with α at several φ-values

$$\xi_{r\theta} = \frac{B \sin 2\psi}{r^2 \left(\sin\varphi + \cos 2\psi\right)\left(\cos 2\psi + \sin\varphi - c\right)}. \tag{226}$$

It is evident that the normal strain rates are bounded and $\xi_{r\theta} \to \infty$ as $\psi \to \psi_w$. Therefore, Eq. (6) in which ξ_τ is replaced with $\xi_{r\theta}$ is valid. Expanding the right hand side of (225) in a series in the vicinity of $\psi = \psi_w$ gives

$$\xi_{r\theta} = -\frac{B}{2cr^2\left(\psi_w - \psi\right)} + o\left[\left(\psi_w - \psi\right)^{-1}\right] \quad \text{as} \quad \psi \to \psi_w. \tag{227}$$

Combining (225) and (227) leads to

$$\xi_{r\theta} = -\frac{B\sqrt{\cos\varphi}}{2c^{3/2}r^2\left(\alpha - \theta\right)^{1/2}} + o\left[\left(\alpha - \theta\right)^{-1/2}\right] \quad \text{as} \quad \theta \to \alpha. \tag{228}$$

Comparing (6) and (228) shows that

$$D = -\frac{B\sqrt{\cos\varphi}}{\sqrt{3}\,(\mathrm{cr})^{3/2}}. \tag{229}$$

Substituting (218) into (63) and using (219) yields

$$B = -\frac{Q}{2}\left[\int_0^{\psi_w} \frac{\left(\sin\varphi + \cos 2\psi\right)}{\left(\cos 2\psi + \sin\varphi - c\right)^2} d\psi\right]^{-1}. \tag{230}$$

Since c has been found (Fig. 32), the integral here can be evaluated. Eliminating B in (229) by means of (230) shows that the strain rate intensity factor is a linear function of Q. In order to reveal the effect of α and φ on the strain rate intensity factor, it is convenient to introduce the dimensionless strain rate intensity factor, d, as the ratio of the strain rate intensity factor given by (229) to the strain rate intensity factor given by (62). The variation of d with α at several φ-values is depicted in Fig. 33. In this figure, curve 1 corresponds to $\varphi = 0.1$, curve 2 to $\varphi = 0.15$, curve 3 to $\varphi = 0.2$, curve 4 to $\varphi = 0.25$, and curve 5 to $\varphi = 0.3$. It is seen from this figure that the strain rate intensity factor at $\varphi \neq 0$ is smaller than the strain rate intensity factor for pressure-independent material in the entire range of parameters used in this study.

5.4 Compression of a Plastic Layer Between Cylindrical Surfaces

This boundary value problem has been formulated and solved for pressure-independent material in Sect. 3.4 (see Fig. 10). An extension of this solution to the double shearing model has been proposed in [37]. Let ψ_w be the value of ψ at $r = R_1$ and ψ_f be the value of ψ at $r = R_2$. The direction of flow in the region $\theta > 0$ demands

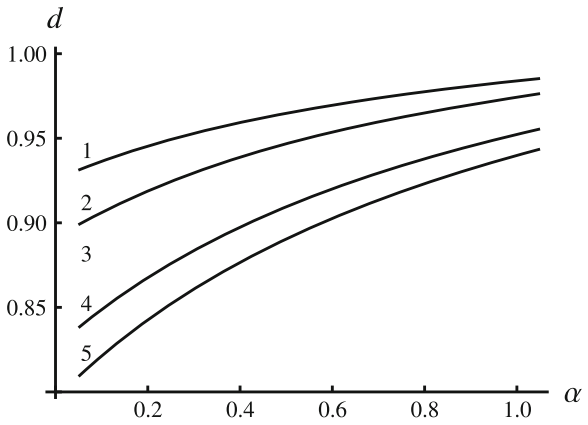

Fig. 33 Variation of the dimensionless strain rate intensity factor with α at several φ-values

$\sigma_{r\theta} > 0$ in the vicinity of the surface $r = R_1$ and $\sigma_{r\theta} < 0$ in the vicinity of the surface $r = R_2$. Then, it follows from (199) that

$$0 < \psi_w < \frac{\pi}{2} \quad \text{and} \quad \frac{\pi}{2} < \psi_f < \pi. \tag{231}$$

The maximum friction surfaces are orthogonal to the r-axis. Therefore, $\phi_1 = \pi/2$ or $\phi_2 = \pi/2$ in (198). The condition $\phi_1 = \pi/2$ contradicts (231) for ψ_w, and the condition $\phi_2 = \pi/2$ contradicts (231) for ψ_f. Therefore,

$$\psi = \psi_w = \frac{\pi}{4} - \frac{\varphi}{2} \qquad \text{for} \quad r = R_1 \tag{232}$$

and

$$\psi = \psi_f = \frac{3\pi}{4} + \frac{\varphi}{2} \qquad \text{for} \quad r = R_2. \tag{233}$$

It is seen from (232) and (233) that ψ is independent of θ at the maximum friction surfaces. Therefore, a natural assumption to find an approximate solution is that ψ is independent of θ. In this case substituting (199) into (42) and eliminating p by means of (191) result in

$$\begin{gathered}
\frac{(\cos 2\psi \sin\varphi - 1)}{\sin\varphi}\frac{\partial \ln q}{\partial r} + \sin 2\psi \frac{\partial \ln q}{r\partial\theta} \\
- 2\sin 2\psi \frac{d\psi}{dr} + \frac{2\cos 2\psi}{r} = 0, \\
- \frac{(\cos 2\psi \sin\varphi + 1)}{\sin\varphi}\frac{\partial \ln q}{r\partial\theta} + \sin 2\psi \frac{\partial \ln q}{\partial r} + 2\cos 2\psi \frac{d\psi}{dr} + \frac{2\sin 2\psi}{r} = 0.
\end{gathered} \tag{234}$$

Eliminating the derivative $\partial \ln q/\partial r$ between these two equations gives

$$-\cos\varphi\cot\varphi\frac{\partial\ln q}{r\partial\theta}+2\left(\cos 2\psi-\sin\varphi\right)\frac{d\psi}{dr}+\frac{2\sin 2\psi}{r}=0. \tag{235}$$

Since ψ is independent of θ, the first term of this equation must be independent of θ as well. It is possible if and only if

$$\ln\left(\frac{q}{k}\right)=\frac{2c\tan\varphi}{\cos\varphi}\theta+Q\left(\psi\right) \tag{236}$$

and

$$r\left(\cos 2\psi-\sin\phi\right)\frac{d\psi}{dr}=c-\sin 2\psi. \tag{237}$$

Here c is constant and $Q\left(\psi\right)$ is an arbitrary function of ψ. The function $Q\left(\psi\right)$ has no effect on the strain rate intensity factor. Therefore, Eq. (236) is not considered in the present chapter. The solution for the function $Q\left(\psi\right)$ is given in [37]. Equation (237) can be integrated in elementary functions. It is however more convenient to represent its solution satisfying the boundary condition (232) in the form

$$\ln\frac{r}{R_1}=\int\limits_{\psi_w}^{\psi}\frac{\left(\cos 2\gamma-\sin\varphi\right)}{\left(c-\sin 2\gamma\right)}d\gamma. \tag{238}$$

Here γ is a dummy variable of integration. Substituting the boundary condition (233) into (238) leads to the following equation for c

$$\ln\frac{R_2}{R_1}=\int\limits_{\psi_w}^{\psi_f}\frac{\left(\cos 2\gamma-\sin\varphi\right)}{\left(c-\sin 2\gamma\right)}d\gamma. \tag{239}$$

Numerical solution to this equation is illustrated in Fig. 34. The broken line corresponds to $\varphi=0$ (pressure-independent material), curve 1 to $\varphi=0.1$, curve 2 to $\varphi=0.2$, and curve 3 to $\varphi=0.3$.

The main assumption concerning the velocity field is that the radial velocity is independent of θ. Since ψ is also independent of θ, the radial velocity can be represented as

$$u_r=\dot{R}_1 v\left(\psi\right), \tag{240}$$

where $v(\psi)$ is an arbitrary function of ψ. It follows from (67), (68), (232) and (233) that the function $v(\psi)$ must satisfy the conditions

$$v=0\quad\text{at}\quad\psi=\psi_f\quad(\text{or}\quad r=R_2) \tag{241}$$

and

$$v=1\quad\text{at}\quad\psi=\psi_w\quad(\text{or}\quad r=R_1). \tag{242}$$

Substituting (240) into $(203)_1$ and taking into account that $v(\psi)$ is independent of θ yields

$$\frac{\partial u_\theta}{\dot{R}_1 \partial \theta} = -\frac{d\,(r\nu)}{dr}. \tag{243}$$

The right hand side of this equation is independent of θ. Therefore, integrating (243) gives

$$\frac{u_\theta}{\dot{R}_1} = -\theta \frac{d\,(r\nu)}{dr} + V\,(\psi)\,, \tag{244}$$

where $V\,(\psi)$ is an arbitrary function of ψ.

A distinguished feature of the present solution, as compared to the solutions given in Sects. 5.2 and 5.3, is that $\dot{\psi} \neq 0$. In particular, substituting (237) and (240) into $(202)_2$ and taking into account that $\partial\psi/\partial\theta = 0$ and $\partial\psi/\partial t = \dot{R}_1 \partial\psi/\partial R_1$ gives

$$\frac{\dot{\psi}}{\dot{R}_1} = \frac{\partial \psi}{\partial R_1} + \frac{v\,(c - \sin 2\psi)}{r\,(\cos 2\psi - \sin \varphi)}. \tag{245}$$

In order to find the derivative $\partial\psi/\partial R_1$, it is necessary to differentiate (238). Since ψ_w is constant, one gets

$$d\psi = \frac{(c - \sin 2\psi)}{r\,(\cos 2\psi - \sin \varphi)} dr + \frac{(c - \sin 2\psi)}{(\cos 2\psi - \sin \varphi)} \left[\frac{dc}{dR_1} \int_{\psi_w}^{\psi} \frac{(\cos 2\gamma - \sin \varphi)}{(c - \sin 2\gamma)^2} d\gamma - \frac{1}{R_1} \right] dR_1.$$

It follows from this equation that

$$\frac{\partial \psi}{\partial R_1} = \frac{(c - \sin 2\psi)}{(\cos 2\psi - \sin \varphi)} \left[\frac{dc}{dR_1} \int_{\psi_w}^{\psi} \frac{(\cos 2\gamma - \sin \varphi)}{(c - \sin 2\gamma)^2} d\gamma - \frac{1}{R_1} \right]. \tag{246}$$

In order to find the derivative dc/dR_1, it is necessary to differentiate (239). Since ψ_w, ψ_f and R_2 are constant, one gets

$$\frac{dc}{dR_1} = \frac{1}{R_1} \left[\int_{\psi_w}^{\psi_f} \frac{(\cos 2\gamma - \sin \varphi)}{(c - \sin 2\gamma)^2} d\gamma \right]^{-1}. \tag{247}$$

Substituting (247) into (246) gives

$$\frac{\partial \psi}{\partial R_1} = \frac{(c - \sin 2\psi)}{R_1\,(\cos 2\psi - \sin \varphi)} \left[\int_{\psi_w}^{\psi_f} \frac{(\cos 2\gamma - \sin \varphi)}{(c - \sin 2\gamma)^2} d\gamma \right]^{-1} \left[\int_{\psi_w}^{\psi} \frac{(\cos 2\gamma - \sin \varphi)}{(c - \sin 2\gamma)^2} d\gamma - 1 \right]. \tag{248}$$

Using (240), (243) and (244) Eq. $(203)_2$ transforms to

$$\theta\left[-r\left(\cos 2\psi-\sin\varphi\right)\frac{d^2\left(rv\right)}{dr^2}+\left(\cos 2\psi+\sin\varphi\right)\frac{d\left(rv\right)}{dr}\right]$$
$$+r\left(\cos 2\psi-\sin\varphi\right)\frac{dV}{dr}+2\left[v-\frac{d\left(rv\right)}{dr}\right]\sin 2\psi$$
$$-\left(\cos 2\psi+\sin\varphi\right)V+\frac{2r\dot{\psi}}{\dot{R}_1}\sin\varphi=0. \tag{249}$$

Since ψ, $\dot{\psi}$, v and V are independent of θ, this equation may have a solution if and only if

$$r\left(\cos 2\psi-\sin\varphi\right)\frac{d^2\left(rv\right)}{dr^2}-\left(\cos 2\psi+\sin\varphi\right)\frac{d\left(rv\right)}{dr}=0$$
$$r\left(\cos 2\psi-\sin\varphi\right)\frac{dV}{dr}-\left(\cos 2\psi+\sin\varphi\right)V \tag{250}$$
$$+2\left[v-\frac{d\left(rv\right)}{dr}\right]\sin 2\psi+\frac{2r\dot{\psi}}{\dot{R}_1}\sin\varphi=0.$$

Introduce the following notation $Y\left(\psi\right)=d\left(rv\right)/dr$. Then, Eq. $(244)_1$ transforms to

$$r\left(\cos 2\psi-\sin\varphi\right)\frac{dY}{d\psi}\frac{d\psi}{dr}-\left(\cos 2\psi+\sin\varphi\right)Y=0. \tag{251}$$

Eliminating in this equation the derivative $d\psi/dr$ by means of (237) and integrating yields

$$Y=\frac{d\left(rv\right)}{dr}=Y_0\exp\left[\int\limits_{\psi_w}^{\psi}\frac{\left(\cos 2\gamma+\sin\varphi\right)}{\left(c-\sin 2\gamma\right)}d\gamma\right]. \tag{252}$$

Here Y_0 is a constant of integration. Replacing integration with respect to r with integration with respect to ψ in (252) by means of (237) and integrating with the boundary condition (242) result in

$$v\left(\psi\right)=\frac{R_1}{r}\left(Y_0\int\limits_{\psi_w}^{\psi}\exp\left[\int\limits_{\psi_w}^{\eta}\frac{\left(\cos 2\gamma+\sin\varphi\right)}{\left(c-\sin 2\gamma\right)}d\gamma\right]\frac{\left(\cos 2\eta-\sin\varphi\right)}{\left(c-\sin 2\eta\right)}\frac{r}{R_1}d\eta+1\right). \tag{253}$$

Here η is a dummy variable of integration. The value of Y_0 is determined from the solution (253) and the boundary condition (241) as

$$Y_0 = -\left\{\int_{\psi_w}^{\psi_f} \exp\left[\int_{\psi_w}^{\eta} \frac{(\cos 2\gamma + \sin\varphi)}{(c - \sin 2\gamma)} d\zeta\right] \frac{(\cos 2\eta - \sin\varphi)}{(c - \sin 2\eta)} \frac{r}{R_1} d\eta\right\}^{-1}. \quad (254)$$

Since the value of c has been found (Fig. 34), eliminating r/R_1 by means of (238) the integrals in (253) and (254) can be evaluated numerically. Since r/R_1 and $d\,(rv)/dr$ are known functions of ψ due to (238), (252), (253), and (254), it is evident that Eq. $(250)_2$ is a linear ordinary differential equation for $V\,(\psi)$. Its general solution is

$$V\,(\psi) = 2Y\,(\psi)\left[\int_{\psi_w}^{\psi} \frac{\left\{[Y\,(\gamma) - v\,(\gamma)]\sin 2\gamma - \sin\varphi\dot{\psi}r/\dot{R}_1\right\}}{(c - \sin 2\gamma)\,Y\,(\gamma)} d\gamma + V_0\right]. \quad (255)$$

Here V_0 is a constant of integration. The integral in (255) can be evaluated numerically. The value of V_0 is found from the condition (69) integrated over the thickness of the layer. Using (238), (245) and (248) the quantity $\dot{\psi}r/\dot{R}_1$ is represented as

$$\frac{\dot{\psi}r}{\dot{R}_1} = \frac{(c - \sin 2\psi)}{(\cos 2\psi - \sin\varphi)} m\,(\psi)\,,$$

$$m\,(\psi) = v + \exp\left[\int_{\psi_w}^{\psi} \frac{(\cos 2\gamma - \sin\varphi)}{(c - \sin 2\gamma)} d\gamma\right] \quad (256)$$

$$\times \left\{\left[\int_{\psi_w}^{\psi_f} \frac{(\cos 2\gamma - \sin\varphi)}{(c - \sin 2\gamma)^2} d\gamma\right]^{-1} \int_{\psi_w}^{\psi} \frac{(\cos 2\gamma - \sin\varphi)}{(c - \sin 2\gamma)^2} d\gamma - 1\right\}.$$

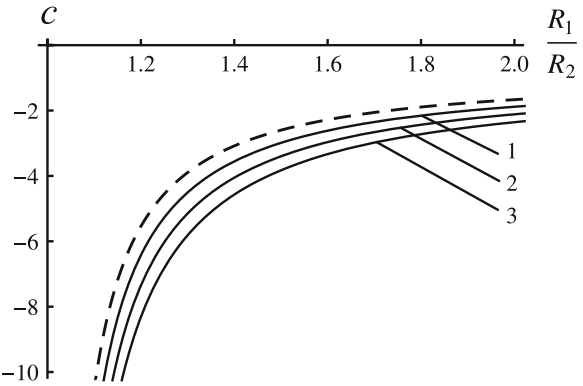

Fig. 34 Variation of c with R_1/R_2 at several φ-values

In order to determine the strain rate intensity factors, it is necessary to find the values of $\dot{\psi} r \dot{R}_1^{-1}$ at the maximum friction surfaces. Moreover, it follows from the boundary conditions (241) and (242) that the right hand side of (256) reduces to the expression $0/0$ at $\psi = \psi_w$ and $\psi = \psi_f$. It is evident that the derivative of the denominator with respect to ψ is equal to a finite value at $\psi = \psi_w$ and $\psi = \psi_f$. It follows from (237) and (253) that $\partial r/\partial\psi = 0$ and $\partial v/\partial\psi = 0$ at these points. Therefore, applying l'Hospital's rule,

$$\frac{\dot{\psi} r}{\dot{R}_1} = 0 \qquad \text{at} \quad \psi = \psi_w \quad \text{and} \psi = \psi_f. \tag{257}$$

The shear strain rate is determined from (41) where differentiation with respect to r is replaced with differentiation with respect to ψ by means of (237). Then,

$$2\xi_{r\theta} = \frac{\partial u_\theta}{r\partial\psi} \frac{(c - \sin 2\psi)}{(\cos 2\psi - \sin\varphi)} - \frac{u_\theta}{r}. \tag{258}$$

It has been taken into account here that $\partial u_r/\partial\theta = 0$. It is now necessary to find the derivative $\partial u_\theta/\partial\psi$ at $\psi = \psi_w$ and $\psi = \psi_f$. It follows from (244) and (252) that

$$\frac{\partial u_\theta}{U\partial\psi} = -\theta\frac{dY}{d\psi} + \frac{dV}{d\psi}. \tag{259}$$

The derivative $dY/d\psi$ at $\psi = \psi_w$ and $\psi = \psi_f$ is found from (252) as

$$\left.\frac{dY}{d\psi}\right|_{\psi=\psi_w} = \frac{2Y_0 \sin\varphi}{c - \cos\varphi}, \quad \left.\frac{dY}{d\psi}\right|_{\psi=\psi_f} = \frac{2wY_0 \sin\varphi}{c + \cos\varphi}, \tag{260}$$
$$w = \exp\left[\int_{\psi_w}^{\psi_f} \frac{(\cos 2\gamma + \sin\varphi)}{(c - \sin 2\gamma)} d\gamma\right].$$

It is seen from (255) and (260) that the derivative $dV/d\psi$ is finite at $\psi = \psi_w$ and $\psi = \psi_f$. Therefore, it is evident from (258) that $|\xi_{r\theta}| \to \infty$ as $\psi \to \psi_w$ and $\psi \to \psi_f$. The second term in (258) has no effect on this singular behaviour of the shear strain rate since the value of u_θ is finite. Therefore, expanding $\cos 2\psi - \sin\varphi$ in a series in the vicinity of points $\psi = \psi_w$ and $\psi = \psi_f$ Eq. (258) is represented as

$$\begin{aligned}
\xi_{r\theta} &= -\frac{\dot{R}_1 (c - \cos\varphi)}{4R_1 \cos\varphi} \left(\frac{dV}{d\psi} - \theta\frac{dY}{d\psi}\right)\Bigg|_{\psi=\psi_w} (\psi - \psi_w)^{-1} \\
&\quad + o\left[(\psi - \psi_w)^{-1}\right] \quad \text{as} \quad \psi \to \psi_w \\
\xi_{r\theta} &= -\frac{U (c + \cos\varphi)}{4R_2 \cos\varphi} \left(\frac{dV}{d\psi} - \theta\frac{dY}{d\psi}\right)\Bigg|_{\psi=\psi_f} (\psi_f - \psi)^{-1} \\
&\quad + o\left[(\psi_f - \psi)^{-1}\right] \quad \text{as} \quad \psi \to \psi_f.
\end{aligned} \tag{261}$$

Here Eq. (259) has been taken into account. Differentiating (255) with the use of (241), (242), (252), (257), and (260) gives

$$\begin{aligned} \left.\frac{dV}{d\psi}\right|_{\psi=\psi_w} &= \tfrac{2}{(c-\cos\varphi)}\left[2Y_0V_0\sin\varphi+(Y_0-1)\cos\varphi\right], \\ \left.\frac{dV}{d\psi}\right|_{\psi=\psi_f} &= \frac{2Y_0w}{(c+\cos\varphi)}\left[2\left(V_0+w_1\right)\sin\varphi-\cos\varphi\right], \end{aligned} \tag{262}$$

where

$$w_1=\int\limits_{\psi_w}^{\psi_f}\frac{\left\{\left[Y\left(\gamma\right)-v\left(\gamma\right)\right]\sin 2\gamma-\sin\varphi\dot{\psi}r/\dot{R}_1\right\}}{\left(c-\sin 2\gamma\right)Y\left(\gamma\right)}d\gamma. \tag{263}$$

Substituting (260) and (262) into (261) yields

$$\begin{aligned} \xi_{r\theta} =& -\frac{U}{2R_1\cos\varphi}\left[2Y_0V_0\sin\varphi+(Y_0-1)\cos\varphi-\theta Y_0\sin\varphi\right]\left(\psi-\psi_w\right)^{-1} \\ &+o\left[\left(\psi-\psi_w\right)^{-1}\right] \quad \text{as} \quad \psi\to\psi_w, \\ \xi_{r\theta} =& -\frac{UY_0w}{2R_2\cos\varphi}\left[2\left(V_0+w_1\right)\sin\varphi-\cos\varphi-\theta\sin\varphi\right]\left(\psi_f-\psi\right)^{-1} \\ &+o\left[\left(\psi_f-\psi\right)^{-1}\right] \quad \text{as} \quad \psi\to\psi_f. \end{aligned} \tag{264}$$

Equation (237) in the vicinity of points $\psi=\psi_w$ and $\psi=\psi_f$ is represented as

$$\begin{aligned} \frac{d\psi}{dr} &= -\frac{(c-\cos\varphi)}{2R_1\cos\varphi\left(\psi-\psi_w\right)}+o\left[\left(\psi-\psi_w\right)^{-1}\right] \quad \text{as} \quad \psi\to\psi_w, \\ \frac{d\psi}{dr} &= -\frac{(c+\cos\varphi)}{2R_2\cos\varphi\left(\psi_f-\psi\right)}+o\left[\left(\psi_f-\psi\right)^{-1}\right] \quad \text{as} \quad \psi\to\psi_f, \end{aligned} \tag{265}$$

respectively. Integrating the first of these equations with the boundary condition (232) gives

$$\psi-\psi_w=\sqrt{-\frac{(c-\cos\varphi)}{R_1\cos\varphi}}\sqrt{r-R_1}+o\left(\sqrt{r-R_1}\right) \quad \text{as} \quad r\to R_1. \tag{266}$$

Integrating $(265)_2$ with the boundary condition (233) gives

$$\psi_f-\psi=\sqrt{-\frac{(c+\cos\varphi)}{R_2\cos\varphi}}\sqrt{R_2-r}+o\left(\sqrt{R_2-r}\right) \quad \text{as} \quad r\to R_2. \tag{267}$$

Since the normal strain rates are finite as $r\to R_1$ and $r\to R_2$, Eq. (6) in which ξ_τ should be replaced with $\xi_{r\theta}$ is valid. Substituting (266) into $(264)_1$ and comparing

to (6) show that

$$D_1 = \frac{\dot{R}_1}{\sqrt{3R_1 \cos\varphi}} \frac{|2Y_0V_0 \sin\varphi + (Y_0 - 1)\cos\varphi - \theta Y_0 \sin\varphi|}{\sqrt{\cos\varphi - c}}, \tag{268}$$

where D_1 is the strain rate intensity factor corresponding to the maximum friction surface $r = R_1$. Analogously, it follows from $(265)_2$, (267) and (6) that the strain rate intensity factor corresponding to the maximum friction surface $r = R_2$ is

$$D_2 = \frac{\dot{R}_1 |Y_0 w|}{\sqrt{3R_2 \cos\varphi}} \frac{|2(V_0 + w_1)\sin\varphi - \cos\varphi - \theta \sin\varphi|}{\sqrt{-(c + \cos\varphi)}}. \tag{269}$$

The right hand sides of (268) and (269) can be evaluated using (254) and (263) .

It is of interest to introduce the ratio $\Delta = D_1/D_2$. It follows from (268) and (269) that

$$\Delta = \sqrt{\frac{R_2}{R_1}} \frac{|2Y_0V_0 \sin\varphi + (Y_0 - 1)\cos\varphi - \theta Y_0 \sin\varphi| \sqrt{-(c + \cos\varphi)}}{|Y_0 w|\,|2(V_0 + w_1)\sin\varphi - \cos\varphi - \theta \sin\varphi| \sqrt{\cos\varphi - c}}. \tag{270}$$

The variation of Δ with R_1/R_2 at $\theta = 1$ and $\theta = 1.5$ is shown in Figs. 35 and 36, respectively. The broken line corresponds to the solution for pressure-independent material (see Sect. 3.4) curve 1 corresponds to $\varphi = 0.1$, curve 2 to $\varphi = 0.15$, curve 3 to $\varphi = 0.2$, curve 4 to $\varphi = 0.25$, and curve 5 to $\varphi = 0.3$. The dependence of Δ on θ for several values of R_1/R_2 at $\varphi = 0.1$, $\varphi = 0.2$ and $\varphi = 0.3$ is depicted in Figs. 37, 38 and 39, respectively. Curve 1 corresponds to $R_1/R_2 = 0.5$, curve 2 to $R_1/R_2 = 0.7$, and curve 3 to $R_1/R_2 = 0.9$. In order to illustrate the effect of pressure-dependency of the yield criterion on the strain rate intensity factors, it is convenient to introduce the ratios of the strain rate intensity factors given in (268) and (269) to the respective strain rate intensity factors from the solution for the pressure-independent model. These ratios are denoted by d_1 and d_2 where d_1 is related to the surface $r = R_1$ and d_2 to the surface $r = R_2$. Since the strain rate intensity factors for the model of pressure-independent plasticity are given in (78), the values of d_1 and d_2 can be found with no difficulty. It is evident from (78), (268) and (269) that d_1 and d_2 are linear functions of θ. The dependence of d_1 on θ at $\varphi = 0.1$, $\varphi = 0.2$ and $\varphi = 0.3$ is depicted in Figs. 40, 41 and 42, and the dependence of d_2 on θ at the same values of φ in Figs. 43, 44 and 45 (curve 1 corresponds to $R_1/R_2 = 0.5$, curve 2 to $R_1/R_2 = 0.7$, curve 3 to $R_1/R_2 = 0.9$). The variation of d_1 and d_2 with R_1/R_2 at $\theta = 1$ is depicted in Figs. 46 and 47, respectively. In these figures, curve 1 corresponds to $\varphi = 0.1$, curve 2 to $\varphi = 0.15$, curve 3 to $\varphi = 0.2$, curve 4 to $\varphi = 0.25$, and curve 5 to $\varphi = 0.3$. It is seen from Figs. 40, 41, 42, 43, 44, 45, 46 and 47 that $d_1 < 1$ and $d_2 < 1$. Thus pressure-dependency of the yield criterion leads to a decrease in the magnitude of the strain rate intensity factor in the process under consideration.

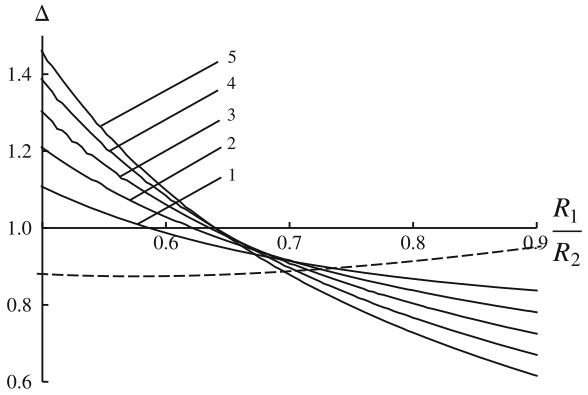

Fig. 35 Variation of Δ with R_1/R_2 at $\theta = 1$

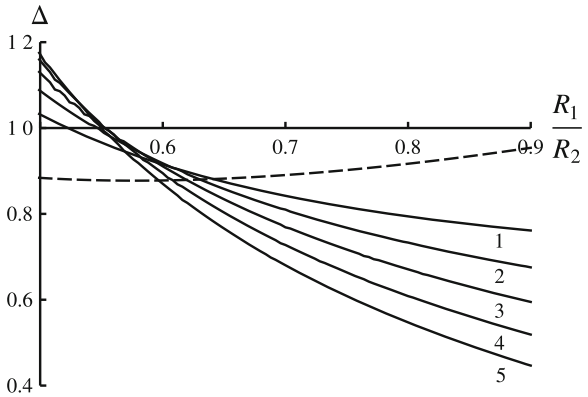

Fig. 36 Variation of Δ with R_1/R_2 at $\theta = 1.5$

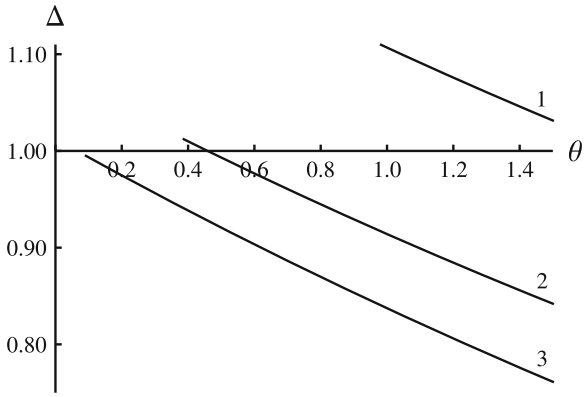

Fig. 37 Dependence of Δ on θ at $\varphi = 0.1$ and several R_1/R_2-values

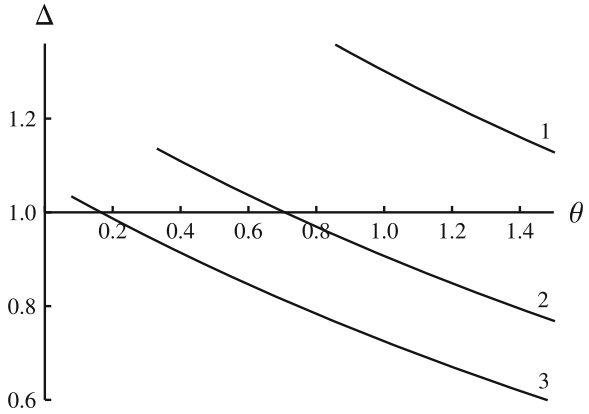

Fig. 38 Dependence of Δ on θ at $\varphi = 0.2$ and several R_1/R_2-values

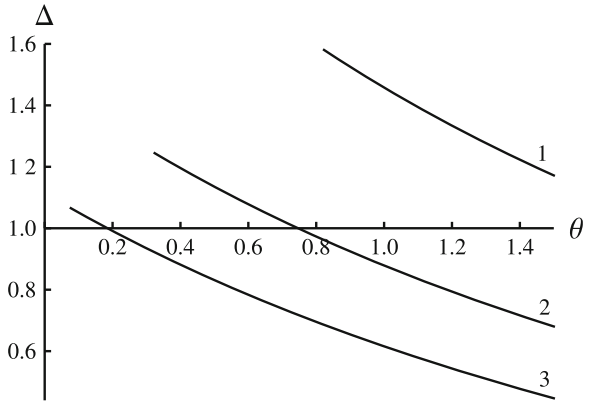

Fig. 39 Dependence of Δ on θ at $\varphi = 0.3$ and several R_1/R_2-values

5.5 Compression of a Plastic Layer Between Rotating Plates I

This boundary value problem has been formulated and solved for pressure-independent material in Sect. 3.5 (see Fig. 11). An extension of this solution to the double shearing model has been proposed in [38].

Let ψ_w be the value of ψ at the maximum friction surface $\theta = \alpha$. The direction of flow (Fig. 11) dictates that $\sigma_{r\theta} < 0$ near the friction surface. Therefore, it follows from (199) that

$$-\frac{\pi}{2} < \psi_w < 0. \tag{271}$$

The maximum friction surface is parallel to the r-axis. Therefore, $\phi_1 = 0$ or $\phi_2 = 0$ in (204). The equation $\phi_1 = 0$ contradicts (271). Therefore, $\phi_2 = 0$ and

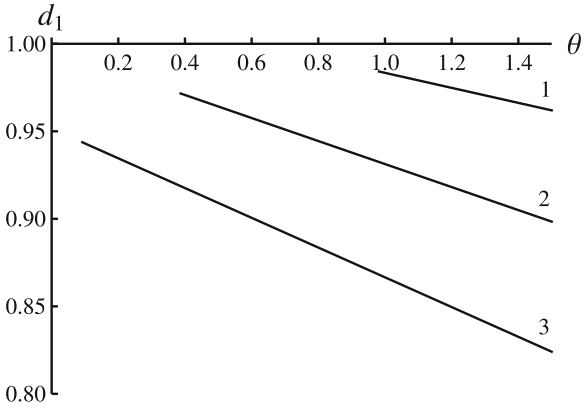

Fig. 40 Dependence of d_1 on θ at $\varphi = 0.1$ and several R_1/R_2-values

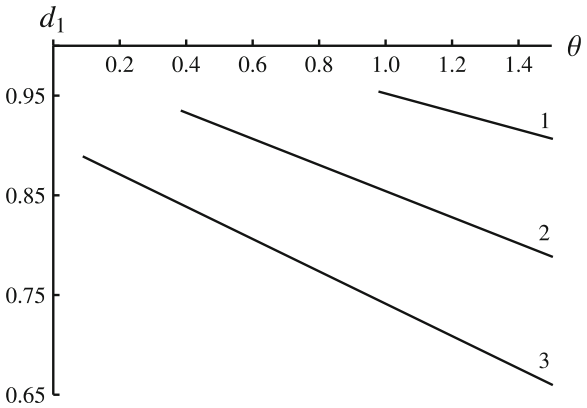

Fig. 41 Dependence of d_1 on θ at $\varphi = 0.2$ and several R_1/R_2-values

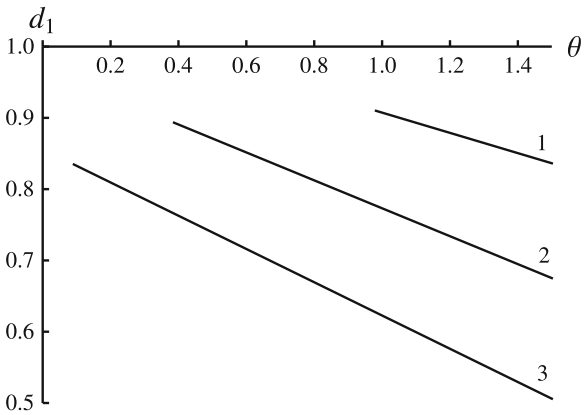

Fig. 42 Dependence of d_1 on θ at $\varphi = 0.3$ and several R_1/R_2-values

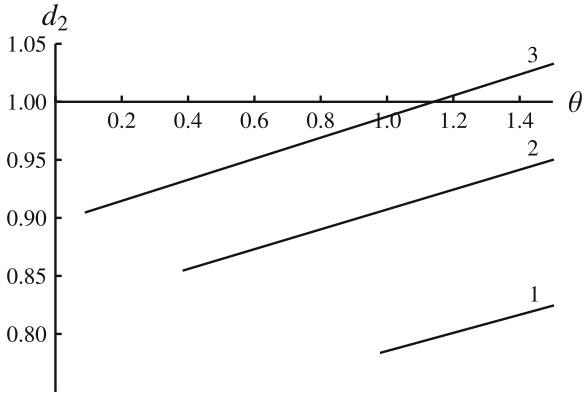

Fig. 43 Dependence of d_2 on θ at $\varphi = 0.1$ and several R_1/R_2-values

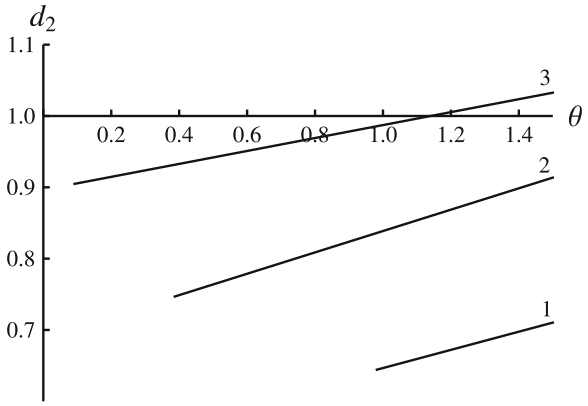

Fig. 44 Dependence of d_2 on θ at $\varphi = 0.2$ and several R_1/R_2-values

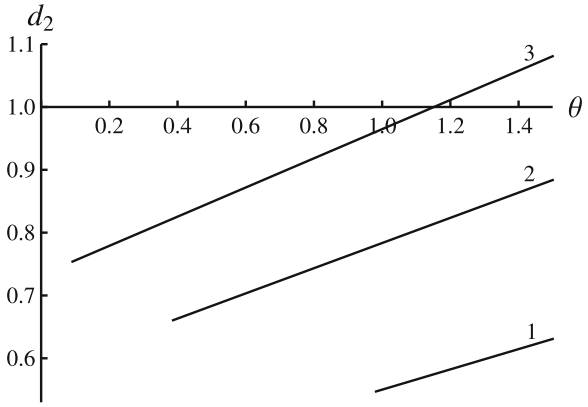

Fig. 45 Dependence of d_2 on θ at $\varphi = 0.3$ and several R_1/R_2-values

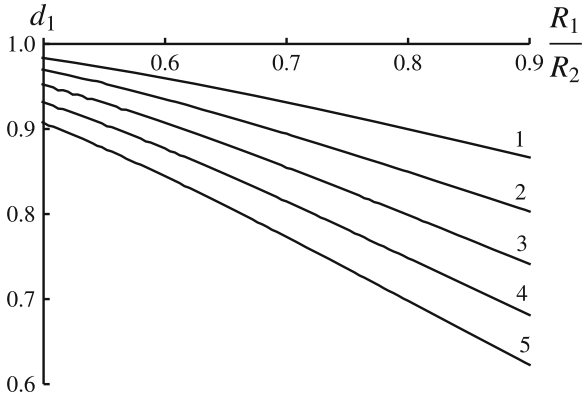

Fig. 46 Variation of d_1 with R_1/R_2 at $\theta = 1$ and at several φ-values

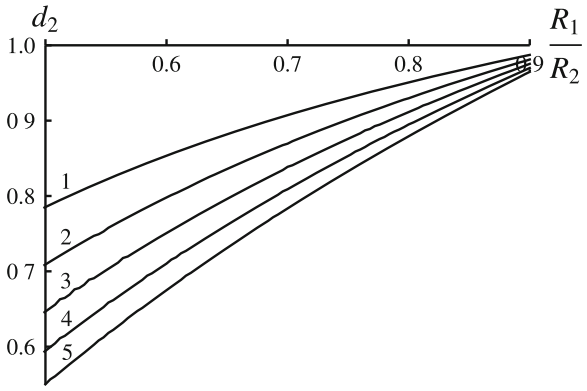

Fig. 47 Variation of d_2 with R_1/R_2 at $\theta = 1$ and at several φ-values

$$\psi = \psi_w = -\frac{\pi}{4} - \frac{\varphi}{2} \quad \text{for} \quad \theta = \alpha. \tag{272}$$

The main assumption accepted in [38] is that ψ is independent of r. Note that this assumption is in agreement with (272). Substituting (191) and (199) into (42) gives

$$\begin{aligned} r\frac{(\cos 2\psi \sin\varphi - 1)}{\sin\varphi}\frac{\partial \ln q}{\partial r} + \sin 2\psi \frac{\partial \ln q}{\partial \theta} + 2\cos 2\psi \left(\frac{d\psi}{d\theta} + 1\right) = 0, \\ -\frac{(\cos 2\psi \sin\varphi + 1)}{\sin\varphi}\frac{\partial \ln q}{\partial \theta} + r\sin 2\psi \frac{\partial \ln q}{\partial r} + 2\sin 2\psi \left(\frac{d\psi}{d\theta} + 1\right) = 0. \end{aligned} \tag{273}$$

Eliminating the derivative $\partial \ln q/\partial\theta$ between these equations yields

$$r\frac{\partial \ln q}{\partial r} = \frac{2\sin\varphi\,(\sin\varphi + \cos 2\psi)}{\cos^2\varphi}\left(\frac{d\psi}{d\theta} + 1\right). \tag{274}$$

The right hand side of this equation is independent of r. Therefore, integrating gives

$$\ln q = \frac{2\sin\varphi\,(\sin\varphi+\cos 2\psi)}{\cos^2\varphi}\left(\frac{d\psi}{d\theta}+1\right)\ln r + Q\,(\theta)\,, \tag{275}$$

where $Q\,(\theta)$ is an arbitrary function of θ. Substituting (275) into $(273)_2$ results in

$$-\frac{2\,(\cos 2\psi\sin\varphi+1)}{\cos^2\varphi}\frac{d}{d\theta}\left[(\sin\varphi+\cos 2\psi)\left(\frac{d\psi}{d\theta}+1\right)\right]\ln r \tag{276}$$
$$-\frac{dQ}{d\theta}\frac{(\cos 2\psi\sin\varphi+1)}{\sin\varphi}+\frac{2\sin 2\psi\,(1+\sin\varphi\cos 2\psi)}{\cos^2\varphi}\left(\frac{d\psi}{d\theta}+1\right)=0.$$

This equation can have a solution if and only if the coefficient of $\ln r$ vanishes. Therefore,

$$(\sin\varphi+\cos 2\psi)\left(\frac{d\psi}{d\theta}+1\right)=c, \tag{277}$$

where c is constant. Substituting (277) into (276) results in

$$\frac{dQ}{d\theta}=\frac{2c\sin\varphi\sin 2\psi}{\cos^2\varphi\,(\sin\varphi+\cos 2\psi)}. \tag{278}$$

Replacing here differentiation with respect to θ with differentiation with respect to ψ by means of (277) and integrating yield

$$Q=\frac{c\sin\varphi}{\cos^2\varphi}\ln|c-\sin\varphi-\cos 2\psi|+Q_0, \tag{279}$$

where Q_0 is a constant of integration. The solution to Eq. (277) satisfying the boundary condition (272) is

$$\theta=\alpha-\int_{\psi}^{\psi_w}\frac{(\sin\varphi+\cos 2\gamma)}{(c-\sin\varphi-\cos 2\gamma)}d\gamma, \tag{280}$$

where γ is a dummy variable of integration. It follows from (37) and (81) that $\psi=0$ at $\theta=0$. Using this condition the equation for c is obtained from (280) in the form

$$\alpha=\int_{0}^{\psi_w}\frac{(\sin\varphi+\cos 2\gamma)}{(c-\sin\varphi-\cos 2\gamma)}d\gamma. \tag{281}$$

Numerical solution to this equation is illustrated in Fig. 48. The broken line corresponds to pressure-independent material, curve 1 to $\varphi=0.1$, curve 2 to $\varphi=0.2$,

and curve 3 to $\varphi = 0.3$. In the case of $c = 0$ Eq. (281) is immediately integrated to give $\alpha = \pi/4 + \varphi/2$. It is seen from Fig. 48 that $c < 0$ for $\alpha < \pi/4 + \varphi/2$.

It is necessary to find the derivative $dc/d\alpha$ to determine the strain rate intensity factor. Differentiating (281) gives

$$\frac{dc}{d\alpha} = -\left[\int_0^{\psi_w} \frac{(\sin\varphi + \cos 2\gamma)}{(c - \sin\varphi - \cos 2\gamma)^2} d\gamma\right]^{-1}. \tag{282}$$

At $c = 0$ one gets

$$I(\psi) = \int_0^{\psi} \frac{(\sin\phi + \cos 2\zeta)}{(A - \sin\phi - \cos 2\zeta)^2} d\zeta = \int_0^{\psi} \frac{d\zeta}{(\sin\phi + \cos 2\zeta)}$$
$$= \operatorname{arctanh}\left(\frac{\cos\phi \tan\psi}{1 + \sin\phi}\right) \frac{1}{\cos\phi}.$$

Hence $\lim\limits_{\psi \to \psi_w} I(\psi) = -\infty$ and it follows from (282) that

$$\frac{dc}{d\alpha} = 0 \quad \text{at} \quad c = 0. \tag{283}$$

The velocity field is sought in the form [38]

$$u_r = \frac{\omega r}{2} \frac{\partial g(\psi, \alpha)}{\partial \theta}, \qquad u_\theta = -\omega r g(\psi, \alpha), \tag{284}$$

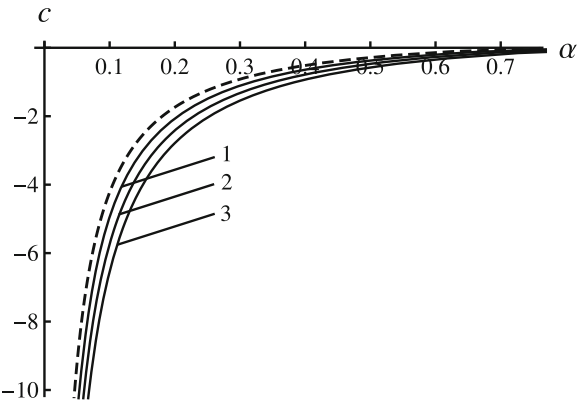

Fig. 48 Variation of c with α at several φ-values

where $g\ (\psi,\ \alpha)$ is an arbitrary function of ψ and α. The velocity field (284) automatically satisfies the equation of incompressibility $(203)_1$. Using (284) the boundary conditions (79) and (80) transform to

$$g = 0 \quad \text{for} \quad \theta = 0 \quad (\text{or} \quad \psi = 0) \tag{285}$$

and

$$g = 1 \quad \text{for} \quad \theta = \alpha \quad (\text{or} \quad \psi = \psi_w). \tag{286}$$

Substituting (284) into $(203)_2$ gives

$$(\cos 2\psi + \sin\varphi)\frac{d^2g}{d\theta^2} - 2\sin 2\psi\frac{dg}{d\theta} + 4g\sin\varphi + 4\sin\varphi\frac{\dot{\psi}}{\omega} = 0. \tag{287}$$

The derivative $d\psi/d\theta$ is found from (277). Subsequent differentiation of this derivative with respect to θ gives

$$\frac{d^2\psi}{d\theta^2} = \frac{2c\sin 2\psi\,(c - \sin\varphi - \cos 2\psi)}{(\sin\varphi + \cos 2\psi)^3}. \tag{288}$$

On the other hand,

$$\frac{dg}{d\theta} = \frac{dg}{d\psi}\frac{d\psi}{d\theta}, \quad \frac{d^2g}{d\theta^2} = \frac{d^2g}{d\psi^2}\left(\frac{d\psi}{d\theta}\right)^2 + \frac{dg}{d\psi}\frac{d^2\psi}{d\theta^2}. \tag{289}$$

Replacing in (287) differentiation with respect to θ with differentiation with respect to ψ by means of (289) and using (277) and (288) leads to

$$\begin{aligned}(\sin\varphi + \cos 2\psi)\frac{d^2g}{d\psi^2} + 2\sin 2\psi\frac{dg}{d\psi}\\ + \frac{4\sin\varphi\,(\sin\varphi + \cos 2\psi)^2}{(c - \sin\varphi - \cos 2\psi)^2}\left(g + \frac{\dot{\psi}}{\omega}\right) = 0.\end{aligned} \tag{290}$$

Since $\partial\psi/\partial t = -\omega\partial\psi/\partial\alpha$, it follows from (202) and (277) that

$$\frac{\dot{\psi}}{\omega} = -\frac{\partial\psi}{\partial\theta_0} - \left(\frac{c - \sin\varphi - \cos 2\psi}{\sin\varphi + \cos 2\psi}\right)g. \tag{291}$$

Differentiating (280) gives

$$\frac{(\sin\varphi+\cos 2\psi)}{(c-\sin\varphi-\cos 2\psi)}d\psi + \left\{1+\frac{dc}{d\alpha}\left[\int_{\psi}^{\psi_w}\frac{(\sin\varphi+\cos 2\gamma)}{(c-\sin\varphi-\cos 2\gamma)^2}d\gamma\right]\right\}d\alpha - d\theta = 0. \tag{292}$$

Determining the derivative $\partial\psi/\partial\alpha$ from this equation and substituting it into (291) lead to

$$\frac{\dot{\psi}}{\omega} = \left\{1-g+\frac{dc}{d\alpha}\left[\int_{\psi}^{\psi_w}\frac{(\sin\varphi+\cos 2\gamma)}{(c-\sin\varphi-\cos 2\gamma)^2}d\gamma\right]\right\} \times\frac{(c-\sin\varphi-\cos 2\psi)}{(\sin\varphi+\cos 2\psi)}. \tag{293}$$

Eliminating $\dot{\psi}/\omega$ in (290) by means of (293) results in a linear ordinary differential equation for $g\,(\psi)$ in the form

$$\begin{aligned}(\sin\varphi+\cos 2\psi)\frac{d^2g}{d\psi^2}+2\sin 2\psi\frac{dg}{d\psi}+P_1(\psi)\,g &= P_0(\psi),\\ P_1(\psi) &= \frac{4\sin\varphi\,(\sin\varphi+\cos 2\psi)\,(2\sin\varphi+2\cos 2\psi-c)}{(c-\sin\varphi-\cos 2\psi)^2},\\ P_0(\psi) &= -\frac{4\sin\varphi\,(\sin\varphi+\cos 2\psi)}{(c-\sin\varphi-\cos 2\psi)}\left\{\frac{dc}{d\alpha}\left[\int_{\psi}^{\psi_w}\frac{(\sin\varphi+\cos 2\gamma)}{(c-\sin\varphi-\cos 2\gamma)^2}d\gamma\right]+1\right\}.\end{aligned} \tag{294}$$

Expanding the coefficients of this equation in series in the vicinity of $\psi=\psi_w$ gives

$$\begin{aligned}\sin\varphi+\cos 2\psi =& 2\cos\varphi\,(\psi-\psi_w)+2\sin\varphi\,(\psi-\psi_w)^2\\ &-\frac{4}{3}\cos\varphi\,(\psi-\psi_w)^3+o\left[(\psi-\psi_w)^3\right],\\ 2\sin 2\psi =& -2\cos\varphi-4\sin\varphi\,(\psi-\psi_w)+4\cos\varphi\,(\psi-\psi_w)^2\\ &+\frac{8}{3}\sin\varphi\,(\psi-\psi_w)^3+o\left[(\psi-\psi_w)^3\right],\\ P_1(\psi) =& -\frac{4\sin 2\varphi}{c}(\psi-\psi_w)-\frac{8\sin^2\varphi}{c}(\psi-\psi_w)^2\\ &+\frac{8\sin 2\varphi}{c}\left(\frac{1}{3}+\frac{2\cos^2\varphi}{c^2}\right)(\psi-\psi_w)^3+o\left[(\psi-\psi_w)^3\right],\end{aligned} \tag{295}$$

$$P_0(\psi) = -\frac{4\sin 2\varphi}{c}(\psi-\psi_w) - \frac{8\sin\varphi\,(1+\cos 2\varphi + c\sin\varphi)}{c^2}(\psi-\psi_w)^2 - \frac{4\sin 2\varphi}{3c^3}\left[2\left(3-c^2+3\cos 2\varphi+6c\sin\varphi\right) - 3\cos\varphi\frac{dc}{d\alpha}\right](\psi-\psi_w)^3 + o\left[(\psi-\psi_w)^3\right]$$

as $\psi \to \psi_w$. It is seen from (295) that $\psi = \psi_w$ is a regular singular point of Eq. (294). Using a standard procedure it is possible to find that the two linearly independent primitive solutions of the corresponding homogeneous equation are represented as

$$g_1 = O\left[(\psi-\psi_w)^2\right] \quad \text{as} \quad \psi \to \psi_w \tag{296}$$

and

$$g_2 = P(\psi) + Cg_1 \ln(\psi-\psi_w), \tag{297}$$

where $P(\psi)$ is a function of ψ represented by a Taylor series in the vicinity of $\psi = \psi_w$ and C is an arbitrary constant. It is possible to show (see [38]) that C must vanish and that $P(\psi)$ does not contain the term $O(\psi-\psi_w)$ as $\psi \to \psi_w$. Then, it follows from (296), (297) and the boundary condition (286) that the function $g(\psi)$ is approximated by

$$g = 1 + c_2(\psi-\psi_w)^2 + c_3(\psi-\psi_w)^3 \tag{298}$$

in the vicinity of point $\psi = \psi_w$. Substituting (295) and (298) into (294) yields

$$c_3 = \frac{2}{3}c_2\tan\varphi - \frac{4\sin 2\varphi}{3c^2}. \tag{299}$$

It has been shown before that $c \le 0$ (Fig. 48). However, it follows from (295) and (299) that the special case $c = 0$ should be treated separately. In order to clarify the general structure of the solution for values of c in the vicinity of $c = 0$, it is necessary to find the radial velocity at $\psi = \psi_w$ (i.e. at the maximum friction surface). It follows from (277), (284), (295), and (298) that

$$u_r = \frac{\omega r}{2}\frac{cc_2}{\cos\varphi} + o(1) \quad \text{as} \quad \psi \to \psi_w. \tag{300}$$

It is seen from this equation that u_r at $\psi = \psi_w$ vanishes if $c_2 = 0$. This means that the regime of sticking occurs. Let $\alpha_{\rm cr}$ be the value of α corresponding to the condition $c_2 = 0$. Assume that

$$0 < \alpha_{\rm cr} < \frac{\pi}{4} + \frac{\varphi}{2}. \tag{301}$$

Then, the general structure of the solution is as follows. The found solution at sliding is valid if $\alpha < \alpha_{\rm cr}$. The condition (301) ensures that $c < 0$ (Fig. 48). Then, since

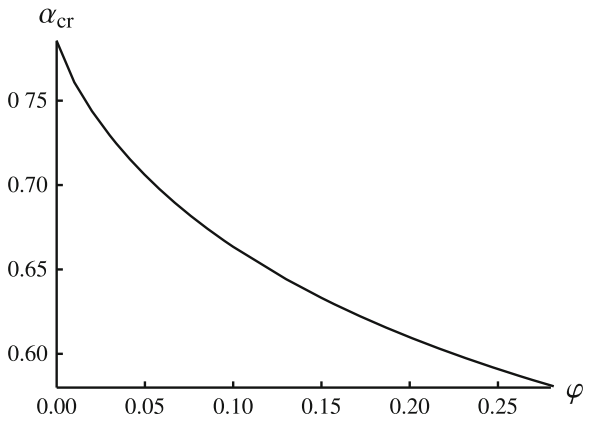

Fig. 49 The variation of α_{cr} with φ

$u_r > 0$, it follows from (300) that

$$c_2 < 0. \tag{302}$$

A limit case occurs at $\alpha = \alpha_{cr}$. In this case the found solution is valid but the regime of sticking takes place at the maximum friction surface. If $\alpha > \alpha_{cr}$, a rigid zone appears near the plate. This case is not important for the present chapter since the solution is not singular. In order to show that the structure of the solution proposed is possible, it is necessary to verify (301). To this end Eq. (294) has been solved numerically at $c_2 = 0$. The representation of the solution given in (298) has been used in the range $\psi_w \geq \psi \geq \psi_w (1 - \delta)$ where $0 < \delta << 1$. The value of c_3 in this representation has been eliminated by means of (299). The solution found must satisfy the boundary condition (285). The value of c corresponding to the limit case is determined from this boundary condition. It is evident that this value is related to α_{cr} by Eq. (281) in which α should be replaced with α_{cr}. The numerical solution is illustrated in Fig. 49. It is seen from this figure that the inequality (301) is satisfied. In what follows, it is assumed that $\alpha \leq \alpha_{cr}$.

Using (277), (284), (288) and (289) the shear strain rate is determined from (41) as

$$\xi_{r\theta} = \frac{\omega\,(c - \sin\varphi - \cos 2\psi)}{4\,(\sin\varphi + \cos 2\psi)^2}\left[(c - \sin\varphi - \cos 2\psi)\,\frac{d^2 g}{d\psi^2} + \frac{2c\sin 2\psi}{(\sin\varphi + \cos 2\psi)}\,\frac{dg}{d\psi}\right]. \tag{303}$$

Substituting (298) into (303) and using (295) and (299) yield the representation of the shear strain rate in the vicinity of the maximum friction surface in the form

$$\xi_{r\theta} = -\frac{\omega}{4\cos\varphi}\,\frac{\left[4\sin\varphi + c\left(c_2 + \tan^2\varphi\right)\right]}{(\psi - \psi_w)} + o\left[(\psi - \psi_w)^{-1}\right] \quad \text{as} \quad \psi \to \psi_w. \tag{304}$$

In the vicinity of the maximum friction surface (277) is written as

$$\frac{d\psi}{d\theta} = \frac{c}{2\cos\varphi\,(\psi - \psi_w)} + o\left[(\psi - \psi_w)^{-1}\right] \quad \text{as} \quad \psi \to \psi_w.$$

Integrating with the use of the boundary condition (272) gives

$$\psi - \psi_w = \frac{\sqrt{-c}}{\sqrt{\cos\varphi}}\,(\alpha - \theta)^{1/2} + o\left[(\alpha - \theta)^{1/2}\right] \quad \text{as} \quad \theta \to \alpha. \tag{305}$$

Substituting (305) into (304) yields

$$|\xi_{r\theta}| = \frac{\omega}{4\sqrt{\cos\varphi}} \frac{\left[4\sin\varphi + c\left(c_2 + \tan^2\varphi\right)\right]}{\sqrt{-c}\sqrt{\alpha - \theta}} + o\left[(\alpha - \theta)^{-1/2}\right] \quad \text{as} \quad \theta \to \alpha. \tag{306}$$

Equation (6) in which ξ_τ should be replased with $\xi_{r\theta}$ is valid. Therefore, the strain rate intensity factor is given by

$$D = \frac{\omega}{2\sqrt{3}\sqrt{\cos\varphi}} \frac{\left[4\sin\varphi + c\left(c_2 + \tan^2\varphi\right)\right]\sqrt{r}}{\sqrt{-c}}. \tag{307}$$

It is convenient to introduce the dimensionless strain rate intensity factor by

$$d = \frac{D}{\omega\sqrt{r}}. \tag{308}$$

The same definition for the dimensionless strain rate intensity factor has been adopted for the pressure-independent model in Sect. 3.5 (see Fig. 12). The variation of the dimensionless strain rate intensity factor found by means of (307) and (308) as well as the dimensionless strain rate intensity factor for the pressure-independent model is depicted in Fig. 50. The broken line corresponds to pressure-independent material, curve 1 to $\varphi = 0.1$, curve 2 to $\varphi = 0.2$, and curve 3 to $\varphi = 0.3$. The right ends of these curves are determined by the condition $\alpha = \alpha_{\rm cr}$. It is seen from this figure that the strain rate intensity factor for pressure-independent material is larger than the strain rate intensity factor for pressure-dependent material at smaller values of α and smaller than the strain rate intensity factor for pressure-dependent material at larger values of α.

5.6 Compression of a Plastic Layer Between Rotating Plates II

This boundary value problem has been formulated and solved for pressure-independent material in Sect. 3.6 (see Fig. 14). An extension of this solution to the double shearing model has been proposed in [39].

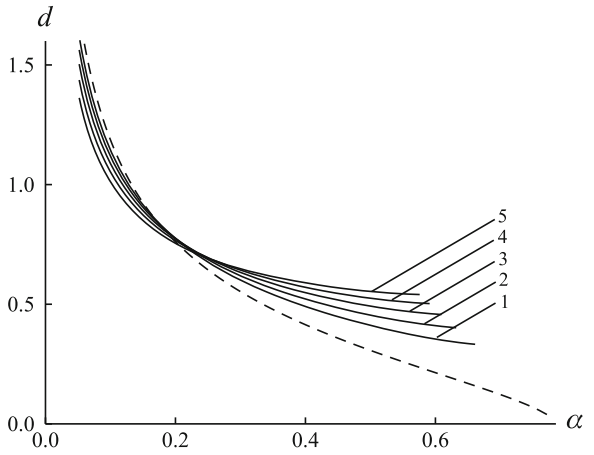

Fig. 50 Variation of the dimensionless strain rate intensity factor with α at several φ-values

Let ψ_w be the value of ψ at the maximum friction surface $\theta = \alpha$. The direction of flow (Fig. 14) dictates that $\sigma_{r\theta} > 0$ near the friction surface. Therefore, it follows from (199) that

$$0 < \psi_w < \frac{\pi}{2}. \tag{309}$$

The maximum friction surface is parallel to the r-axis. Therefore, $\phi_1 = 0$ or $\phi_2 = 0$ in (204). The equation $\phi_2 = 0$ contradicts (309). Therefore, $\phi_1 = 0$ and

$$\psi = \psi_w = \frac{\pi}{4} + \frac{\varphi}{2} \quad \text{for} \quad \theta = \alpha. \tag{310}$$

The main assumption accepted in [39] is that ψ is independent of r. Note that this assumption is in agreement with (310). The general solution for the stress equations given in the previous section is valid. In particular, the dependence of ψ on θ follows from (277) or, after integration, from (280). Then, the value of c involved in (277) is determined from (281) where ψ_w should be eliminated by means of (310). Numerical solution of this equation is illustrated in Fig. 51. The broken line corresponds to the solution for pressure-independent material, curve 1 to $\varphi = 0.1$, curve 2 to $\varphi = 0.2$, and curve 3 to $\varphi = 0.3$. It is seen from this figure that $c > 0$. The derivative $dc/d\alpha$ is given by (282). The velocity field is sought in the form [39]

$$u_r = \frac{\omega r}{2} \frac{\partial g\,(\psi,\ \alpha)}{\partial \theta} + \omega \frac{G\,(\psi,\ \alpha)}{r}, \quad u_\theta = -\omega r g\,(\psi,\ \alpha)\,, \tag{311}$$

where $g\,(\psi,\ \alpha)$ and $G\,(\psi,\ \alpha)$ are arbitrary functions of ψ and α. It is possible to verify by inspection that $(203)_1$ is automatically satisfied. Using (310) and (311) the boundary conditions (79) and (80) are transformed to

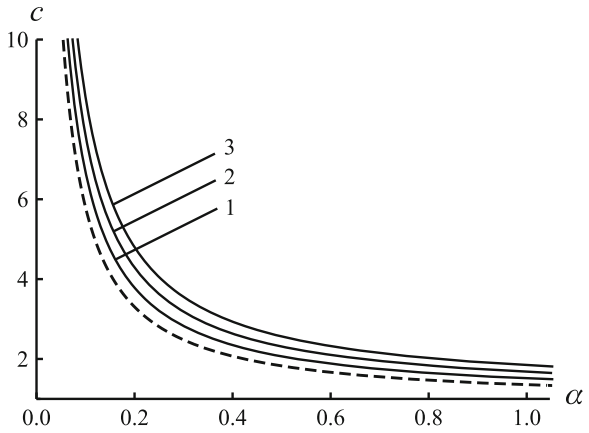

Fig. 51 Variation of c with α

$$g = 0 \quad \text{at} \quad \theta = 0 \quad (\text{or} \quad \psi = 0) \tag{312}$$

and

$$g = 1 \quad \text{at} \quad \theta = \alpha \quad (\text{or} \quad \psi = \psi_w), \tag{313}$$

respectively. Substituting (311) into $(203)_2$ yields

$$\begin{aligned}(\cos 2\psi + \sin\varphi)\,\frac{\partial^2 g}{\partial\theta^2} - 2\sin 2\psi\frac{\partial g}{\partial\theta} + 4g\sin\varphi + 4\sin\varphi\frac{\dot{\psi}}{\omega}\\ +\frac{2}{r^2}\left[(\cos 2\psi + \sin\varphi)\,\frac{dG}{d\theta} + 2G\sin 2\psi\right] = 0.\end{aligned} \tag{314}$$

Since ψ and $\dot{\psi}$ are independent of r, this equation may have a solution if and only if

$$\begin{aligned}(\cos 2\psi + \sin\varphi)\,\frac{\partial^2 g}{\partial\theta^2} - 2\sin 2\psi\frac{\partial g}{\partial\theta} + 4g\sin\varphi + 4\sin\varphi\frac{\dot{\psi}}{\omega} = 0,\\ (\cos 2\psi + \sin\varphi)\,\frac{\partial G}{\partial\theta} + 2G\sin 2\psi = 0.\end{aligned} \tag{315}$$

Replacing here the derivatives $\partial^2 g/\partial\theta^2$ and $\partial g/\partial\theta$ with the derivatives $\partial^2 g/\partial\psi^2$ and $\partial g/\partial\psi$ by means of (289) and eliminating the derivatives $d^2\psi/d\theta^2$ and $d\psi/d\theta$ by means of (277) and (288) result in

$$
\begin{aligned}
&(\sin\varphi+\cos 2\psi)\,\frac{\partial^2 g}{\partial\psi^2}+2\sin 2\psi\,\frac{\partial g}{\partial\psi}\\
&+\frac{4\sin\varphi\,(\sin\varphi+\cos 2\psi)^2}{(c-\sin\varphi-\cos 2\psi)^2}\left(g+\frac{\dot{\psi}}{\omega}\right)=0,\\
&\frac{dG}{d\psi}+\frac{2G\sin 2\psi}{c-\sin\varphi-\cos 2\psi}=0.
\end{aligned}
\tag{316}
$$

Integrating $(316)_2$ gives

$$
G=\frac{B}{c-\sin\varphi-\cos 2\psi},
\tag{317}
$$

where B is a constant of integration. The derivative $\dot{\psi}$ is given by (293). Therefore, Eq. $(316)_1$ transforms to (294). However, in contrast to (295), it is now necessary to investigate the coefficients of Eq. (294) in the vicinity of $\psi=\psi_w=\pi/4+\varphi/2$. Expanding these coefficients in series near this point yields

$$
\begin{aligned}
\sin\varphi+\cos 2\psi=&-2\cos\varphi\,(\psi-\psi_w)+2\sin\varphi\,(\psi-\psi_w)^2\\
&+\frac{4}{3}\cos\varphi\,(\psi-\psi_w)^3+o\left[(\psi-\psi_w)^3\right],\\
2\sin 2\psi=&\,2\cos\varphi-4\sin\varphi\,(\psi-\psi_w)-4\cos\varphi\,(\psi-\psi_w)^2\\
&+\frac{8}{3}\sin\varphi\,(\psi-\psi_w)^3+o\left[(\psi-\psi_w)^3\right],\\
P_1(\psi)=&\,\frac{4\sin 2\varphi}{c}\,(\psi-\psi_w)-\frac{8\sin^2\varphi}{c}\,(\psi-\psi_w)^2\\
&-\frac{8\sin 2\varphi}{c}\left(\frac{1}{3}+\frac{2\cos^2\varphi}{A^2}\right)(\psi-\psi_w)^3+o\left[(\psi-\psi_w)^3\right],\\
P_0(\psi)=&\,\frac{4\sin 2\varphi}{c}\,(\psi-\psi_w)-\frac{8\sin\varphi\,(1+\cos 2\varphi+A\sin\varphi)}{c^2}\,(\psi-\psi_w)^2\\
&+\frac{4\sin 2\varphi}{3c^3}\Big[2\left(3-c^2+3\cos 2\varphi+6c\sin\varphi\right)\\
&+3\cos\varphi\frac{dc}{d\alpha}\Big](\psi-\psi_w)^3+o\left[(\psi-\psi_w)^3\right]
\end{aligned}
\tag{318}
$$

as $\psi\to\psi_w$. It is seen from (294) and (318) that $\psi=\psi_w$ is a regular singular point of Eq. (294). Using a standard procedure it is possible to find that the solution to this equation in the vicinity of $\psi=\psi_w$ is represented by

$$
g=1+c_2\,(\psi-\psi_w)^2+c_3\,(\psi-\psi_w)^3.
\tag{319}
$$

It has been taken into account here that the solution must satisfy the boundary condition (313). Substituting (318) and (319) into (294) and collecting the coefficients of $(\psi-\psi_w)^2$ give

$$c_3=-\frac{2}{3}c_2\tan\varphi+\frac{4\sin 2\varphi}{3c^2}. \tag{320}$$

The shear strain rate is determined from (41) and (311) as

$$\frac{\xi_{r\theta}}{\omega}=\frac{1}{4}\frac{\partial^2 g}{\partial\theta^2}+\frac{1}{2r^2}\frac{\partial G}{\partial\theta}. \tag{321}$$

Replacing here differentiation with respect to θ with differentiation with respect to ψ by means of (289), eliminating G by means of (317) and using (277) and (288) result in

$$\begin{aligned}\xi_{r\theta}&=\frac{\omega}{4}\left(\frac{c-\sin\varphi-\cos 2\psi}{\sin\varphi+\cos 2\psi}\right)Q\left(r,\psi\right),\\ Q\left(r,\psi\right)&=\left(\frac{c-\sin\varphi-\cos 2\psi}{\sin\varphi+\cos 2\psi}\right)\frac{\partial^2 g}{\partial\psi^2}\\ &\quad+\frac{2c\sin 2\psi}{\left(\sin\varphi+\cos 2\psi\right)^2}\frac{\partial g}{\partial\psi}-\frac{4B\sin 2\psi}{r^2\left(c-\sin\varphi-\cos 2\psi\right)^2}.\end{aligned} \tag{322}$$

Substituting (319) into (322), eliminating c_3 by means of (320) and expanding the resulting expression in a series in the vicinity of $\psi=\psi_w$ yield

$$\xi_{r\theta}=-\frac{\omega}{2}\left(\frac{B}{cr^2}+\frac{cc_2}{2\cos\varphi}+\tan\varphi\right)\left(\psi_w-\psi\right)^{-1}+o\left[\left(\psi_w-\psi\right)^{-1}\right] \quad \text{as} \quad \psi\to\psi_w. \tag{323}$$

In the vicinity of this point Eq. (277) is represented as

$$\frac{d\psi}{d\theta}=\frac{c}{2\cos\varphi\left(\psi_w-\psi\right)}+o\left[\left(\psi_w-\psi\right)^{-1}\right] \quad \text{as} \quad \psi\to\psi_w.$$

Integrating with the boundary condition (310) gives

$$\psi_w-\psi=\sqrt{\frac{c}{\cos\varphi}}\sqrt{\alpha-\theta}+o\left(\sqrt{\alpha-\theta}\right) \quad \text{as} \quad \theta\to\alpha. \tag{324}$$

Substituting (324) into (323) yields

$$\begin{aligned}\left|\xi_{r\theta}\right|=&-\frac{\omega}{2}\left(\frac{B}{cr^2}+\frac{cc_2}{2\cos\varphi}+\tan\varphi\right)\sqrt{\frac{\cos\varphi}{c}}\left(\alpha-\theta\right)^{-1/2}\\ &+o\left[\left(\alpha-\theta\right)^{-1/2}\right] \quad \text{as} \quad \theta\to\alpha.\end{aligned} \tag{325}$$

Equation (6) in which ξ_τ should be replaced with $\xi_{r\theta}$ is valid. Therefore, the strain rate intensity factor is determined from (325) as

$$D = -\frac{\omega\sqrt{r}}{\sqrt{3}}\left(\frac{B}{cr^2} + \frac{cc_2}{2\cos\varphi} + \tan\phi\right)\sqrt{\frac{\cos\varphi}{c}}. \tag{326}$$

The value of c_2 is found from numerical solution of Eq. (294). The variation of c_2 with α at several values of φ is illustrated in Fig. 52. The broken line corresponds to the model of pressure-independent material. In this case $c_2 = -2$. Curve 1 corresponds to $\varphi = 0.1$, curve 2 to $\varphi = 0.15$, curve 3 to $\varphi = 0.2$, curve 4 to $\varphi = 0.25$, and curve 5 to $\varphi = 0.3$.

The direction of friction stress (Fig. 14) demands $u_r < 0$ at $\theta = \alpha$ (or $\psi = \psi_w$). Taking into account (311), (317) and (319) this inequality is rewritten as

$$u_r|_{\theta=\alpha} = -\frac{rcc_2}{2\cos\varphi} + \frac{B}{rc} < 0.$$

Therefore, the solution found is valid in the range

$$r < r_{\rm cr} = \frac{1}{c}\sqrt{\frac{2B\cos\varphi}{c_2}}. \tag{327}$$

The values of c and c_2 have been already determined (Figs. 51 and 52). In order to find the value of B, it is necessary to formulate an additional condition in integral form (similar to the condition (49) accepted in the classical problem considered in Sect. 3.2). A reasonable condition is

$$\int_0^\alpha u_r|_{r=R}\, d\theta = 0. \tag{328}$$

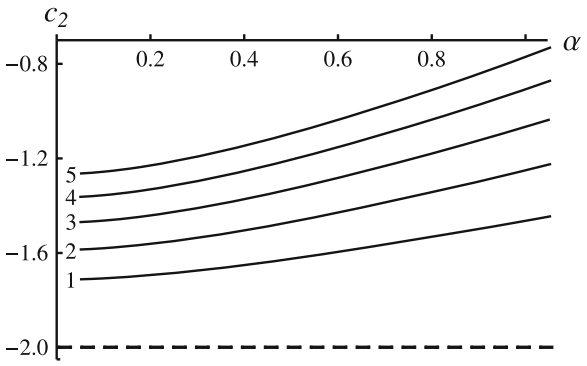

Fig. 52 Variation of c_2 with α at several φ-values

Here R is some prescribed radius. Substituting the radial velocity from (311) into (328), eliminating G by means of (317) and replacing integration with respect to θ with integration with respect to ψ by means of (277) result in

$$B = -\frac{R^2}{2}\left[\int_0^{\psi_w} \frac{(\sin\varphi + \cos 2\psi)}{(c - \sin\varphi - \cos 2\psi)^2} d\psi\right]^{-1}. \tag{329}$$

Eliminating B in (327) by means of (329) determines the dependence of $r_{\rm cr}/R$ on φ and α. The dependence of $r_{\rm cr}/R$ on α at several values of φ is depicted in Fig. 53. The broken line corresponds to the model of pressure-independent material, curve 1 to $\varphi = 0.1$, curve 2 to $\varphi = 0.15$, curve 3 to $\varphi = 0.2$, curve 4 to $\varphi = 0.25$, and curve 5 to $\varphi = 0.3$. Eliminating B in (326) by means of (329), it is possible to conclude that the strain rate intensity factor depends on φ, α and r/R. Consider first the dependence of D on φ and α assuming that $r/R = \mu = \text{constant} < r_{\rm cr}/R$. It is convenient to introduce the dimensionless strain rate intensity factor, d, as the ratio of the strain rate intensity factor given by (326) to the strain rate intensity factor for pressure-independent material given by (105). The variation of d with α at several values of φ is shown in Fig. 54 at $\mu = 0.3$, Fig. 55 at $\mu = 0.2$, and Fig. 56 at $\mu = 0.1$. In these figures, curve 1 corresponds to $\varphi = 0.1$, curve 2 to $\varphi = 0.15$, curve 3 to $\varphi = 0.2$, curve 4 to $\varphi = 0.25$, and curve 5 to $\varphi = 0.3$. In order to illustrate the variation of the strain rate intensity factor with r/R, it is necessary to take into account that $r_{\rm cr}/R$ depends on φ (Fig. 53). Therefore, it is more convenient in this case to introduce the dimensionless strain rate intensity factor by

$$d = D/\left(\omega\sqrt{r}\right).$$

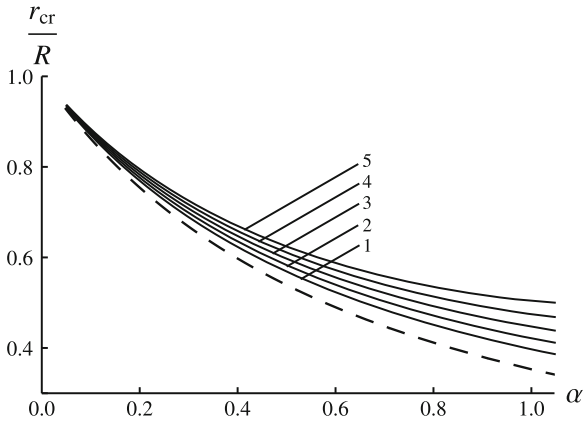

Fig. 53 Variation of $r_{\rm cr}/R$ with α at several φ-values

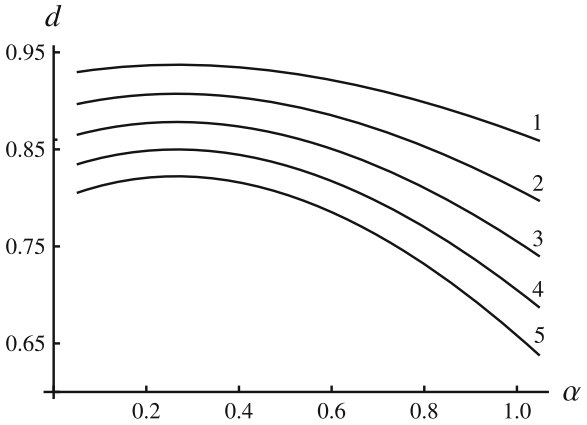

Fig. 54 Variation of the dimensionless strain rate intensity factor with α at several φ-values and $\mu = 0.3$

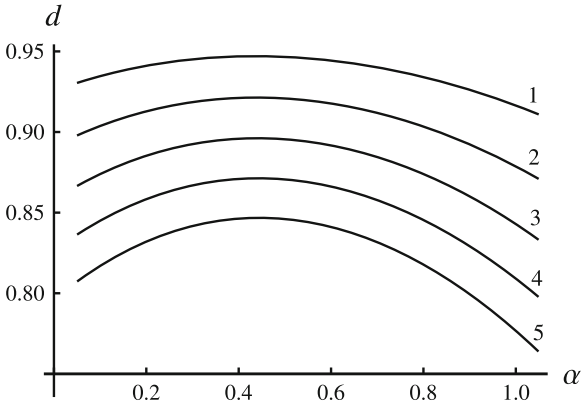

Fig. 55 Variation of the dimensionless strain rate intensity factor with α at several φ-values and $\mu = 0.2$

Note that the same definition has been adopted for the dimensionless strain rate intensity factor depicted in Fig. 15. The variation of d with r/R in the range $0.2 \leq r/R \leq r_{cr}/R$ is illustrated in Figs. 57, 58, 59 and 60. In Figs. 57 and 58 the value of α is fixed ($\alpha = \pi/36$ in Fig. 57 and $\alpha = \pi/6$ in Fig. 58) and the curves correspond to different values of φ (the broken line corresponds to the model of pressure-independent material, curve 1 to $\varphi = 0.1$, curve 2 to $\varphi = 0.2$ and curve 3 to $\varphi = 0.3$). In Figs. 59 and 60 the value of φ is fixed ($\varphi = 0.1$ in Fig. 59 and $\varphi = 0.3$ in Fig. 60) and the curves correspond to different values of α (curve 1 corresponds to $\alpha = \pi/36$, curve 2 to $\alpha = \pi/18$, curve 3 to $\alpha = \pi/12$, curve 4 to $\alpha = \pi/9$, and curve 5 to $\alpha = \pi/6$).

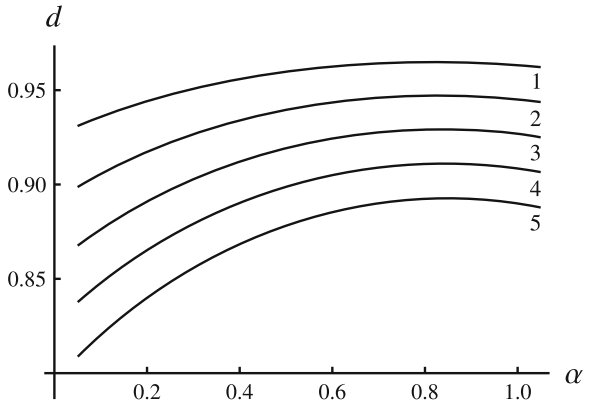

Fig. 56 Variation of the dimensionless strain rate intensity factor with α at several φ-values and $\mu = 0.1$

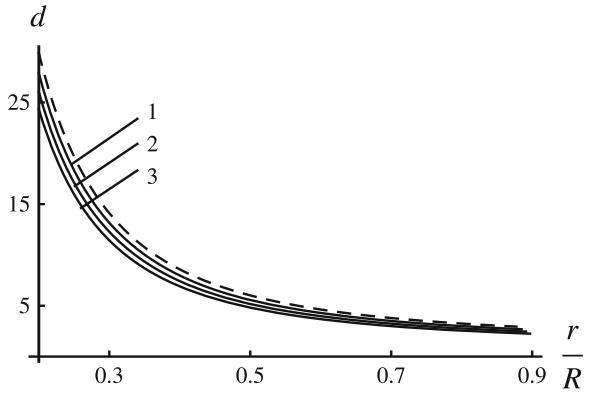

Fig. 57 Variation of the dimensionless strain rate intensity factor with r/R at several φ-values and $\alpha = \pi/36$

It is seen from Figs. 54, 55, 56, 57 and 58 that the strain rate intensity factor for pressure-dependent material is smaller than the strain rate intensity factor for pressure-independent material.

5.7 Simultaneous Shearing and Expansion of a Hollow Cylinder

This boundary value problem has been formulated and solved for pressure-independent material in Sect. 3.7 (see Fig. 17). An extension of this solution to the double shearing model has been proposed in [5].

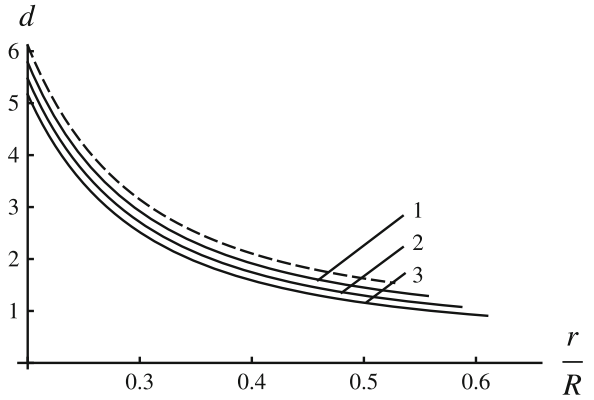

Fig. 58 Variation of the dimensionless strain rate intensity factor with r/R at several φ-values and $\alpha = \pi/6$

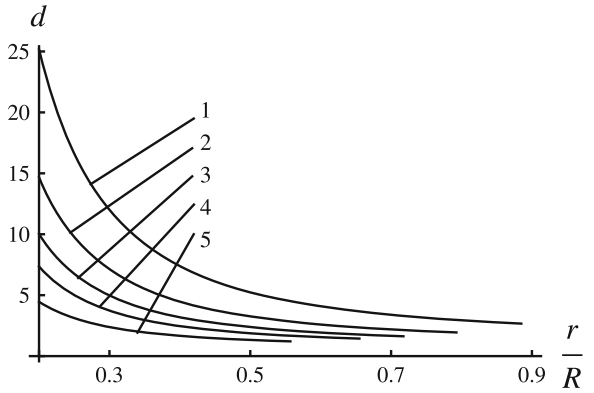

Fig. 59 Variation of the dimensionless strain rate intensity factor with r/R at several α-values and $\varphi = 0.1$

Let ψ_w be the value of ψ at the maximum friction surface $r = a$. The direction of rotation of the rigid rod (Fig. 17) dictates that $\sigma_{r\theta} > 0$ near the friction surface. Therefore, it follows from (199) that

$$0 < \psi_w < \frac{\pi}{2}. \tag{330}$$

The maximum friction surface is perpendicular to the r-axis. Therefore, $\phi_1 = \pi/2$ or $\phi_2 = \pi/2$ in (204). The equation $\phi_1 = \pi/2$ contradicts (330). Therefore, $\phi_2 = \pi/2$ and

$$\psi = \psi_w = \frac{\pi}{4} - \frac{\varphi}{2} \quad \text{for} \quad r = a. \tag{331}$$

The solution is independent of θ. Therefore, the equilibrium Eq. (42) become

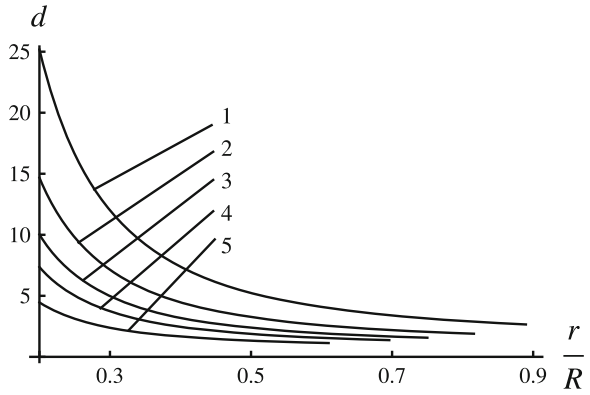

Fig. 60 Variation of the dimensionless strain rate intensity factor with r/R at several α-values and $\varphi = 0.3$

$$\frac{\partial \sigma_{rr}}{\partial r} + \frac{\sigma_{rr} - \sigma_{\theta\theta}}{r} = 0, \quad \frac{\partial \sigma_{r\theta}}{\partial r} + \frac{2\sigma_{r\theta}}{r} = 0. \tag{332}$$

The general solution to Eq. $(332)_2$ is

$$\frac{\sigma_{r\theta}}{k} = \frac{C^2}{r^2}, \tag{333}$$

where C is a constant of integration. Using (191), (200) and (333) the normal stresses are expressed as

$$\begin{aligned} \frac{\sigma_{rr}}{k} &= \cot\varphi - \frac{C^2\,(1 - \cos 2\psi \sin\varphi)}{r^2 \sin 2\psi \sin\varphi}, \\ \frac{\sigma_{\theta\theta}}{k} &= \cot\varphi - \frac{C^2\,(1 + \cos 2\psi \sin\varphi)}{r^2 \sin 2\psi \sin\varphi}. \end{aligned} \tag{334}$$

Substituting (334) into $(332)_1$ gives the following equation for ψ

$$\frac{\partial \psi}{\partial r} = -\frac{\sin 2\psi}{r\,(\cos 2\psi - \sin\varphi)}. \tag{335}$$

Integrating this equation with the boundary condition (331) results in

$$\frac{r}{a} = \frac{\cos\psi_w \tan^m \psi_w}{\cos\psi \tan^m \psi}, \quad m = \frac{1 - \sin\varphi}{2}. \tag{336}$$

This equation determines ψ as a function of r in implicit form. Let ψ_b be the value of ψ at $r = b$. Then, it follows from (336) that

$$\frac{b}{a} = \frac{\cos\psi_w \tan^m \psi_w}{\cos\psi_b \tan^m \psi_b}. \tag{337}$$

This equation should be solved numerically to find the value of ψ_b.

Since the solution is independent of θ, the solution to the incompressibility Eq. $(302)_1$ satisfying the boundary condition (106) is

$$u_r = \frac{\dot{a}a}{r}. \tag{338}$$

Since ψ is independent of θ, $\partial\psi/\partial r$ is given by (335) and $\partial\psi/\partial t = \dot{a}\partial\psi/\partial a$, Eq. $(301)_2$ becomes

$$\dot{\psi} = \dot{a}\frac{\partial\psi}{\partial a} - \frac{\dot{a}a \sin 2\psi}{r^2 (\cos 2\psi - \sin\varphi)}. \tag{339}$$

Here the radial velocity has been eliminated by means of (338). Substituting (338) and (339) into $(302)_2$ gives

$$\sin 2\psi \frac{\partial u_\theta}{\partial\psi} + (\cos 2\psi + \sin\varphi)\, u_\theta - \frac{2a\dot{a}\sin 2\psi}{r} - 2\dot{a}r \sin\varphi \frac{\partial\psi}{\partial a} + \frac{2a\dot{a}\sin\varphi}{r}\frac{\sin 2\psi}{(\cos 2\psi - \sin\varphi)} = 0. \tag{340}$$

Since ψ_w is constant, it follows from (336) that

$$\frac{\partial\psi}{\partial a} = \frac{\sin 2\psi}{a(\cos 2\psi - \sin\varphi)}. \tag{341}$$

Substituting (336) and (341) into (340) leads to

$$\frac{\partial u_\theta}{\partial\psi} + \frac{(\cos 2\psi + \sin\varphi)}{\sin 2\psi} u_\theta = P(\psi),$$
$$P(\psi) = \frac{2\dot{a}\tan^m\psi\cos\psi}{\cos\psi_w \tan^m\psi_w (\cos 2\psi - \sin\varphi)} \times \left(\frac{\sin\varphi\cos\varphi\tan^{\sin\varphi}\psi}{\tan^{\sin\varphi}\psi_w \sin 2\psi} + \cos 2\psi - 2\sin\varphi\right). \tag{342}$$

Applying l'Hospital's rule it is possible to find that $\lim_{\psi\to\psi_w} P(\psi) = 2\dot{a} > 0$. Then, it follows from (342) that

$$\left.\frac{\partial u_\theta}{\partial\psi}\right|_{\psi=\psi_w} = 2(\dot{a} - u_a \tan\varphi). \tag{343}$$

Here u_a is the value of the circumferential velocity at $r = a$. Taking into account that the solution is independent of θ and replacing differentiation with respect to r with differentiation with respect to ψ by means of (335) the shear strain rate is determined from (41) as

$$\xi_{r\theta} = \frac{(\dot{a} - u_a \tan\varphi)}{2a\,(\psi - \psi_w)} + o\left[(\psi - \psi_w)^{-1}\right] \quad \text{as} \quad \psi \to \psi_w. \tag{344}$$

Here Eq. (343) has been used to eliminate the derivative $\partial u_\theta / \partial \psi$. Equation (335) in the vicinity of $r = a$ (or $\psi = \psi_w$) is represented as

$$\frac{\partial \psi}{\partial r} = \frac{1}{2a\,(\psi - \psi_w)} + o\left[(\psi - \psi_w)^{-1}\right] \quad \text{as} \quad \psi \to \psi_w. \tag{345}$$

Integrating this equation with the boundary condition (331) gives

$$\psi - \psi_w = \frac{\sqrt{r-a}}{\sqrt{a}} + o\left(\sqrt{r-a}\right) \quad \text{as} \quad r \to a. \tag{346}$$

Substituting (346) into (344) leads to

$$\xi_{r\theta} = \frac{(\dot{a} - u_a \tan\varphi)}{2\sqrt{a}\sqrt{r-a}} + o\left[(r-a)^{-1/2}\right] \quad \text{as} \quad r \to a. \tag{347}$$

Equation (6) in which ξ_τ should be replaced with $\xi_{r\theta}$ is valid. Therefore, the strain rate intensity factor is determined using (347) as

$$D = \frac{(\dot{a} - u_a \tan\varphi)}{\sqrt{3a}}. \tag{348}$$

It is convenient to introduce the dimensionless strain rate intensity factor, d, as the ratio of the strain rate intensity factor given by (348) to the strain rate intensity factor given by (112). As a result,

$$d = 1 - \frac{u_a}{\dot{a}} \tan\varphi. \tag{349}$$

The solution of Eq. (342) satisfying the boundary condition (107) is

$$\frac{u_\theta}{\dot{a}} = \frac{\tan^m \psi}{\cos\psi_w \tan^{m+\sin\varphi} \psi_w \sin\psi} \times \int_{\psi_b}^{\psi} \frac{\left[\sin\varphi \cos\varphi \tan^{\sin\varphi}\gamma + \tan^{\sin\varphi}\psi_w \sin 2\gamma\,(\cos 2\gamma - 2\sin\varphi)\right]}{(\cos 2\gamma - \sin\varphi)} d\gamma. \tag{350}$$

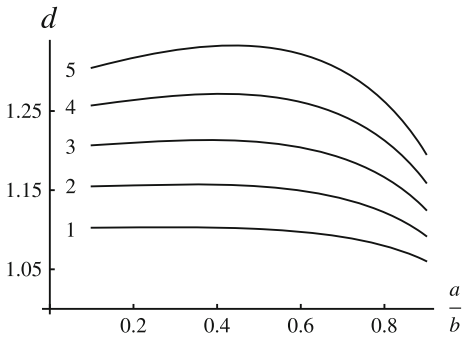

Fig. 61 Variation of the dimensionless strain rate intensity factor with α at several φ-values

Here γ is a dummy variable of integration and ψ_b is determined from the solution of Eq. (337). It follows from the definition for u_a and (350) that

$$-\frac{u_a}{\dot{a}} = \frac{2}{\cos\varphi}\int_{\psi_w}^{\psi_b} \frac{\left[\sin\varphi\cos\varphi\,(\tan\gamma/\tan\psi_w)^{\sin\varphi} + \sin 2\gamma\,(\cos 2\gamma - 2\sin\varphi)\right]}{(\cos 2\gamma - \sin\varphi)} d\gamma. \tag{351}$$

The integrand reduces to the expression $0/0$ at $\gamma = \psi_w$. Applying l'Hospital's rule yields

$$\lim_{\gamma\to\psi_w}\left\{\frac{\sin\varphi\cos\varphi\,(\tan\gamma\cot\psi_w)^{\sin\varphi} + \sin 2\gamma\,(\cos 2\gamma - 2\sin\varphi)}{(\cos 2\gamma - \sin\varphi)}\right\} = \cos\varphi. \tag{352}$$

Using (352) the integral in (351) can be evaluated numerically with no difficulty. Substituting the value of u_a found into (349) gives the dimensionless strain rate intensity factor. Its variation with the ratio a/b at several values of φ is depicted in Fig. 61 (curve 1 corresponds to $\varphi = 0.1$, curve 2 to $\varphi = 0.15$, curve 3 to $\varphi = 0.2$, curve 4 to $\varphi = 0.25$, and curve 5 to $\varphi = 0.3$). It is seen from this figure that the strain rate intensity factor for pressure-independent material is smaller than the strain rate intensity factor for pressure-dependent material.

6 Axisymmetric Solutions for the Double-Shearing Model

6.1 Basic Equations

Section 6 is concerned with axisymmetric solutions for the double-shearing model. In this section, a spherical coordinate system (r, θ, ϑ) will be employed. The solutions are independent of ϑ, the stress $\sigma_{\vartheta\vartheta}$ is one of the principal stresses and the velocity

u_ϑ vanishes. A cross-section of the Mohr-Coulomb yield surface by a plane $\sigma_{\vartheta\vartheta} =$ constant is shown in Fig. 62. In general, various regimes of flow arise depending on the relative magnitudes of $\sigma_{\vartheta\vartheta}$, σ_1 and σ_2. However, in what follows, regime A only is of interest. In this regime

$$\sigma_1 (1 + \sin\varphi) = 2k\cos\varphi + \sigma_{\vartheta\vartheta} (1 - \sin\varphi), \quad \sigma_2 = \sigma_{\vartheta\vartheta}. \tag{353}$$

Using the transformation equations for stress components in $r\theta$-planes the stress components in the spherical coordinate system are expressed as (Fig. 21)

$$\sigma_{rr} = -p + q\cos 2\psi, \quad \sigma_{\theta\theta} = -p - q\cos 2\psi, \quad \sigma_{r\theta} = q\sin 2\psi. \tag{354}$$

Here p and q are given by (192). Using (354) the yield criterion (353) transforms to

$$q - p\sin\varphi = k\cos\varphi, \quad \sigma_{\vartheta\vartheta} = -p - q. \tag{355}$$

The velocity equations have been given in [10]. Those are

$$\begin{gathered} \xi_{rr} + \xi_{\theta\theta} + \xi_{\vartheta\vartheta} = 0, \\ 2\xi_{r\theta}\cos 2\psi - (\xi_{rr} - \xi_{\theta\theta})\sin 2\psi + \sin\varphi\left(\omega_{r\theta} + \dot{\psi}\right) = 0. \end{gathered} \tag{356}$$

The components of the strain rate tensor are given by (124). Equation $(356)_1$ is equivalent to (128). The only non-zero spin component is

$$\omega_{r\theta} = \frac{1}{2r}\left(\frac{\partial u_r}{\partial\theta} - r\frac{\partial u_\theta}{\partial r} - u_\theta\right). \tag{357}$$

Since $u_\vartheta = 0$, the derivative $\dot{\psi}$ is given by

$$\dot{\psi} = \frac{\partial\psi}{\partial t} + u_r\frac{\partial\psi}{\partial r} + \frac{u_\theta}{r}\frac{\partial\psi}{\partial\theta}. \tag{358}$$

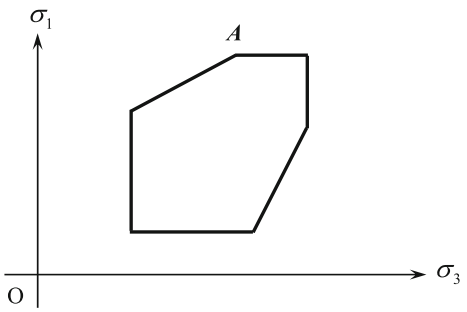

Fig. 62 Cross-section of the Mohr-Coulomb yield surface by plane $\sigma_{\vartheta\vartheta} =$ constant

Equation (131) is replaced with

$$\phi_1 = \psi - \frac{\pi}{4} - \frac{\varphi}{2}, \quad \phi_2 = \psi + \frac{\pi}{4} + \frac{\varphi}{2}. \tag{359}$$

The equilibrium equations are given by (125).

6.2 *Flow of Plastic Material Through an Converging Conical Channel*

This boundary value problem has been formulated and solved for pressure-independent material in Sect. 4.3 (see Fig. 23). An extension of this solution to the double shearing model has been outlined in [10].

Let ψ_w be the value of ψ at the maximum friction surface $\theta = \alpha$. The direction of flow (Fig. 23) dictates that $\sigma_{r\theta} > 0$ near the friction surface. Therefore, it follows from (354) that

$$0 < \psi_w < \frac{\pi}{2}. \tag{360}$$

The orientation of the maximum friction surface shows that $\phi_1 = 0$ or $\phi_2 = 0$ in (359). The equation $\phi_2 = 0$ contradicts (360). Therefore, $\phi_1 = 0$ and

$$\psi = \psi_w = \frac{\pi}{4} + \frac{\varphi}{2} \quad \text{for} \quad \theta = \alpha. \tag{361}$$

The main assumptions accepted in [10] are that ψ is independent of r and $u_\theta = 0$. Note that the former is in agreement with (361) and the latter automatically satisfies the boundary conditions (147). Equation (128) reduces to

$$\frac{\partial u_r}{\partial r} + 2\frac{u_r}{r} = 0.$$

The general solution of this equation is

$$u_r = -\frac{U(\theta)}{r^2}, \tag{362}$$

where $U(\theta) > 0$ is an arbitrary function of θ. The solution for stresses is sought in the form [40]

$$q = \exp[f(\theta)]\, r^n. \tag{363}$$

Here $f(\theta)$ is an arbitrary function of θ and $n =$ constant. Using (355) and (363) it is possible to find that

$$p = \frac{\exp\left[f\left(\theta\right)\right] r^n}{\sin\varphi} - k\cot\varphi, \tag{364}$$
$$\sigma_{\vartheta\vartheta} = -\exp\left[f\left(\theta\right)\right] r^n \left(\frac{1}{\sin\varphi} + 1\right) + k\cot\varphi.$$

Substituting (363) and (364) into (354) gives the stresses in terms of $f\left(\theta\right)$ and r. Substituting these stresses and $\sigma_{\vartheta\vartheta}$ from (364) into the equilibrium Eq. (125) results in the following equations for $\psi\left(\theta\right)$ and $f\left(\theta\right)$

$$\frac{d\psi}{d\theta} = \frac{n\cos^2\varphi - \sin\varphi\omega_0(\psi,\theta)}{2\sin\varphi\left(\sin\varphi + \cos 2\psi\right)}, \tag{365}$$
$$\omega_0\left(\psi,\theta\right) = 3\sin\varphi + 1 + \cos 2\psi\left(3 + \sin\varphi\right) + \cot\theta\sin 2\psi\left(1 + \sin\varphi\right),$$

and

$$\frac{df}{d\theta} = \frac{n\sin 2\psi - \sin\varphi\left[\cot\theta\left(1 - \cos 2\psi\right) + \sin 2\psi\right]}{\sin\varphi + \cos 2\psi}, \tag{366}$$

respectively. Using (365) Eq. (366) can be rewritten as

$$\frac{df}{d\psi} = \frac{2\sin\varphi\left\{n\sin 2\psi - \sin\varphi\left[\cot\theta\left(1 - \cos 2\psi\right) + \sin 2\psi\right]\right\}}{n\cos^2\varphi - \sin\varphi\omega_0(\psi,\theta)}. \tag{367}$$

An advantage of Eq. (367) over Eq. (366) is that the denominator in (366) vanishes at $\psi = \psi_w$. For the same reason, it is advantageous to rewrite Eq. (365) as

$$\frac{d\theta}{d\psi} = \frac{2\sin\varphi\left(\sin\varphi + \cos 2\psi\right)}{n\cos^2\varphi - \sin\varphi\omega_0(\psi,\theta)}. \tag{368}$$

The process is stationary. Therefore, $\partial\psi/\partial t = 0$. Moreover, by assumption, $u_\theta = 0$ and $\partial\psi/\partial r = 0$. Therefore, it follows from (358) that $\dot{\psi} = 0$. Then, using (124) and (357) it is possible to simplify Eq. $(356)_2$ to

$$\left(\cos 2\psi + \sin\varphi\right)\frac{\partial u_r}{\partial\theta} - \sin 2\psi\left(r\frac{\partial u_r}{\partial r} - u_r\right) = 0.$$

Substituting (362) into this equation gives

$$\left(\cos 2\psi + \sin\varphi\right)\frac{dU}{d\theta} + 3U\sin 2\psi = 0. \tag{369}$$

The coefficient of the derivative vanishes at $\psi = \psi_w$. Therefore, using (368) it is advantageous to rewrite (369) as

$$\frac{dU}{d\psi} = \frac{-6U\sin\varphi\sin 2\psi}{n\cos^2\varphi - \sin\varphi\omega_0(\psi,\theta)}. \tag{370}$$

In the case under consideration, the shear strain rate is determined from (124), (362) and (369) as

$$\xi_{r\theta} = -\frac{1}{2r^3}\frac{dU}{d\theta} = \frac{3U\sin 2\psi}{2r^3\left(\cos 2\psi + \sin\varphi\right)}. \tag{371}$$

Let U_w be the value of U at $\theta = \alpha$ (or $\psi = \psi_w$). Then, expanding the right hand side of (371) in a series in the vicinity of $\psi = \psi_w$ yields

$$\xi_{r\theta} = \frac{3U_w}{4r^3\left(\psi_w - \psi\right)} + o\left(\frac{1}{\psi_w - \psi}\right) \quad \text{as} \quad \psi \to \psi_w. \tag{372}$$

Equation (368) in the vicinity of $\psi = \psi_w$ (or $\theta = \alpha$) becomes

$$\frac{d\theta}{d\psi} = \frac{4\sin\varphi\left(\psi_w - \psi\right)}{n\cos\varphi - \sin\varphi\left[\cos\varphi + \cot\alpha\left(1 + \sin\varphi\right)\right]} + o\left(\psi_w - \psi\right) \quad \text{as} \quad \psi \to \psi_w.$$

Integrating this equation gives

$$\left(\psi_w - \psi\right)^2 = \frac{\left\{n\cos\varphi - \sin\varphi\left[\cos\varphi + \cot\alpha\left(1 + \sin\varphi\right)\right]\right\}}{2\sin\varphi}\left(\alpha - \theta\right) \tag{373}$$

to leading order. Substituting (373) into (372) gives

$$\xi_{r\theta} = \frac{3\sqrt{2\sin\varphi}U_w}{4r^3\sqrt{n\cos\varphi - \sin\varphi\left[\cos\varphi + \cot\alpha\left(1 + \sin\varphi\right)\right]}\sqrt{\alpha - \theta}} + o\left(\frac{1}{\sqrt{\alpha - \theta}}\right) \quad \text{as} \quad \theta \to \alpha. \tag{374}$$

The normal strain rates are bounded in the vicinity of the maximum friction surface and $|\xi_{r\theta}| \to \infty$ as $\theta \to \alpha$. Therefore, Eq. (6) in which ξ_τ should be replaced with $\xi_{r\theta}$ is valid. Then, it follows from (6) and (374) that the strain rate intensity factor is

$$D = \frac{\sqrt{6\sin\varphi}U_w}{2r^{5/2}\sqrt{n\cos\varphi - \sin\varphi\left[\cos\varphi + \cot\alpha\left(1 + \sin\varphi\right)\right]}}. \tag{375}$$

A difficulty with solving (367), (368) and (370) numerically is that the right hand sides of these equations contain the expression $0\cdot\infty$ as $\theta \to 0$ and $\psi \to 0$. Represent the function $\psi\left(\theta\right)$ in the form

$$\psi\left(\theta\right) = A\theta + B\theta^2 + O\left(\theta^3\right) \quad \text{as} \quad \theta \to 0. \tag{376}$$

Substituting this representation into (365) gives

$$A + 2B\theta = \frac{1}{2}\left(\frac{n}{\sin\varphi} - n - 4 - 2A\right) - B\theta \quad \text{as} \quad \theta \to 0. \tag{377}$$

Therefore,

$$A = -1 + \frac{n}{4}\left(\frac{1}{\sin\varphi} - 1\right), \quad B = 0$$

and Eq. (376) becomes

$$\psi(\theta) = \left[\frac{n}{4}\left(\frac{1}{\sin\varphi} - 1\right) - 1\right]\theta + O\left(\theta^3\right) \quad \text{as} \quad \theta \to 0. \tag{378}$$

Substituting this representation into (367) and (370) yields

$$\frac{df}{d\psi} = n\left(\frac{1}{2} + \frac{1}{1 + \sin\varphi}\right)\theta + O\left(\theta^3\right) \quad \text{as} \quad \theta \to 0 \tag{379}$$

and

$$\frac{dU}{d\psi} = -\frac{6U}{(1 + \sin\varphi)}\theta + O\left(\theta^3\right) \quad \text{as} \quad \theta \to 0, \tag{380}$$

respectively. It follows from (378)-(380) that

$$\begin{aligned} f &= f_0 + \frac{n\sin\varphi\,(3 + \sin\varphi)}{(1 + \sin\varphi)\,[n\,(1 - \sin\varphi) - 4\sin\varphi]}\psi^2 + o\left(\psi^2\right) \quad \text{as} \quad \psi \to 0, \\ \ln\frac{U}{U_0} &= -\frac{12\sin\varphi}{\left[n\cos^2\varphi - 4\sin\varphi\,(1 + \sin\varphi)\right]}\psi^2 + o\left(\psi^2\right) \quad \text{as} \quad \psi \to 0, \end{aligned} \tag{381}$$

where f_0 and U_0 are constants of integration. It is seen from (375) that the function $f(\theta)$ is not involved in the expression for the strain rate intensity factor. Therefore, Eq. (367) is not solved here. The solution of Eq. (370) is

$$U = U_w w(\psi), \tag{382}$$

$$w(\psi) = \exp\left\{-6\sin\varphi\int_{\psi_w}^{\psi}\frac{\sin 2\gamma}{n\cos^2\varphi - \sin\varphi\omega_0\left[\gamma, \theta(\gamma)\right]}d\gamma\right\}.$$

Equation (168) should be used to determine U_w. In particular, substituting (362) and (382) into this equation gives

$$Q = 2\pi U_w\int_0^{\alpha} w(\psi)\sin\theta d\theta.$$

Replacing here integration with respect to θ with integration with respect to ψ by means of (368) yields

$$U_w = \frac{Q}{4\pi \sin\varphi}\left[\int_0^{\psi_w} \frac{\sin\theta\,(\sin\varphi + \cos 2\psi)\,w\,(\psi)}{n\cos^2\varphi - \sin\varphi\omega_0\,(\psi,\theta)}d\psi\right]^{-1}. \tag{383}$$

In order to make comparison with the solution for pressure-independent material (Sect. 4.3), it is convenient to introduce the dimensionless strain rate intensity factor, d, by (170).

Using (378) Eq. (368) can be solved numerically if a value of n is specified. An iterative procedure should be adopted to determine the value of n using the boundary condition (361). The variation of n with α at several values of φ is depicted in Fig. 63 (curve 1 corresponds to $\varphi = 0.1$, curve 2 to $\varphi = 0.15$, curve 3 to $\varphi = 0.2$, curve 4 to $\varphi = 0.25$, and curve 5 to $\varphi = 0.3$). Having the solution to Eq. (368) the integrals in (382) and (383) can be evaluated. Finally, the dimensionless strain rate intensity factor is determined from (170) and (375). The variation of d with α at several values of φ is depicted in Fig. 64. The broken line corresponds to the model of pressure-independent plasticity. It is seen that the effect of φ on d is not significant (the solid curves cover the range $0.1 \le \varphi \le 0.3$). It is more pronounced at smaller α-angles (Fig. 65). In this figure, curve 1 corresponds to $\varphi = 0.1$, curve 2 to $\varphi = 0.15$, curve 3 to $\varphi = 0.2$, curve 4 to $\varphi = 0.25$, and curve 5 to $\varphi = 0.3$. It is seen that the dimensionless strain rate intensity factor increases with φ. It is interesting to mention that the opposite tendency occurs at larger α-angles (Fig. 66).

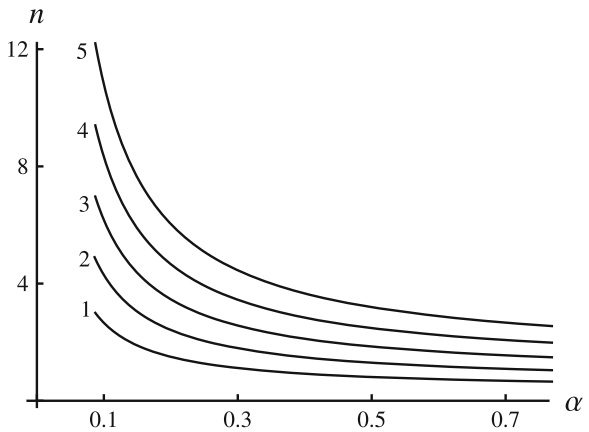

Fig. 63 Variation of n with α at several φ-values

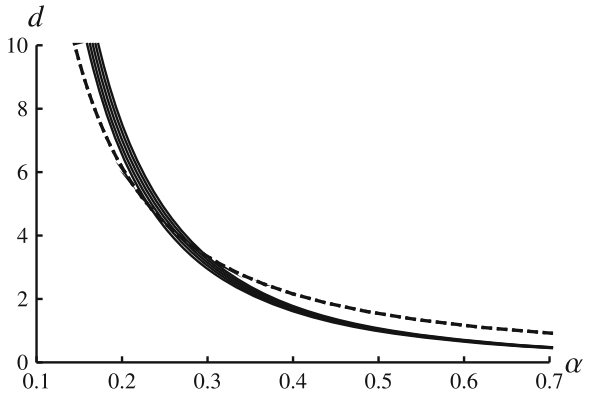

Fig. 64 Variation of the dimensionless strain rate intensity factor with α at several φ-values

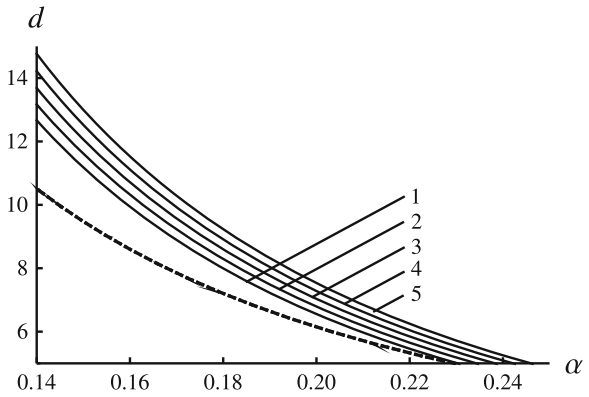

Fig. 65 Variation of the dimensionless strain rate intensity factor with α at several φ-values (small α-values)

6.3 Radial Flow Between Two Conical Surfaces

This boundary value problem has been formulated and solved for pressure-independent material in Sect. 4.4 (see Fig. 26). An extension of this solution to the double shearing model has been given in [40].

Let ψ_f be the value of ψ at the maximum friction surface $\theta = \theta_0$ and ψ_w be the value of ψ at the maximum friction surface $\theta = \theta_1$. The direction of flow (Fig. 26) dictates that $\sigma_{r\theta} < 0$ near the friction surface $\theta = \theta_0$ and $\sigma_{r\theta} > 0$ near the friction surface $\theta = \theta_1$. Therefore, it follows from (354) that

$$-\frac{\pi}{2} < \psi_f < 0 \quad \text{and} \quad 0 < \psi_w < \frac{\pi}{2}. \tag{384}$$

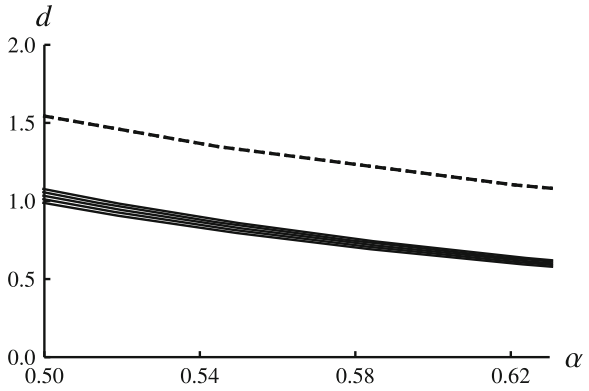

Fig. 66 Variation of the dimensionless strain rate intensity factor with α at several φ-values (large α-values)

The orientation of the normal to the maximum friction surfaces shows that $\phi_1 = 0$ or $\phi_2 = 0$ in (359). Equation $\phi_1 = 0$ contradicts $(384)_1$ and equation $\phi_2 = 0$ to $(384)_2$. Therefore,

$$\psi = \psi_f = -\frac{\pi}{4} - \frac{\varphi}{2} \quad \text{for} \quad \theta = \theta_0 \tag{385}$$

and

$$\psi = \psi_w = \frac{\pi}{4} + \frac{\varphi}{2} \quad \text{for} \quad \theta = \theta_1. \tag{386}$$

The velocity boundary conditions (172) are automatically satisfied assuming that $u_\theta = 0$. Then, the radial velocity is given by (362). The general solution for stresses given in the previous section is also valid. In particular, the dependence of ψ on θ and the value of n are determined from (368) and the boundary conditions (385) and (386). Equations (370) and (371) are also valid. Since the boundary condition (386) coincides with (361), the strain rate intensity factor corresponding to the maximum friction surface $\theta = \theta_1$ is given by (375). Using the nomenclature of the present section the expression for this strain rate intensity factor becomes

$$D_{\text{ex}} = \frac{\sqrt{6 \sin \varphi} U_w}{2r^{5/2} \sqrt{n \cos \varphi - \sin \varphi \left[\cos \varphi + \cot \theta_1 \left(1 + \sin \varphi\right)\right]}}. \tag{387}$$

Here U_w is the value of U at $\theta = \theta_1$. Expanding the right hand side of (371) in a series in the vicinity of $\psi = \psi_f$ (or $\theta = \theta_0$) yields

$$\xi_{r\theta} = -\frac{3U_f}{4r^3 \left(\psi - \psi_f\right)} + o\left(\frac{1}{\psi - \psi_f}\right) \quad \text{as} \quad \psi \to \psi_f. \tag{388}$$

Here U_f is the value of U at $\theta = \theta_0$. Equation (368) in the vicinity of $\psi = \psi_f$ becomes

$$\frac{d\theta}{d\psi} = \frac{4\sin\varphi\left(\psi - \psi_f\right)}{n\cos\varphi - \sin\varphi\left[\cos\varphi - \cot\theta_0\left(1 + \sin\varphi\right)\right]} + o\left(\psi - \psi_f\right) \quad \text{as} \quad \psi \to \psi_f. \tag{389}$$

Integrating this equation gives

$$\left(\psi - \psi_f\right)^2 = \frac{\left\{n\cos\varphi - \sin\varphi\left[\cos\varphi - \cot\theta_0\left(1 + \sin\varphi\right)\right]\right\}}{2\sin\varphi}\left(\theta - \theta_0\right) \tag{390}$$

to leading order. Substituting (390) into (388) yields

$$\xi_{r\theta} = -\frac{3\sqrt{2\sin\varphi}U_f}{4r^3\sqrt{n\cos\varphi - \sin\varphi\left[\cos\varphi - \cot\theta_0\left(1 + \sin\varphi\right)\right]}\sqrt{\theta - \theta_0}} + o\left(\frac{1}{\sqrt{\theta - \theta_0}}\right) \quad \text{as} \quad \theta \to \theta_0. \tag{391}$$

The normal strain rates are bounded in the vicinity of the maximum friction surface $\theta = \theta_0$ and $\xi_{r\theta} \to \infty$ as $\theta \to \theta_0$. Therefore, Eq. (6) in which ξ_τ should be replaced with $\xi_{r\theta}$ is valid. Then, it follows from (6) and (391) that the strain rate intensity factor corresponding to the friction surface $\theta = \theta_0$ is

$$D_{in} = \frac{\sqrt{6\sin\varphi}U_f}{2r^{5/2}\sqrt{n\cos\varphi - \sin\varphi\left[\cos\varphi - \cot\theta_0\left(1 + \sin\varphi\right)\right]}}. \tag{392}$$

The solution of Eq. (370) is given by (382). The condition (187) should be used to determine U_w. In particular, substituting (362) and (382) into this condition results in

$$Q = 2\pi U_w \int_{\theta_0}^{\theta_1} w\left(\psi\right)\sin\theta d\theta.$$

Replacing here integration with respect to θ with integration with respect to ψ by means of (368) yields

$$\frac{U_w}{Q} = \frac{1}{4\pi\sin\varphi}\left[\int_{\psi_f}^{\psi_w} \frac{\sin\theta\left(\sin\varphi + \cos 2\psi\right)w\left(\psi\right)}{n\cos^2\varphi - \sin\varphi\omega_0\left(\psi, \theta\right)} d\psi\right]^{-1}, \tag{393}$$

where $\omega_0(\psi, \theta)$ is defined in (365). The value of U_f is found from (382) as

$$U_f = U_w w\left(\psi_f\right). \tag{394}$$

In order to make comparison with the solution for pressure-independent material (Sect. 4.4), it is convenient to introduce the dimensionless strain rate intensity factors, d_{ex} and d_{in}, by Eq. (170). Then, using Eqs. (387), (392) and (394) yields

$$d_{\mathrm{ex}} = \frac{\sqrt{6\sin\varphi}}{2\sqrt{n\cos\varphi - \sin\varphi\,[\cos\varphi + \cot\theta_1\,(1+\sin\varphi)]}}\left(\frac{U_w}{Q}\right) \tag{395}$$

and

$$d_{in} = \frac{\sqrt{6\sin\varphi}w\left(\psi_f\right)}{2\sqrt{n\cos\varphi - \sin\varphi\,[\cos\varphi - \cot\theta_0\,(1+\sin\varphi)]}}\left(\frac{U_w}{Q}\right). \tag{396}$$

The ratio U_w/Q in Eqs. (395) and (396) should be eliminated by means of (393).

7 Concluding Remarks

The present chapter provides a comprehensive review of solutions for the strain rate intensity factor for the model of classical pressure-independent plasticity and the double-shearing model of pressure-dependent plasticity. Comparison made allows one to estimate the effect of pressure-dependency of the yield criterion on the magnitude of the strain rate intensity factor. The importance of this quantity for applications is that it controls the intensity of plastic deformation and, as a consequence, the intensity of physical processes in a narrow layer near frictional interfaces. Some theories have been already proposed to use the strain rate intensity factor in constitutive equations [41, 42]. In certain sense, these theories are similar to some theories in the mechanics of cracks based on the stress intensity factor [43]. Since the latter are very successful in engineering applications, it is expected that the theories based on the strain rate intensity factor can be successful as well.

Acknowledgments The research described in this chapter has been supported by the grant RFBR-11-01-00987. A part of this work was done while the first author was with National Chung Cheng University (Taiwan) as a research scholar under the recruitment program supported by the National Science Council of Taiwan (contact 99-2811-E-194-009).

References

1. Alexandrov, S., Richmond, O.: Int. J. Non-Linear Mech. **36**(1), 1 (2001)
2. Alexandrov, S., Lyamina, E.: Dokl. Phys. **47**(4), 308 (2002)
3. Alexandrov, S., Mishuris, G.: J. Eng. Math. **65**(2), 143 (2009)
4. Alexandrov, S.: In: Proceedings of 10th Biennial ASME Conference on Engineering Systems Design and Analysis (ESDA 2010) ESDA2010-24021 (2010)
5. Alexandrov, S., Harris, D.: Int. J. Mech. Sci. **48**(7), 750 (2006)
6. Moylan, S., Kompella, S., Chandrasekar, S., Farris, T.: Trans. ASME J. Manuf. Sci. Eng. **125**(2), 310 (2003)

7. Trunina, T., Kokovkhin, E.: J. Mach. Manuf. Reliab. **37**(2), 160 (2008)
8. Alexandrov, S., Grabko, D., Shikimaka, O.: J. Mach. Manuf. Reliab. **38**(3), 277 (2009)
9. Fries, T.P., Belytschko, T.: Int. J. Numer. Meth. Eng. **84**, 253 (2010)
10. Spencer, A.: Mechanics of Solids, pp. 607–652. Pergamon Press, Oxford (1982)
11. Hill, R.: The Mathematical Theory of Plasticity. Clarendon Press, Oxford (1950)
12. Rees, D.: Basic Engineering Plasticity. Butterworth-Heinemann, Oxford (2006)
13. Shield, R.: Proc. Roy. Soc. **233A**(1193), 267 (1955)
14. Druyanov, B., Nepershin, R.: Problems of Technological Plasticity. Elsevier, Amsterdam (1994)
15. Menrabadi, M., Cowin, S.: J. Mech. Phys. Solids **26**, 269 (2001)
16. Alexandrov, S., Druyanov, B.: Mech. Solids **27**(4), 110 (1992)
17. Druyanov, B., Alexandrov, S.: Int. J. Plast. **8**(7), 819 (1992)
18. Alexandrov, S.: Sov. Phys. Dokl. **37**(6), 283 (1992)
19. Alexandrov, S.: Mech. Solids **30**(5), 111 (1995)
20. Alexandrov, S., Richmond, O.: Dokl. Phys. **43**(6), 362 (1998)
21. Alexandrov, S.: J. Appl. Mech. Tech. Phys. **46**(5), 766 (2005)
22. Alexandrov, S., Mishuris, G.: Arch. Appl. Mech. **77**(1), 35 (2007)
23. Alexandrov, S.: J. Appl. Mech. Tech. Phys. **50**(5), 886 (2009)
24. Alexandrov, S., Harris, D.: Eur. J. Mech. A. Solids **29**(6), 966 (2010)
25. Alexandrov, S.: J. Appl. Mech. Tech. Phys **52**(3), 483 (2011)
26. Alexandrov, S.: Mater. Sci. Forum **623**, 1 (2009)
27. Alexandrov, S., Jeng, Y.R.: J. Eng. Math. **71**(4), 339 (2011)
28. Alexandrov, S., Lyamina, E.: J. Appl. Mech. Tech. Phys. **50**(3), 504 (2009)
29. Alexandrov, S., Kocak, M.: Fatigue Fract. Eng. Mater. Struct. **30**(4), 351 (2007)
30. Alexandrov, S., Richmond, O.: Fatigue Fract. Eng. Mater. Struct. 723–728 (2000)
31. Spencer, A.: Int. J. Mech. Sci. **7**, 197 (1965)
32. Shield, R.: J. Mech. Phys. Solids **3**, 246 (1955)
33. Alexandrov, S., Lyamina, E.: Mech. Solids **43**(5), 751 (2008)
34. Spencer, A.: J. Mech. Phys. Solids **12**, 337 (1964)
35. Marshall, E.: Acta Mech. **3**, 82 (1967)
36. Pemberton, C.: J. Mech. Phys. Solids **13**(6), 351 (1965)
37. Alexandrov S., Lyamina, E.: Mech. Solids (in press)
38. Alexandrov, S., Lyamina, E.: Mech. Solids **38**(6), 40 (2003)
39. Alexandrov, S., Lyamina, E.: Int. J. Mech. Sci. **45**(9), 1505 (2003)
40. Alexandrov, S., Lyamina, E.: Acta Mech. **187**, 37 (2006)
41. Alexandrov, S., Lyamina, E.: J. Appl. Mech. Tech. Phys. **47**(5), 757 (2006)
42. Alexandrov, S., Lyamina, E.: J. Appl. Mech. Tech. Phys. **52**(4), 657 (2011)
43. Kanninen, M., Popelar, C.: Advanced Fracture Mechanics. Oxford University Press, New York (1985)